CARBOHYDRATE-CENTERED PAMAM DENDRIMERS FOR USE IN GROWING LIVER CELLS

JEREMY DANIEL LEASE
(BS ChE, UIUC; MS, UIUC)

A THESIS SUBMITTED

FOR THE DEGREE OF DOCTOR OF PHILOSOPHY OF ENGINEERING

DEPARTMENT OF CHEMICAL AND BIOMOLECULAR ENGINEERING

NATIONAL UNIVERSITY OF SINGAPORE

2007

ACKNOWLEDGEMENTS

First and foremost I would like to thank my supervisor, Dr. Tong Yen Wah, for his guidance throughout this research project. I would also like to express thanks to my colleagues, Shih Tak, Chao "Superman" Ren, and Xin Hao for their intriguing conversation, various inputs and generous assistance throughout this duration of this research. I also have to give thanks to the many laboratory officers and others who dedicated their time and support in assisting with the running of numerous analytical equipment; Michelle Mok (MALDI-TOF-MS), Choon Yen (HPLC), Dr. Rajarathnam (FTIR), Dr. Yuan Ze Liang (XPS & LLS), Mao Ning (TEM), and Novel Chew (GPC). I would also like to thank Alice Low, "the Rube", Ayman Al(l)ian, Bigmac, my family and the Cubs; without whom I may not have kept my sanity throughout this arduous journey.

TABLE OF CONTENTS

SUMMARY

In the current study, a galactose-centered polyamidoamine dendrimer was synthesized. Synthesis of the core molecule, through two main reaction pathways, involved conversion of the five hydroxyls of galactose into amines. A two-step iterative reaction sequence followed for side arm dendrimer growth extending from the core. Growth was continued up to a fourth generation dendrimer, at which point particles should contain eighty reactive amine end groups. These dendrimer nanoparticles were then surface modified, up to fifty percent reaction of end group amines, with a galactose moiety utilizing a zero length coupling reaction to improve biocompatibility and increase cellular interactions for future use. Products were analyzed using combinations of FTIR, NMR, MALDI-TOF-MS, HPLC and elemental analysis.

Synthesized dendrimers, both modified and unmodified, were then crosslinked into gel form for further use as tissue engineering cell scaffolds, specifically for growing Hep3B hepatoma cells. Several crosslinking agents were utilized for reaction, including poly(ethylene glycol 400 diglycidyl ether) (PEG-DGE), poly(ethylene glycol 400 diacrylate) (PEG-DA) and glutaraldehyde. Reaction in both aqueous and organic solvents were studied. Results found PEG-DGE to be the best suited crosslinking reagent, with swelling ratios ranging anywhere from 3 to 12, depending on reaction conditions used. Swelling abilities of the gels could be manipulated by varying crosslinking densities, which is accomplished by varying reactant and solvent contents (crosslinker vs. dendrimer vs. solvent). Higher crosslinker content and less solvent quantity resulted in harder materials of higher crosslinking densities and reduced swelling abilities. Gels

synthesized with modified dendrimers were found to exhibit higher swelling ratios. FTIR and thermal studies were also performed on the acquired gel materials.

Final experiments involved cell culture studies on PEG-DGE and glutaraldehyde crosslinked dendrimer gel samples, as well as the dendrimes themselves. ISO 10993-5 cytotoxicity studes on dendrimer particles indicate decreased toxic effects for higher percentages of dendrimer surface modification. This was expected, as an increase in galactose surface groups will serve to elimate and shield the positive surface charge that is brought about by the large number of amine end groups present on the dendrimers. Toxicity of glutaraldehyde crosslinked samples was found to be high, which may be due to unreacted glutaraldehyde leaching from the samples. Most PEG-DGE crosslinked dendrimer gels, however, were found to exhibit little to no signs of toxicity, with exception to those comprised of high dendrimer concentration (40 wt%).

Hep3B cells were typically observed to grow into a number of large spheroids over the course of a couple of weeks of culture. To study actual cell function of cells cultured onto the gel mateirals, MTT, EROD and ELISA functional assays were also conducted. EROD and ELISA studies found increased levles of P450 and albumin synthesis in a number of PEG-DGE crosslinked gel samples in comparison to positive controls. Enhanced performance was generally found for gels consisting of more highly surface modified dendrimers. These initial findings indicate possible future applications for use of such materials in the areas of tissue engineering.

Several alternate methods for acquiring amine end groups on a carbohydrate core were also studied. A one-step coupling reaction of trehalose with glycine-Fmoc was found to be the most promising, with up to six substitutions clearly observed in mass spectra.

NOMENCLATURE

BE	-	Binding Energy
FWHM	-	Full Width at Half Maximum
ACN	-	Acetonitrile
amu	-	Atomic mass units
BAL	-	Bio artificial liver
BSA	-	Bovine serum albumin
CHCN	-	α–cyano-4-hydroxycinnamic acid
DBA	-	Dibenzylamine
DCC	-	N,N'-dicylohexylcarbodiimide
DCE	-	Dichloroethane
DCM	-	Dichloromethane
DHB	-	2,5-dihydroxybenzoic acid
DMEM	-	Dulbecco's modified Eagle's medium
DMSO	-	Dimethyl sulfoxide
EA	-	Elemental analysis
EDTA	-	Ethylenediamine Tetraacetic Acid
FTIR	-	Fourier Transform Infrared
G4M25	-	Fourth generation glycodendrimer with 23% surface modification
G4M50	-	Fourth generation glycodendrimer with 46% surface modification
GPC	-	Gel Permeation Chromatography
HPLC	-	High Pressure Liquid Chromatography
LBA	-	Lactobionic Acid
MALDI-TOF	-	Matrix Assisted Laser Desorption Ionization-Time of Flight
LLS	-	Laser Light Scattering
MS	-	Mass Spectroscopy
NaOH	-	Sodium Hydroxide
NHS	-	N-Hydroxysuccinimide
NMR	-	Nuclear Magnetic Resonance
PAMAM	-	Poly(amido amine)
PBS	-	Phosphate Buffered Saline
PE	-	Polyethylene
PEG-DA	-	Poly (ethylene glycol 400 diacrylate)
PEG-DGE	-	Poly (ethylene glycol 400 diglycidyl ether)
PEO	-	Poly(ethylene oxide)
PET	-	Poly(ethylene terephthalate)
PhthN	-	Potassium Phthalimide
PLGA	-	Poly(lactic-co-glycolic acid)
PU	-	Polyurethane
PVDF	-	Poly(vinylidene fluoride)
SEM	-	Scanning Electron Microscopy
TBABr	-	Tetrabutylammonium Bromide
TEM	-	Transmission Electron Microscopy
TFA	-	Trifluoroacetic Acid
THF	-	Tetrahydrofuran

TLC	-	Thin Layer Chromatography
TMB	-	3,3',5',5-tetramethylbenzidine
UV	-	Ultraviolet

LIST OF FIGURES

LIST OF TABLES

CHAPTER 1: INTRODUCTION

The area of bioengineering is taking an ever-increasing precedence in the research world today. Stem cell research, genetics, and tissue engineering are the major fields at the forefront of such research. Tissue engineering, in specific, is a multidisciplinary field involving collaboration from a broad array of educational sectors. It comes as no surprise the chemical engineering field is becoming intrinsically involved in this area, with the chemistry, materials science, and engineering knowledge it has to offer. Tissue engineering remains an emerging, rapidly expanding field that mixes new age studies with age old engineering principles in an attempt to mimic or control biology by means of achieving specific biological response.

The liver, in particular, is an area of major focus due to the already prevalent and increasing presence of liver disease in the world today. There is a constant shortage of donor organs that are available for transplants, which is pushing the demand for the availability of alternative tissue sources. One such source could be obtained through in vitro cultivation of liver cells on engineered biocompatible scaffolds. The liver, however, is a complex organ comprised of several different cell types. A great deal of further research is still needed to attain complete mimicry that is capable of performing all of the livers functions. For this reason, cultivated cells at this point in time are typically used in temporary life support systems until a donor liver becomes available.

The primary objective of this research was to synthesize a material to be used in the development of a scaffold for use in tissue engineering, specifically for assisted liver cell growth. The first area of consideration was in exactly what type of material/s were going to be used for scaffold synthesis and construction. A wide range of materials, both

natural and synthetic, have already been studied for use in growing liver cells with variations in such properties as hydrophobicity, surface roughness and charge. Dendrimers, a unique relatively recent type of polymer, are an area that has not yet been highly implemented or studied in terms of being applied as major components in the makeup of tissue engineering scaffolds. Due to their unique characteristics and physical properties it was thought that dendrimers would be interesting molecules with great potential to consider for use in such applications.

Once chosen as the material of interest, the *type* of dendrimer had to be considered and what exactly was going to be its chemical makeup. Since biocompatibility is of primary concern in tissue engineering scaffold design, glycodendrimers (carbohydrate based) were perceived as a suitable choice to start due to the advantages in biocompatibility carbohydrates offer. Polyamidoamine (PAMAM) dendrimer, the first synthesized dendrimer, has shown various degrees of success in such applications as gene and drug delivery and in general has been quite extensively studied. In addition, PAMAM synthesis reactions are simple, straightforward and performed under ambient conditions. Although this dendrimer has been shown to exhibit some toxic effects in its amine terminated form, these effects have been shown to be reduced when surface modified with different functional groups. For these reasons, PAMAM was chosen as the material to use in combination with carbohydrates for dendrimer synthesis. Putting these two materials together, a galactose centered dendrimer consisting of PAMAM branching arm units was decided upon for final dendrimer construct.

It was envisioned that combining the advantageous properties inherent in dendrimers with the biocompatibility of carbohydrates would form a material that would be suitable to support and maintain the growth of liver cells by enabling high cell-scaffold

interactions, and thereby increasing cell survivability and functionality. This principle objective can then be broken down into sub-objectives such as (a) glycodendrimer synthesis, (b) formation of the dendrimer into a scaffold material suitable for cellular studies and (c) the performance and function of cell culture on the acquired materials.

For dendrimer synthesis, a galactose-centered polyamidoamine dendrimer will be synthesized through a sequence of chemical reactions, ending in globular shaped nanoparticles with a large number of reactive amine endgroups. As increased positive charges resulting from large numbers of surface amines have been shown to affect cytotoxicity, end group modification of the dendrimers to further improve biocompatibility by shielding this effect was viewed to be not necessarily compulsory but most likely beneficial. Carbohydrates were again chosen for use as the modifying ligand, specifically utilizing the galactose moiety due its documented interactions with the asialoglycoprotein receptors of hepatocytes. Surface modification of the dendrimer will be performed through a zero-length crosslinking reaction, similar to that implemented in protein synthesis, to introduce the galactose moieties onto the outermost dendrimer surface.

The acquired dendrimer nanoparticles will then need to be crosslinked into a material construct that is suitable for cell culture conditions. The next consideration was then toward which type of scaffold geometry to construct, i.e. 2D versus 3D. A 3D structure was decided upon for the benefits it has been shown to provide in the culturing of hepatocytes versus thin films. With the desired geometry decided upon, the next step was to figure out *how* to form the dendrimers into a 3D material. Due to the large number of reactive end groups present in the dendrimers, crosslinking was thought to be an appropriate and viable option. Several crosslinking agents capable of reaction with amine

groups were then chosen for crosslinking consideration; these included glutaraldehyde, poly(ethylene glycol 400 diglycidyl ether) and poly(ethylene glycol 400 diacrylate. PEG containing crosslinking agents were chosen for their biocompatibilities. The idea was to have the dendrimer nanoparticles crosslink together into a gel form in which the cells could be grown and cultured. This could be envisioned as something resembling the ball and stick construct depicted in **Figure 1-1**. Surface modification of dendrimers will therefore have to be limited to a degree that will still leave adequate numbers of amines to enable bonded networks to form with the crosslinking agents.

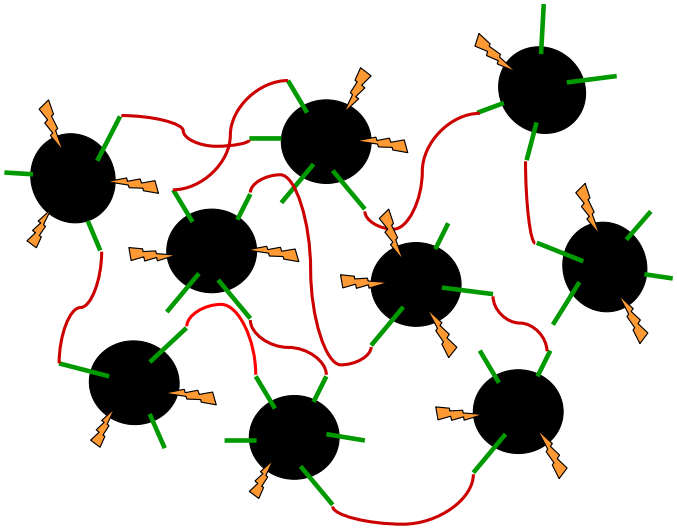

Figure 1-1: Illustration of dendrimer crosslinking. (green=amine, yellow=carbohydrate, red=crosslinking agent)

Cytotoxicity and functional studies will then need to be performed on cells seeded with the materials. The Hep3B hepatoma cell line was chosen for its relatively easy culture requirements, faster proliferation (being of a cancer cell line) and display of several key testable liver functions such as albumin and P450 productions. L929 mouse fibroblasts will be used for toxicity studies performed using ISO-10993 protocols.

In addition to the decided upon reaction pathways for core dendrimer production, alternative methods to acquire end group amines on carbohydrates were also looked into in attempts at decreasing the overall number of reaction steps required. Such methods included a one-pot conversion method of alcohols to amines and the direct coupling of peptides to carbohydrates using zero length crosslinking agents. A review of objectives and overview of thesis topics and organization follows below.

The objectives of this work can be summarized into the following:

- Synthesize a galactose-centered PAMAM dendrimer that will be used for scaffold construction in support of Hep3B cell culture.
    - Alter endgroups through surface modification to improve biocompatibility.
- Through use of amine reactive crosslinking agents, crosslink acquired dendrimers into a gel state suitable for the support of cell growth and function.
    - Study crosslinker, dendrimer, and solvent concentration effects on gel performance.
- Perform cytotoxicity and cellular studies on dendrimer and dendrimer gel materials.
    - It is hypothesized that the formed dendrimer constructs will provide biocompatible, nontoxic surfaces that will promote high cellular interaction and function through the presence of large numbers of surface groups that can be modified to ligands of choice to induce specific cellular reaction.

A literature review covering areas of tissue engineering scaffolds and dendrimers is presented in **CHAPTER 2**. A general background on the liver, its physical makeup

and its chemical functions is first included to highlight the vital roles this organ plays in the human body as well as its complexity. This is followed by an overview of tissue scaffold materials and geometries that have been applied towards the culturing of liver cells, with concentration on thin films and hydrogels. Material properties such as hydrophobicity and surface roughness and the special condition of cocultures are discussed in terms of their effects on cell cultures and resulting cell functionality. Some of the more advanced technologies looking to utilize such scaffold designs for use in human patient treatment are also described. What exactly a dendrimer is as well as their synthesis strategies, properties and various applications are then highlighted, with focus on glycodendrimers and polyamidoamine dendrimers.

Materials and methods of all chemical syntheses and cell culture procedures are found in **CHAPTER 3**. All analytical techniques and instruments are described in detail.

CHAPTER 4 gives an account of dendrimer synthesis methods as well as presents analytical characterization data, including elemental analysis, FTIR, MALDI-TOF-MS and NMR. Two schemes of synthesis are described. The first consists of the sequence of glycosylation, allylation, hydroboration/oxidation, Appel reaction and Gabriel synthesis, and the second of glycosylation, allylation, ozonolysis, reductive amination and heterogeneous catalytic transfer hydrogenation. Surface modification of dendrimers with carbohydrates is also presented within this chapter.

Gelation strategies involved in the crosslinking of dendrimer samples are found in **CHAPTER 5**. Here, results of dendrimer crosslinking utilizing various crosslinking agents, including glutaraldehyde, PEG-DGE and PEG-DA, are discussed. Swelling and thermal studies on the acquired crosslinked materials are presented, with focus on PEG-

DGE crosslinked materials. The effects of variations in crosslinking agent and dendrimer concentration as well as solvent content on gelled products are also studied.

CHAPTER 6 is an account of all cell culture studies. Results of ISO-10993-5 cytotoxicity tests on unmodified and modified dendrimers as well as on PEG-DGE and glutaraldehyde crosslinked samples can be found here. Proliferation studies (MTT) and cell functionality tests, including studies of P-450 (EROD) synthesis, on Hep3B cells seeded onto prepared polymer gels are also presented within this chapter.

The final chapter is an account of several additional studies that were conducted over the course of this research. Included is the testing of several alternate chemical reactions in the attempt to reduce the number of reaction steps necessary in acquiring the final dendrimer product, with focus primarily on dendrimer core preparation. Study of a zero-generation dendrimer reaction with a polypeptide dendron is found here as well.

A summary of conclusions finalizes this document, followed by a compilation of references. Supporting analytical data and additional cull culture documentation can be found at the end of this document in **Appendices A** to **D**.

CHAPTER 2: BACKGROUND & LITERATURE REVIEW

2.1. The Liver

There is a great deal of focus on the liver in tissue engineering due its vital role in the body and high demand in the medical field. Currently, over 20,300 people die from some form of liver disease each year in the U.S. alone, with over 17,700 people still on a waiting list for donor livers [1]. In addition, liver diseases such as hepatitis C and hepatitis B are also on the rise. Hepatitis C alone is responsible for over 8,000 deaths annually and is currently the leading cause for liver transplantation in the United States. [2]. About 5,500 cadaveric livers do become available for transplant each year, but the high costs of surgery, averaging just over US$300,000 after expenses [3], and the possibility of organ rejection once transplanted still remain. For these reasons, an alternate source of suitable liver tissue that could be used in place of cadaveric organs remains a high priority.

The liver is the largest internal organ/gland of the human body, weighing approximately 1.2 to 1.6 kg. It is wedge-like in shape and covered by a network of connective tissue called Glisson's capsule. Situated in the upper right portion of the abdominal cavity, it consists of two major lobes, left and right, and two minor lobes, caudate and quadrate. It is held in position by ligaments to the diaphragm and abdominal walls [4]. The inferior surface of the liver contains a porta, where various vessels, ducts and nerves enter and exit. Venous blood from the gastrointestinal tract is transported to the liver by the hepatic portal vein, constituting about 80% of the blood in the liver. Oxygenated blood supplied by the hepatic artery accounts for the remaining blood supply.

The hepatic portal vein branches between lobules, hexagonally shaped functional units of the liver (see **Figure 1-1**), to eventually form the sinusoids which supply the liver cells with oxygen and nutrients. These lobules consist of hepatic cords that radiate out from a central vein. These cords are composed of hepatocytes, the main functional cells of the liver. Bile canaliculi lie between the cells within each cord. The spaces between these cords are where the sinusoids are located, which are themselves lined with a thin endothelium composed of endothelial cells and hepatic phagocytic cells (Kupffer cells). [5] Blood leaves the liver through the hepatic vein, which is supplied by the central veins that run through each lobule. Bile is removed through the hepatic ducts.

In total, the liver consists of three main cell types; hepatocytes, Kupffer cells and Ito cells. Kupffer cells are fixed macrophages whose primary role is to remove old red cell cells from the blood stream. The red blood cell is broken into parts, where the heme portion is stored and the globin portion is broken down and concentrated as bile in the gall bladder. Kupffer cells also clean bacteria from the blood stream and lead to their

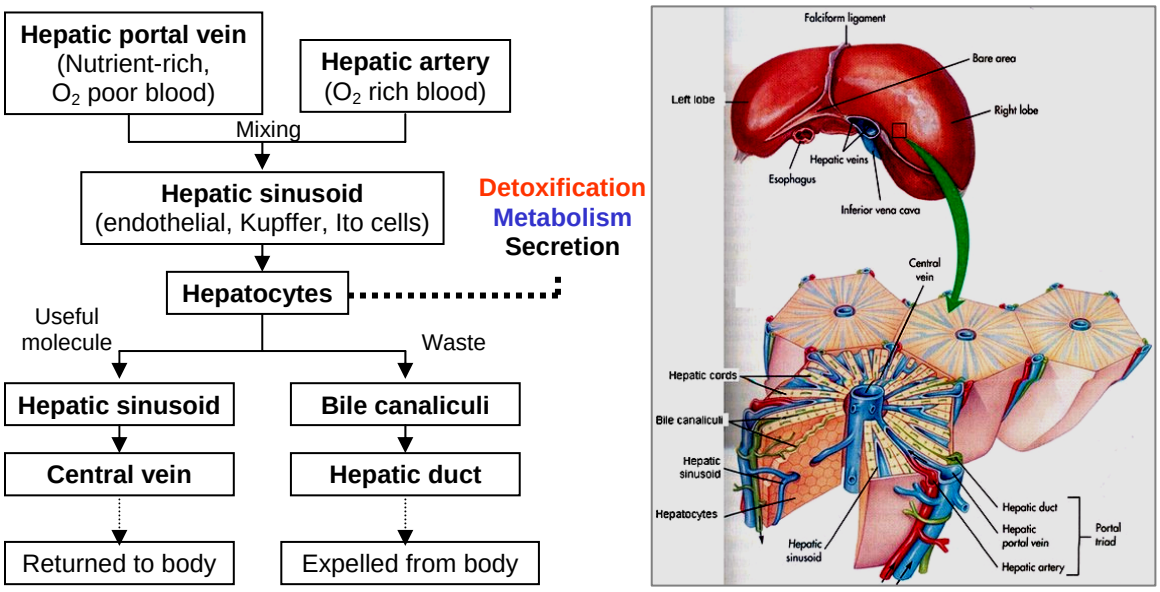

Figure 2-1: (Left) Summary of blood flow through the liver. (Right) Illustration showing the anatomy of the human liver (image from April et al [6])

breakdown [7]. Ito cells are fat-storing cells that are found in the Space of Disse. They are also responsible for vitamin A storage and play a role in wound healing [8]. As previously mentioned, hepatocytes are the main functional cell of the liver. They account for approximately 60% of the cell mass (80% of the volume) in the liver. Hepatocytes are anchorage dependent, highly polarized, polyhedral in shape and range from 13-30 μm in diameter [7]. As pictured in **Figure 2-1**, hepatocytes in the body are observed to grow in sheets one to two cells thick along the hepatic sinusoids [9]. Hepatocytes are different in that they lack protein storage granules, which are present in other protein producing and secreting cells. The unique ability of the liver to regenerate itself comes from the fact that hepatocytes are not terminally differentiated and can still undergo division. Typically only several cells are observed to undergo proliferation, but under stress it has been shown that a vast majority are able to proliferate in order to compensate for any tissue damage or loss. If healthy, large portions (up to 75%) of the liver have been successfully removed from various animals, including human, with a full regenerative recovery still attained [10]. For these reasons various strains of hepatocytes (i.e. primary, Hep3B, HepG2) are most frequently used in research dealing with the liver.

The liver is responsible for a variety of biological functions necessary for maintaining homeostasis within the body, which can be broadly classified into three categories; metabolism, detoxification and secretion. Some of the most important activities include cleansing the blood of carcinogens, alcohol and other poisonous substances; regulating circulating nutrients, such as fat soluble vitamins A and D, hormones and cholesterol; manufacturing proteins such as albumin and clotting factors; producing bile for lipid digestion; lymph production; and producing immune factors to resist infection. Hepatocytes play an integral role in maintaining glucose homeostasis in

the body through processes of glycogenesis (for storage) and glycogenolysis (for use). Under adverse conditions, they can also produce glucose from amino acids or lipids through gluconeogenesis. In total, the liver performs over 500 functions. This complexity, however, also increases susceptibility to damage and disease, as everything that enters the bloodstream eventually passes through the liver, which holds about 13 percent of a person's blood supply at any given time [11].

Hepatocyte functions that are frequently monitored in in-vitro studies are the production of albumin, cytochrome P450 and urea, which are critical, liver-specific functions that can be quantitatively studied through various functional cell assays (i.e. ELISA). Albumin is a blood protein secreted by hepatocytes that is needed for maintaining colloid osmotic pressure, binding and transport, free radical scavenging, acid-base balance, coagulation and vascular permeability. One sign of liver damage is ascites (accumulation of fluid in the abdomen), which is typically a result of low albumin levels in the blood [12]. Many digested substances and by-products of metabolism are toxic to cells within the body if accumulated and not removed. Cytochrome P450 is a group of enzymes that are responsible for the oxidative metabolism of a wide variety of compounds, including many medications.

$$RH + O_2 + 2H^+ + 2e^- \rightarrow ROH + H_2O \tag{2.1}$$

The enzymes work by transforming molecules into more polar compounds that the kidneys can more readily excrete. This is done through catalytic reaction of the iron ion of the haem moiety, the principal component of the active site of all P450s. Ammonia, a by-product of amino acid metabolism, is another substance that is not readily removed from circulation by the kidneys. In the urea cycle (**Figure 2-2**), nitrogen released from

amino and nucleic acids in the form of ammonia or glutamate is converted into urea by hepatocytes. Some of the urea is converted back to ammonia in the gastrointestinal tract by bacterial urease. Ammonia can also be converted to glutamine for transport and storage purposes.

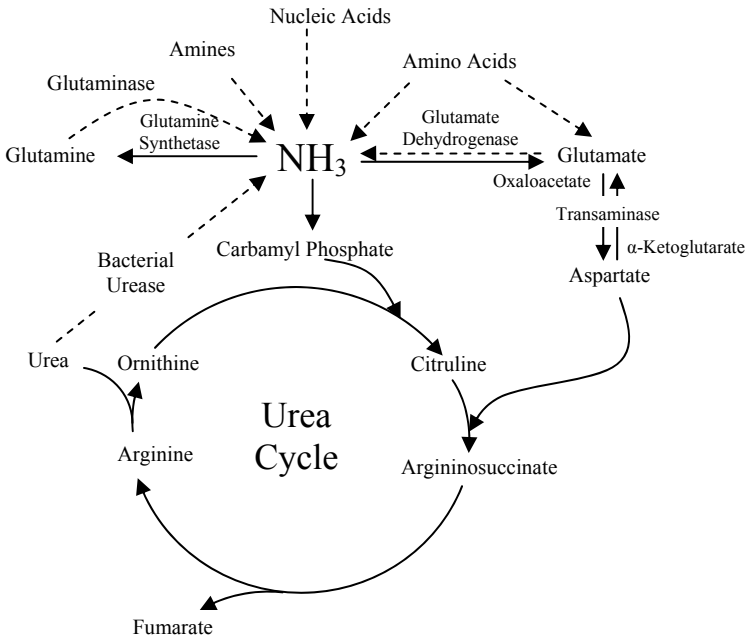

Figure 2-2: Urea Cycle of the liver (Arias et al. [13])

2.2. Scaffolds Used in Liver Tissue Engineering

A number of different constructs have been synthesized for use in liver tissue engineering, involving a wide range of materials. Thin films, hydrogels, nanofibers [14] and microspheres a few examples of the types of scaffolds being explored, with the progression moving from 2-dimensional to 3-dimensional arrangements to better represent natural *in-vivo* conditions. The effects of material properties such as hydrophobicity, surface roughness, ionic charge, dimensional construct and biodegradability have been studied for applicability in liver tissue cultures. In addition, a great deal of research has gone into surface modifications and their effects on biocompatibility and cell-scaffold interactions, specifically cell morphology and functionality. Effects of cell-cell interactions on hepatocyte function have also been studied in cocultures of hepatocytes with other cell types.

2.2.1. Thin Films

Thin films are a widely used scaffold type for initial studies on materials, as they are typically simple to synthesize and provide conditions that allow for easier experimental observation and collection of data than three-dimensional scaffolds. Natural substances such as hyaluronic acid [15] as well as artificial materials such as poly(ethylene terephthalate) (PET) [16, 17], poly-L-lactic acid (PLA) [18], poly(lactic-co-glycolic acid) (PLGA) [19, 20], polypropylene (PP) [21], polytetrafluoroethylene (PTFE) [22] and poly(vinylidene fluoride) (PVDF) [23] have been used in the synthesis of thin films for hepatocyte attachment.

Hydrophobicity, in particular, has been shown to strongly influence cell adhesion, with hydrophilic surfaces promoting increased adhesion over hydrophobic surfaces [24]. This behavior is generally linked to the ability of a surface to adsorb extra cellular matrix (ECM) proteins and has been demonstrated on a number of different materials. Catapano et al. [15], for example, synthesized hyaluronic acid esterified with ethyl (HAE) and benzyl (HAB) esters in both woven and non-woven forms to acquire materials of varying hydrophobicity. Hepatocytes were found to form aggregates on all of the material surfaces, with an increase in aggregate size on the more hydrophobic benzyl ester forms, which was similar to their findings on polypropylene membranes of differing wettabilities [25]. This demonstrates how the hydrophobicity of a surface has a direct effect on cell attachment, with more hydrophobic surfaces inhibiting cell attachment resulting in an increase in cell aggregation and reduction in cell spreading. Hepatocyte function was also found to be elevated and maintained for longer periods of time in the non-woven HAE

form, with this being attributed to the three dimensional structure and reduced hydrophobicity as well as possible effects from surface roughness and mesh size.

Cell adhesion is also influenced by surface roughness, which was demonstrated by Kurosawa et al. [22] in hepatocyte culture studies on expanded hydrophobic PTFE membranes of different pore sizes and surface roughness. Here, it was found that the formation of spheroids occurred on smoother surfaces, while rough surfaces resulted in more flattened and spread cell formations. This may be attributed to an increase in cell-material versus cell-cell interactions on a rough surface. Conceptually it is easy to rationalize that an irregular surface presents more opportunities for a cell to latch onto than a smooth surface. Increased cell function was observed for larger pore sizes of greater than 1 μm. The effect of dissolved oxygen concentration on the function of albumin secretion was demonstrated as well, with oxygen deficiency shown to significantly inhibit cellular performance.

Tanaka et al. [26] also conducted studies on the effect of surface topography by comparing a flat surface to a honeycomb surface of an amphiphilic copolymer of dodecylacrylamide and ω-carboxyhexylacrylamide. Cells were observed flat and spread on the film and to agglomerate into globular shapes on the honeycomb surface (see

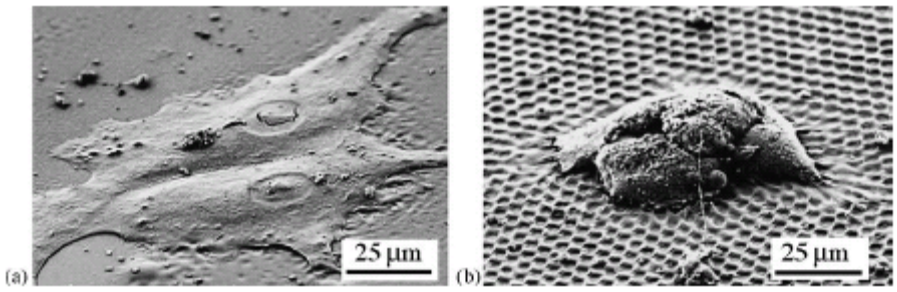

Figure 2-3: Different hepatocyte morphologies on a material surface. (a) Flat surface versus (b) honeycomb surface. SEM cell images from Tanaka et al. [26].

Figure 2-3). The honeycomb surface pattern restricted cell spreading, resulting in the formation of spheroids of approximately 100 μm in size. This behavior may be associated to the amphiphilic nature of the polymer and its method of synthesis, resulting in regions of increased hydrophobicity and hydrophilicity. This would still allow for adequate adhesion but would inhibit the cells from spreading once attached. Urea synthesis was also shown to be significantly higher on the patterned surface, illustrating the effect of cell morphology (spheroid versus spread) on cell function.

In many cases the polymer film itself merely serves as a base for surface modification with various carbohydrates, peptides or other materials to improve biocompatibility and cell-scaffold interactions. A significant amount of research focuses on engineering and designing surfaces with functionalized end groups or binding sites to induce specific cell-scaffold interactions. Several ligands have been identified that improve interactions specifically with liver cells, allowing for increased cell survival and functionality. Galactose, for example, is a widely used ligand in end group modification due to the fact that the asialoglycoprotein receptor of the hepatocyte has been found to specifically bind to this carbohydrate. Parameters such as type, density and orientation have all been shown to have an effect on the morphology, differentiation and proliferation of hepatocytes. Work done by Kim et al. [27] revealed the selectivity of the asialoglycoprotein receptor of hepatocytes, having a higher affinity toward a monosaccharide of terminal galactose and the β-galactose in a disaccharide than a disaccharide of terminal galactose and the α-galactose in a disaccharide. It has also been shown that hepatocytes form spheroids that maintain higher function on surfaces with a higher galactose density [28]. Other ligands found to exhibit specific interaction with liver cells include fructose, which is shown to decrease apoptosis [29], and small peptide

chains such as RGD, which mimics a number of adhesion proteins [30], and GHK, which has been shown to be an activator of hepatoma cells [31]. Extra cellular matrix components and glycosaminoglycans, such as chitosan [32], collagen, and heparin, have also been incorporated into various scaffolds for culturing liver cells.

Attachment and morphological changes of hepatocytes on different modified surfaces were studied by Du et al. [17], using PET films coated with galactose, RGD, collagen, and a galactose-RGD hybrid. The hepatocytes were observed to flatten and spread on both collagen and RGD surfaces, while assembling into spheroids on galactose and hybrid surfaces. Limited spreading occurred on the hybrid surface, resulting in the formation of a so-called '3D monolayer'. 3D spheroids again demonstrated the highest

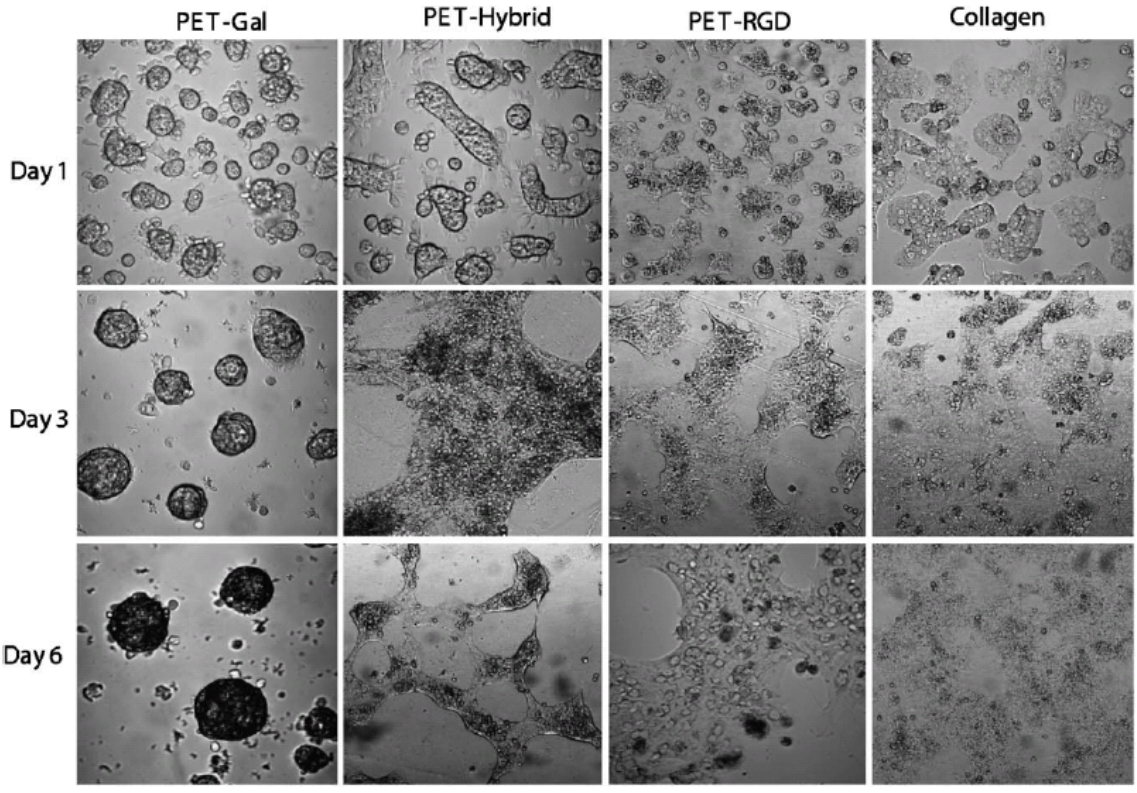

Figure 2-4: Surface ligand effects on hepatocyte morphology. Confocal transmission cell images from Du et al. [17].

function, but possess somewhat weak cell-material interactions that may lead to some detachment from the material surface. The 3D monolayer maintains a middle ground in respect to cell-cell interactions and surface adhesion, while maintaining function near to that of 3D spheroids.

2.2.2. Hydrogels

The primary objective of using hydrogels and other 3-D environments is to more closely mimic in vivo conditions when culturing cells in vitro. Gels offer a balance between support, mechanical stability, and even immunoisolation capabilities, whereas 2-D environments may force cells to conform to a specific flat surface that is otherwise unnatural, which can affect cell performance and function. When using hydrogels as scaffolds, cells can be grown on the surface or encapsulated within the gel either through injection methods or by gelation after cell introduction. A number of different gel systems have been studied, including standard gels, hollow fibers, and microsphere beads [33]. Chitosan, from the exoskeleton of crustaceans, and alginate, from brown seaweed, are probably the most widely studied materials in hydrogel synthesis as they are both derived from naturally occurring biocompatible substances and are found in high abundance. Chitosan, for example, has been used as a base material with various surface modifications [34,35], has been copolymerized with other materials [36,37] and has been used as a surface-modifying agent itself.

The physical properties of gels offer potential for diverse application methods, such as the ability for direct injection, as in the self-cross-linking injectable hydrogel that was devised by Balakrishnan and Jayakrishnan [38]. Here, a periodate-oxidized sodium alginate was cross-linked with gelatin, another commonly used material for gel formation,

in the presence of small amounts of sodium tetraborate (borax). Hepatocytes were encapsulated by first adding them to the alginate solution with borax, followed by the addition of the gelatin to achieve crosslinking. The hepatocytes were observed to maintain a circular morphology, which is common in a gel environment due to the lack of a solid surface for attachment. Albumin secretion was maintained for 16 days, with a weight loss of 50% observed in the gel after a period of five weeks. The gel was also tested as a drug delivery system with primaquine. It was found that after an initial burst release of 40% a relatively smooth release profile was observed to a full release of drug after 5 days for a 57% oxidized alginate dialdehyde gel. This also sheds some light into the multiple functions a 3-D environment can perform, in addition to simply as a surface for attachment.

A major area of concern in 3-D environments is the mass transfer of nutrients and liver proteins. The scaffold should allow for adequate nutrient transfer to maintain cell survival, while in many cases also ensuring immunoisolated conditions. One example of such an environment was created by Honiger et al. [39] using a polyacrylonitrile-sodium methallylsulphonate copolymer to form hollow fibers. A schematic representation of the hollow fiber extrusion synthesis method is depicted in **Figure 2-5**. A chilled saline solution is pumped through an inner tube while the polymer solution is pumped simultaneously through the outer

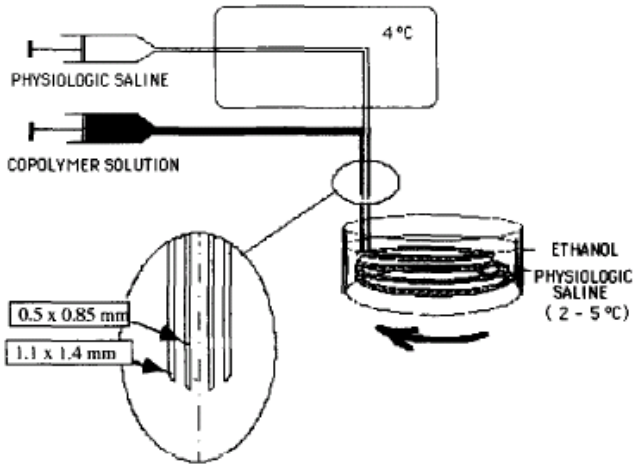

Figure 2-5: Experimental set up for hollow fiber gel synthesis. Image from Honiger et al. [39].

tube, with both directed into a saline bath resulting in fibers with an internal diameter of 800 μm with a 100 μm wall thickness. Similar methodologies can be used for the synthesis of microsphere beads. Cells were introduced into the fibers by a PTFE catheter and were found to exhibit an increase in cell survival and albumin synthesis in comparison to a plastic plate. Cell survival rates of encapsulated hepatocytes were reported as high as 85% at 45 days after transplantation into rats.

Microsphere gel beads are an increasingly common method for hepatocyte encapsulation. Such microenvironments, similar to hollow fibers, offer isolated conditions in a 3-D environment with large surface areas for mass transfer. They have been synthesized in a number of ways, including air jet pellator and syringe pump, to acquire uniform beads of varying sizes. Additional advantages of microsphere encapsulation may vary depending on the materials used. Ringel's et al. [40] alginate microspheres (pictured to the right), for example, offer a stable capsule against mechanical stress, quick encapsulation times (<5 min), and can be quickly liquefied for easy acquisition of the cells. Some possible applications could be in harvesting techniques or for use in bioreactors. The inner and outer surfaces of the microsphere can be modified individually to accommodate surface exposures to different environments. Zhu et al. [41] constructed a microcapsule with an inner surface consisting of half *N*-acetylated chitosan and an outer surface of methacrylic acid-hydroxyethyl methacrylate-methyl methacrylate for encapsulation of hepatocytes. The modified chitosan

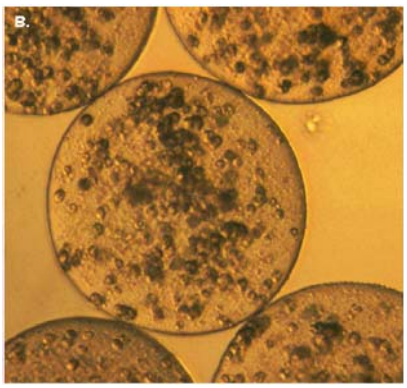

Figure 2-6: Hepatocytes encapsulated within gel microspheres (image from Ringel et al. [40]).

allowed for improved water solubility and preparation at neutral pH. High concentrations of *N*-acetylated chitosan resulted in improved mechanical stability, while lower concentrations increased permeability. Highly permeable microcapsules were tested for cell encapsulation suitability and were found to sustain hepatocyte function at higher levels in comparison to a monolayer culture over a period of seven days.

3-D environments, in general, have been shown to induce higher survival rates and function in cultures of hepatocytes than thin films. This is commonly attributed to the morphological differences that are observed, relating to the proliferation versus function behavior that occurs in cells. As mentioned previously, cells maintain circular morphologies or aggregate into spheroids in gels due to their physical properties and lack of solid surfaces. This maintains the cells in their function behavior instead of differentiating toward proliferation, under which circumstances function is observed to decrease or be lost altogether. Attainment of spheroids is therefore a common goal when designing scaffolds for hepatocyte cultivation.

2.2.3. Bioartificial Liver Assist (BAL) Devices

Great strides have been made in three-dimensional studies involved in the development of bioartificial liver assist devices. These devices are meant to serve as a temporary form of life support until either the liver heals itself or a donor liver becomes available for transplant. Hollow fiber tubes, flat plates, perfused beds, and encapsulation methods are a few of the designs being studied for use, each possessing their own pros and cons (see **Table 2-1**). These devices incorporate variations of previously described scaffold types for culturing cells into their design; thin films, hydrogels, microspheres or

some combination thereof. Designs have also involved the utilization of a range of hepatocyte cell types, including human, porcine and rabbit.

Table 2-1: Different Types of Bioreactors (adapted from Allen et al. [42])

			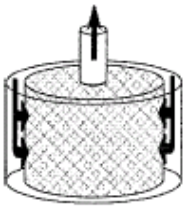	
	Hollow Fiber	**Flat Plat/ Monolayer**	**Perfused Beds/ Scaffolds**	**Encapsulation/ Suspension**
Pros:	Attachment surface, immunoisolation potential, well characterized, cells protected from shear stress	Uniform cell distribution and microenvironment	Ease of scale-up, promotes 3-D architecture, minimal transport barrier	Ease of scale up, uniform microenvironment
Cons:	Nonuniform cell distribution, transport barrier	Complex scale-up, potential large dead volume, cells exposed to shear stress, low surface area-to-volume ratio	Nonuniform perfusion, clogging, cells exposed to shear stress	Poor cell stability, transport barrier in encapsulation, degradation of microcapsules, cells exposed to shear

BAL devices must fulfill two main functions; biochemical (removal of toxins, protein synthesis, etc.) and mechanical (immune protection and cell nourishment). The biochemical aspect would seem to be the easier of the two, utilizing the many scaffold types previously described to culture and maintain hepatocytes that can perform specific liver functions. Mechanical aspects are more challenging, being highly dependent on the membranes used to separate the cultured cells from the patient's blood or plasma. Maintaining cell survivability and functionality for lengthy periods of time continues to be a critical problem. This is especially true in designs incorporating non-human cell

lines, with oxygen and nutrient mass transfer compromised by the necessity to maintain immunoisolation of the cells, most notably against porcine endogenous retrovirus (PERV) when dealing with cells of porcine origin [43].

As of today there is no FDA approved BAL device that utilizes live tissue or cells on the market. The devices currently available offer only dialysis functions, such as HemoTherapies Liver Dialysis Unit (LDU), available since 1999, and Teraklin's MARS® (Molecular Absorbents Recirculating System), which was just recently (June, 2006) approved by the Food and Drug Administration (FDA) for treatment of drug overdoses and poisoning. HemoTherapies went bankrupt in 2001, returning rights to the original developer HemoCleanse, which is now developing a second generation model of the LDU device. For removal of toxins, HemoTherapies' unit utilizes a complex charcoal-based filter, while MARS® employs albumin binding together with membranes that are highly selective towards liver toxins. Although on the market for over five years, HemoTherapies' LDU has not been widely accepted due to lack of clinical testing. It has yet to be seen whether implementation of the MARS® technology will face the same obstacles. Even if available for use, dialysis offers only limited support, as it does account for other functions that the liver performs, such as protein synthesis.

Figure 2-7: Illustration of actual MARS® equipment used for patient treatment. Image from www.leber-dialyse.de [44].

There are a number of tissue inclusive systems that are currently under development and undergoing clinical trials, but have yet to be cleared by the FDA for

common use. To give some insight into the types of technologies being developed, some of the more advanced systems will be mentioned below. Arbios' HepatAssist-2™ , for example, was thought to be the most promising of these systems until it failed its late stage clinical trials and is currently faced with reconducting full phase three testing. Collagen coated dextran in the form of microspheres is used as the cell substrate, which is then loaded into the shell side of hollow fiber membrane cartridges. Cells do not attach to the membrane. The main concern with this system is its use of porcine cells, as the membrane used does not allow for immuno-isolation. This means that extra care must be placed on the supply of the cells, such as screening of animals for viral diseases, to prevent any infectious cells from being used in the system and transferring retroviruses to the patients. Another promising device is Vital Therapies' ELAD® (extracorporeal liver assist device) system, the first to incorporate the use of a human cell line into its design. The specific cell line used is capable of performing a number of liver specific functions and has good proliferation abilities. The cells attach to the external surface of hollow fibers, which are then packed into cartridges for use. This system is currently undergoing phase II clinical trials. Two other more commonly known systems are Sybiol®, which uses aggregated porcine hepatocytes circulated through an interfaced replaceable cartridge, and Matsumura's Alin Bioartificial Liver [45], which utilizes rabbit hepatocytes suspended in solution in conjunction with a semipermeable membrane that is capable of creating immuno-isolated conditions. Although there have been some promising initial results, no system has yet made it to the point of commercial availability.

2.2.4. Hepatocyte Cocultures

A number of groups have shown that prolonged cell life and maintenance of function over longer periods of time can be attained through cocultures of hepatocytes with other cell lines, demonstrating the importance of cell-cell interactions. A number of coculture systems with hepatocytes have been tested, including with fibroblasts, nonparenchymal liver cells (NPCs), bone marrow stromal cells (BMSCs), and endothelial cells. For example, Seo et al. [46] subcultured primary hepatocytes with NIH 3T3 fibroblasts and found a 30-40% increase in albumin and P450 production as well as ammonia elimination. A transwell insert, preventing direct contact but enabling for transfer of proteins and other factors, separated cells. This displays how 'cell signaling' between different cell types can have a direct effect on function.

Higashiyama et al. [47] carried out studies on subcultures of hepatic stellate cells (HSCs) and myofibroblast-like cells (MFBs) with primary hepatocytes. Culture of HSCs in direct contact with hepatocytes was found to result in a decrease in albumin function after six days, while an almost three fold increase resulted in cultivation separated by a semipermeable membrane. The morphology of the HSCs changed to fibroblastic after exposure to FBS, which then led to the trial of MFBs. Two different membranes, one being coated with collagen, were tested in cocultures with MFBs. Using the untreated membrane, viable cells were observed to decrease after six days yet showed a slight increase in urea synthesis. An even greater urea synthesis rate was attained using the collagen-coated membrane, while maintaining a higher number of viable cells, again demonstrating the multiple factors that can influence cell behavior.

BMSCs were cultured with hepatocytes in a similar fashion through use of a semipermeable membrane by Isoda et al. [48]. In this study the BMSCs, as well as treatment with conditioned medium from a BMSC monoculture, were both found to

increase urea and albumin synthesis significantly. This indicates that these cells secrete or synthesize one or more factors that have a direct positive effect on hepatocyte function. Interleukin-6, which is produced by the BMSCs, was found to be the main factor for maintenance of urea synthesis. An additional yet unknown factor is thought accountable for maintaining albumin secretion, as this function was determined to be independent of the presence of interleukin-6.

Tsuda et al. [49] combined surface property manipulation and cocultures of hepatocytes with bovine carotid artery endothelial cells. By using a temperature responsive patterned surface (PIPAAm) hepatocytes were first cultured, attaching and spreading on only the untreated hydrophobic areas. Upon increasing the temperature, the previously hydrophilic areas changed to hydrophobic, to which endothelial cells were then seeded. This created a surface of hepatocyte islets surrounded by endothelial cells. Fluorescent staining indicated an increase in albumin synthesis in areas within 100 to 200 μm to the endothelial cells, with an observable decrease in activity toward the center of larger sized islets. Activities were also maintained for longer periods in these boundary areas, indicating hepatic cellular activity was induced by the interactions occurring with the endothelial cells.

What these works demonstrate is that to attain greater hepatocyte function, experimental conditions must be constructed as close to those found in the body as possible, as with the exposure to other cell types to allow various cell-cell interactions to occur. Although cell signaling is known to play a significant role in determining a cells behavior and function, a great deal is still unknown about the specifics and what factors from what cells affect specific functions.

2.3. Dendrimers

The word dendrimer is derived from the Greek words *dendron* and *meros* meaning "tree" and "part" respectively, and is defined as "a synthetic polymer with a treelike branching structure" [50]. Dendrimers consist of three main parts; a central core, branching units, and functionalized end groups (**Figure 2-8**). The term *dendron* refers to molecules consisting of only the latter two parts, while lacking a central core. As these two terms are often used interchangeably, particular attention must be paid to structure to determine exactly which type of structure is being referred to. Distinction will be made between the two throughout the rest of thesis. Dendrimers are a relatively new class of polymer, first discovered in 1979 by Dr. Donald A. Tomalia of Dow Chemical [51]. The polymeric architecture of dendrimers is recognized as being part of the fourth major class of polymer, which also includes dendrons, dendrigrafts, and hyperbranched polymers [52]. Dendrimer research today has grown exponentially with applications in a wide range of fields.

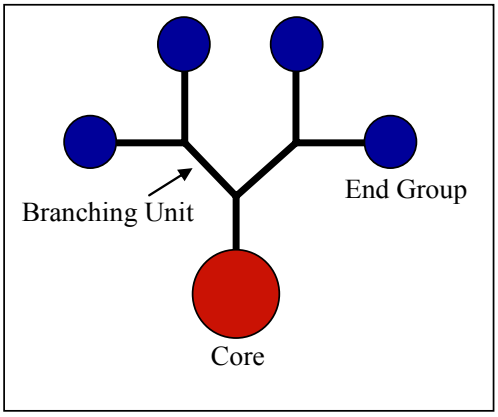

Figure 2-8: Dendrimer building blocks.

2.3.1. Synthesis Methods

2.3.1.1. Divergent Approach

The first of two standard methods used in dendrimer synthesis is the divergent approach (**Figure 2-9**). In this scheme, one starts from a multifunctional core and proceeds to build outward through a sequence of iterative reactions, finally terminating with a functionalized end group. Typically, two different monomers are used in an alternating sequence for the construction of the branching units. In reference to dendrimers, the term 'generation' is used to describe the number of reaction sequences that have taken place. A single generation includes one set of monomer reactions, with the core denoted as generation zero. A half-generation would therefore be after reaction with the first monomer. The earliest dendrimers were synthesized using the divergent approach, including Tomalia's PAMAM dendrimers, Newkome's arborol systems [53], and Mülhaupt [54] and de Brabander's [55] poly (propylene imine) dendrimers (**Figure 2-10**).

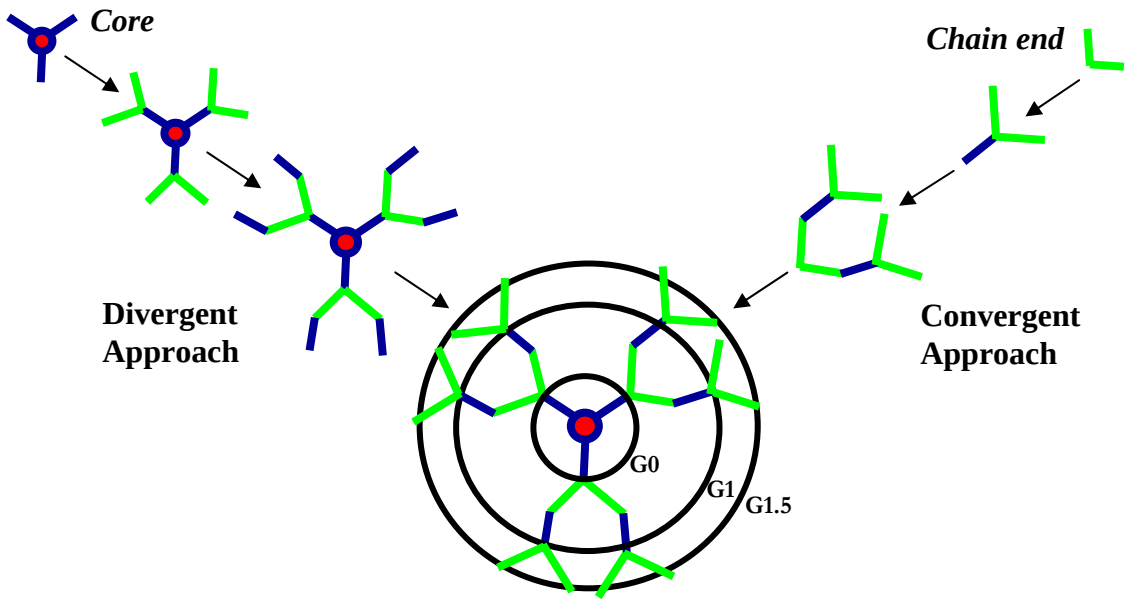

Figure 2-9: Schematic of divergent and convergent dendrimer synthesis, illustrating generations (G) 0, 1, and 1.5.

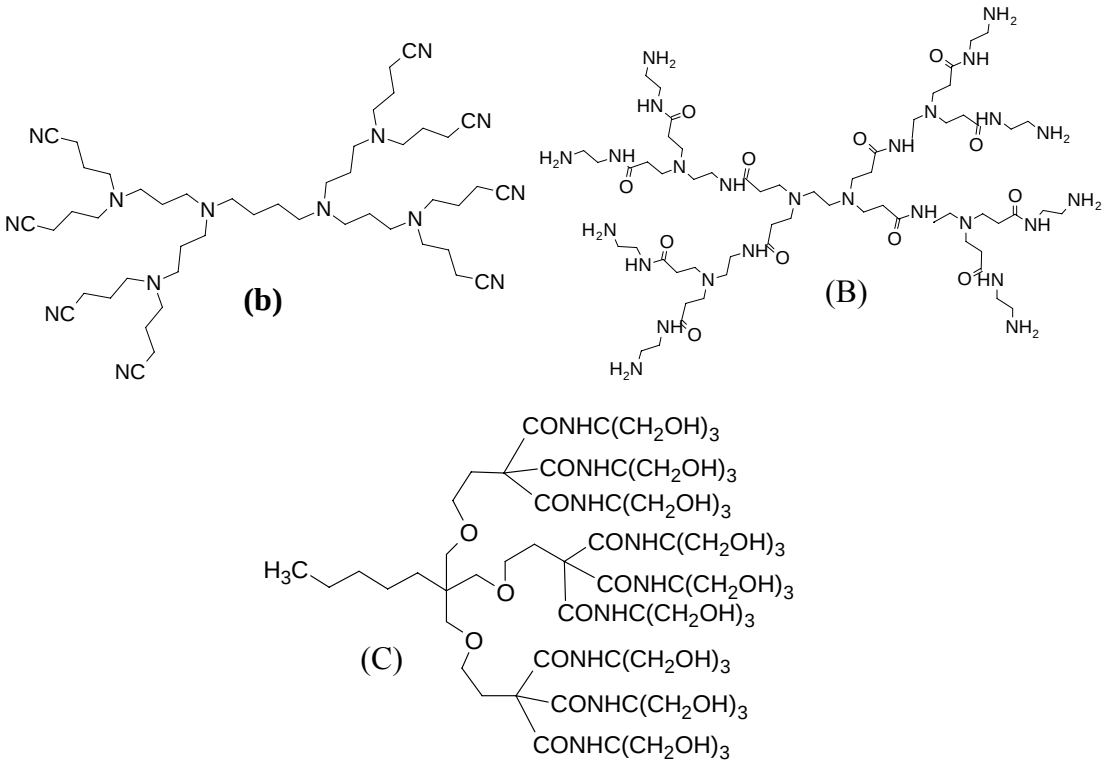

Figure 2-10: (A) Tomalia's generation two PAMAM dendrimer, (B) De Brabander's generation two poly(propylene imine) dendrimer, and (C) Newkome's arborol

The divergent approach is fast and straightforward, but requires an increasing number of reactions for each consecutive step. For this reason, a large excess of reactants is required to ensure complete reaction as well as to suppress side reactions. Side reactions and defects are, however, unavoidable as one proceeds to higher generations, due to the sheer number of reactions involved (e.g. 1024 for a G9 PAMAM dendrimer with an ethylenediamine core), and will become more apparent [56]. Bosman, for example, illustrated that only 29% of a fifth generation poly(propylene imine) dendrimer with 95.5% selectivity per reaction would be defect free [57]. If a perfect structure is required, separation will be a major concern as there is little overall difference in the final structure between perfect and non-perfect high generation end products. The other limiting factor in divergent synthesis is that at the end of each generation there is only one

kind of functional group on the periphery that can be further used for surface modification.

2.3.1.2. Convergent Approach

In the convergent method, the dendrons are initially formed first, starting with the end groups, which are then attached to a central core as a final step. Fréchet first introduced this method in 1990 in the synthesis of aromatic polyether dendrimers [58], followed closely by the phenylacetylene dendrimers of Moore in 1991 [59]. The advantage of this approach is that it allows for a more exact product, while minimizing defects. This is mainly due to easier purification. In this approach defects are more pronounced than those in divergent synthesis (see **Figure 2-11**), as the molecules are much smaller than those formed when building from the core, and are easier to separate out. The number of reactions in the convergent approach is kept to a minimum, decreasing for each subsequent step. This eliminates the need for use of large quantities

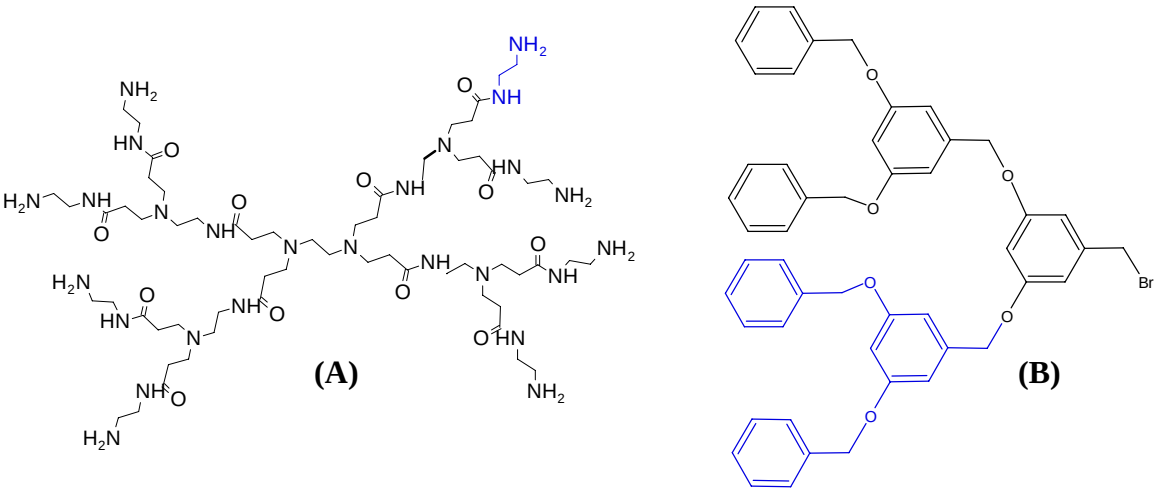

Figure 2-11: Possible defects observed in divergent synthesis (A) G2 PAMAM dendrimer and convergent synthesis (B) G2 aromatic polyether dendrimer due to incomplete reaction. Segments highlighted in blue represent a single reaction and can be visualized to be missing.

of excess reagent and reduces the number of possible side reactions. One limitation however, is that it cannot be used for the construction of high generation dendrimers, as steric hindrance prevents complete dendron attachment to the central core in the final step. In some cases, protection and deprotection reactions may also be required to maintain end group functionality. These protecting groups may contribute to steric hindrance and decrease coupling efficiencies of the reactions [60].

2.3.2. Properties

Dendrimers are highly structured monodisperse branched polymers. Low generation dendrimers exhibit a more open asymmetric shape, while higher generations take on a more globular or spherical shape, forming a membrane-like outer surface as end groups are packed closer and closer together. They typically exhibit high reactivity, due to the large number of reactive end groups on their outer surface, and are amorphous in nature. AB_n type monomers are used as branching units, typically increasing the number of available functional groups 2 to 3 fold each subsequent layer [61]. This growth results in an increase in outer surface area with increasing generation, with the total number of end groups calculated with *Equation 1.2*; where N_c is the core multiplicity, N_r is the number of branches on the monomer unit, and G is the dendrimer generation.

$$End \quad Groups = N_c(N_r)^G \tag{2.2}$$

Dendrimers possess a number of other advantageous physical properties. For one, they are more soluble than linear polymers, which can be beneficial for biomaterials used in applications such as drug delivery. Solubility is highly influenced by the end groups exposed on the outer surface and can be controlled to a great extent through surface modification. For instance, more hydrophilic end groups can be utilized to acquire a

water-soluble molecule, whereas more hydrophobic molecules can be used to attain solubility in nonpolar solvents. Dendrimers also possess lower viscosities due to the lack of chain entanglement that is otherwise present in linear polymers, with intrinsic viscosity actually observed to decrease at higher generations [62]. This phenomenon is explained in that there is an increase in the congestion of end groups in higher generations, which inhibits entanglement between dendrimer molecules [63]. A similar trend is observed in the glass transition temperature (T_g), with T_g leveling off at higher generations.

Probably the most useful trait, however, is that their structures can be easily controlled. Synthesis methods enable virtually complete control of their dimensions, size, and molecular weights, allowing for dendritic polymers of low polydispersity. Monodispersities as low 1.00002 to 1.005 have been reported for polyamidoamine (PAMAM) dendrimers [64]. Typically, the convergent synthesis method results in more monodisperse products. Supramolecular assemblies are possible through integration of molecules with the inner branching units. The presence of internal cavities also allows for the possibility of encapsulation, which can be used for applications in drug delivery or gene therapy.

One limitation of dendrimers is the so-called 'starburst effect'. This is the point at which steric hindrance due to end group crowding disallows any further reaction from taking place. This creates a limit on the number of generations a dendrimer can attain, which varies for each specific dendrimer type. This limit depends a great extent on the multivalency of the core and branching units. The more reactive sites, the faster the growth rate and the quicker this state will be reached. Incomplete reaction and the inability to react all end groups is an indicator as to when this state has been reached.

2.3.3. Glycodendrimers

Glycodendrimers are a specific category of dendrimer that incorporate carbohydrate molecules into their structure. They are divided into four different classes; (A) those with carbohydrates as end groups (i.e. surface modification), (B) those formed in a convergent method starting with a carbohydrate as the end group, (C) those composed of carbohydrate building blocks (i.e. branching units), and (D) those possessing a carbohydrate as the central core [65]. The largest and most researched class is carbohydrates used as end groups. This is because protein-carbohydrate interaction is extremely important in tissue engineering. An inflammatory response, for example, can result in thrombus or scar tissue if proteins are absorbed in a non-specific way onto the surface of a material [66]. It is hoped that by binding carbohydrates onto a materials surface, specific interactions can be tailored to hinder if not completely shield this effect

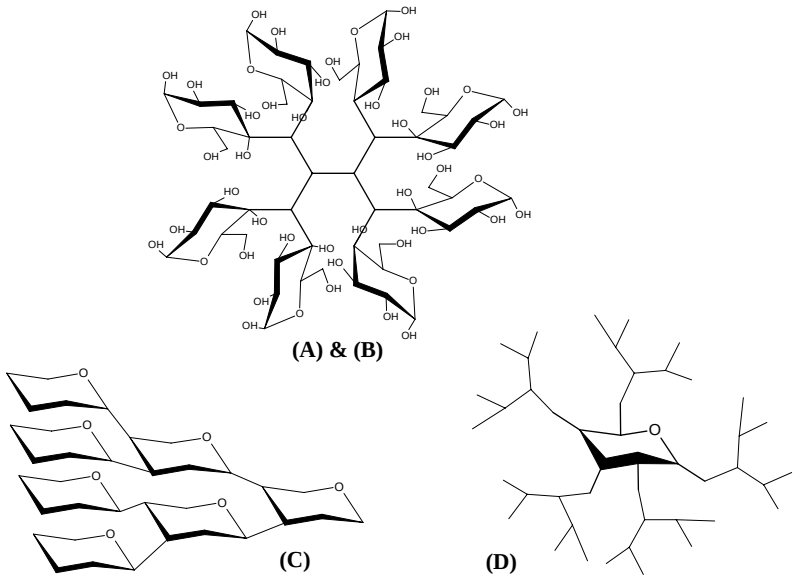

Figure 2-12: Classes of carbohydrate dendrimers. (A) & (B) surface carbohydrates through divergent or convergent synthesis; (C) composed entirely of carbohydrates; (D) carbohydrates as the core.

from occurring. It has also been shown that by increasing the surface concentration of carbohydrates, cell-surface interactions can be increased. This is often referred to as the 'cluster effect' [67].

Some of earliest work on class *A* glycodendrimers was done by Okada [68] and Ashton [69]. Okada's work was done on PAMAM (G=2-4, ammonia core) using the reaction of surface amides with *O*-β-D-galactopyranosyl-(1→4)-D-glucono-1,5-lactone and *O*-β-D-glucopyranosyl-(1→4)-D-glucono-1,5-lactone to form "sugar balls" possessing up to 48 carbohydrates on the periphery. These molecules demonstrated hydrophilic properties by their solubility in water and insolubility in chloroform and ethanol. Ashton performed similar work using DAB (G=1-5). Coupling of amide groups

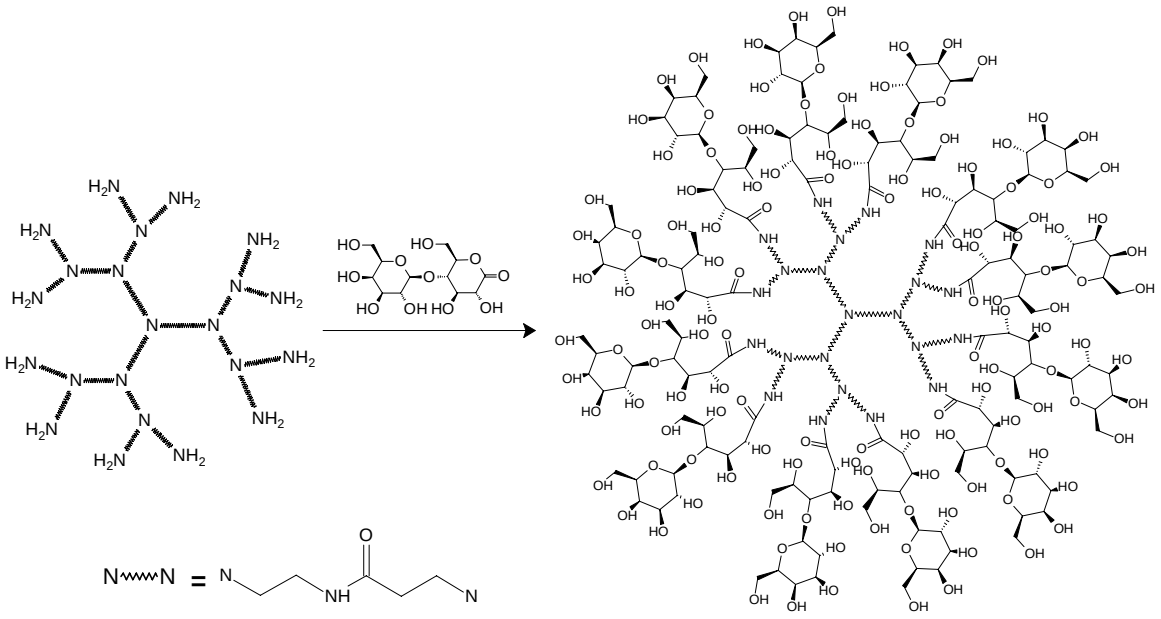

Figure 2-13: Depiction of Okada's "sugar balls". Illustrated is a G2 PAMAM dendrimer (ammonia core) reacted with a carbohydrate functionality to create a glycodendrimer with 12 carbohydrate surface moieties.

and activated ester forms of glucose and lactose using DCC and NHS in dichloromethane resulted in glycodendrimers containing 4 to 64 carbohydrate groups. In this case the sugars were protected in order for efficient coupling to take place.

The convergent approach for constructing glycocoated dendrimers was first encountered in 1996 in work also carried out by Ashton [70]. A TRIS-based cluster glycoside was coupled onto a glycinyl-modified core using DCC and HOBT in a DCM-DMF mixture (2:1), resulting in a molecule containing nine carbohydrate end groups. Protecting groups were again used on the carbohydrates and were removed after coupling. As mentioned previously, this approach is used when a more exact structure is required, with restraints on the number of generations that can be attained due to issues of steric hindrance. As carbohydrates are somewhat bulky end groups, this problem may be

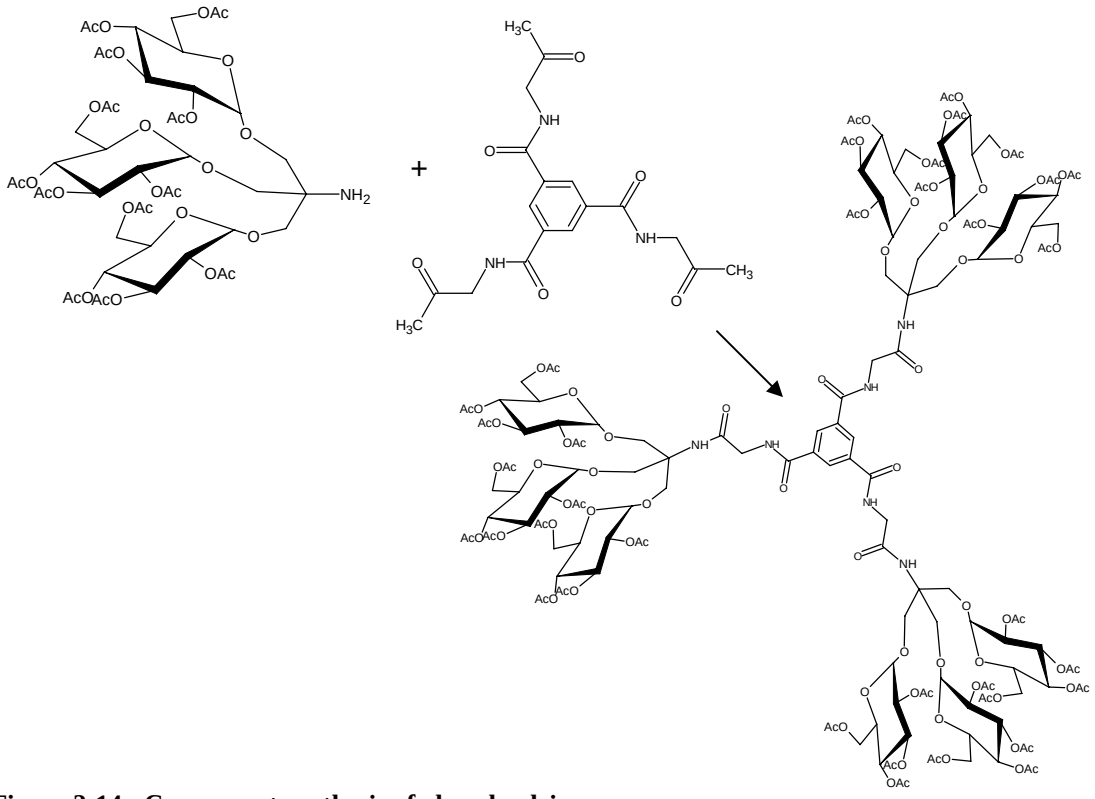

Figure 2-14: Convergent synthesis of glycodendrimer.

further exacerbated. Extending the core or using a spacer arm leading to the reactive site of the dendron can alleviate this setback, as Colonna et al. displayed in their synthesis of

an oligosaccharide dendrimer [71]. Using different protecting groups (4,6-*O*-benzylidine), the same coupling chemistry was performed as in Ashton's synthesis.

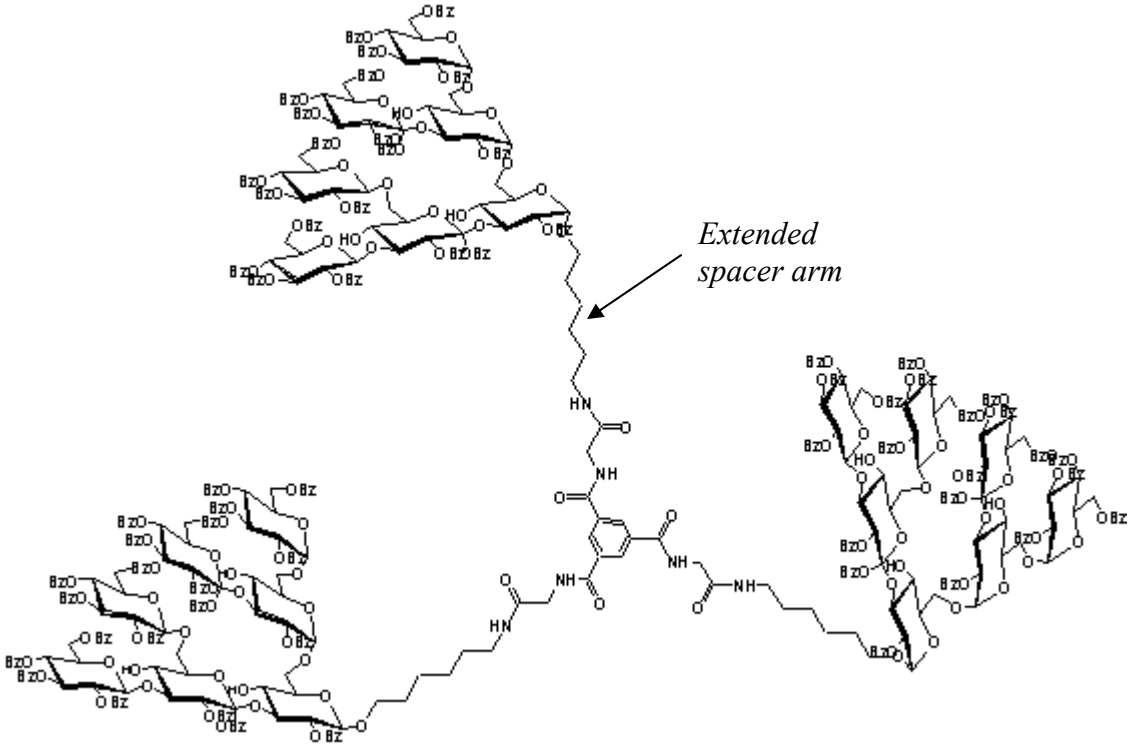

Figure 2-15: Utilization of extended spacer arms for bulkier end groups.

The third glycodendrimer class offers advantages towards biocompatibility in that they can be composed entirely of non-toxic material. They are constructed through glycosylation, peptide coupling and reductive amination reactions. The end groups found in the molecule pictured in **Figure 2-15** for example, can be considered belonging to this group. Two different regioselective glycosylations are involved in its synthesis, in conjunction with the implementation of protecting groups. The molecule itself can be considered a second-generation dendrimer with a carbohydrate core containing a functionalized tether.

Molecules can be synthesized utilizing the same methodology used in peptide synthesis, employing protecting group chemistry (Boc, Fmoc, Mtt) along with coupling reactions, most commonly using DCC/EDC and NHS. Some possible dendron designs composed of carbohydrate building blocks are depicted in **Figure 2-16** [72]. These examples are composed entirely of carbohydrate functional groups and can be synthesized relatively easily using such equipment as a peptide synthesizer with a solid resin support. The primary concern when designing such molecules would be steric hindrance, and allowing enough spatial room for all the desired reactions to take place. Other designs incorporate carbohydrate segments into their branching units albeit contain non-carbohydrate groups as well. Sadalapure and Lindhorst [73] demonstrated such a configuration in their glycopeptide (dendron), coupling together two carbohydrate containing molecules. A carboxylic acid-amine coupling reaction was performed using the uranium based salt HATU together with DIPEA. The final structure consists of

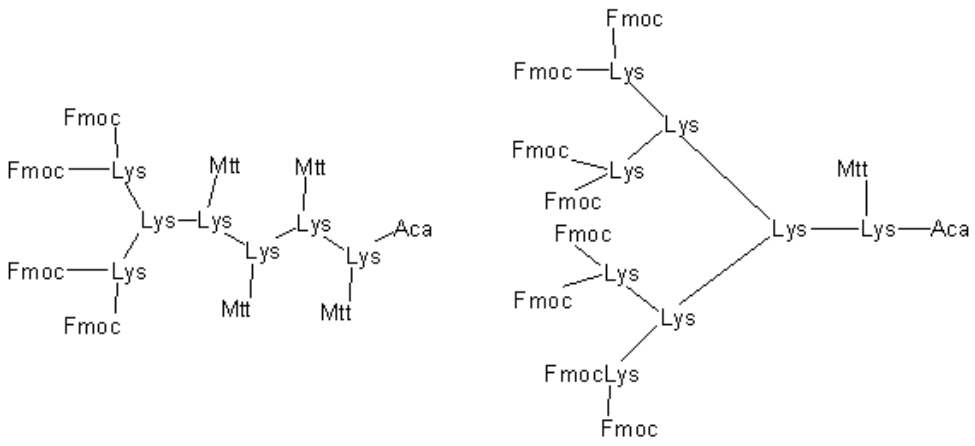

Figure 2-16: Peptide dendrons

carbohydrates connected by the coupled linker arms, with carboxylic acid as the end group functionality.

Finally, reductive amination can be employed as an alternative method for synthesis. Complimentary reactive groups, such as amino and aldehyde, are typically used to undergo reduction with sodium cyanoborohydride (NaCBH). One benefit of this approach is that reaction is usually performed under aqueous conditions without the need for protecting groups. Larger branched oligosaccharides can even be used as the repeating unit, as performed by Turnbull et al. [74] in their use of the trisaccharide β-maltosyl-(1→6)-D-galactose. Two AB_2 type monomers were coupled together using NaCBH resulting in a bis-tertiary amine glycodendrimer.

Carbohydrates used as dendrimer cores are the most current and least studied class of glycodendrimer. Due to their shapes, these molecules have been termed 'octopus glycosides' by their founders, Lindhorst and Dubber [75]. They are different in that the multivalency of their cores is five (monosaccharide) or eight (disaccharide) instead of the typical two or three. Despite the fact that there has yet to be a great deal of research on this type of dendrimer, there are a variety of areas in which they may be applicable. One example of the potential of such constructed molecules is the work done by Kitov et al. [76] in their synthesis of 'STARFISH', a molecule that mimics the structure of subunits of the Verotoxins from *E. coli*. This molecule acts as an inhibitor to SLT-I and SLT-II toxins, protecting cells from prolonged exposure. The inhibition activity of STARFISH was found to be 1 to 10 million times higher than that of monovalent ligands.

Due to the natural chemistry of carbohydrates and the differing reactivity of their hydroxyls, selectively functionalized carbohydrate-centered dendrimers can also be easily attained. This is done by varying the end group on the anomeric carbon, as performed by

Lindhorst et al. [77] in their synthesis of a glucose centered oligosaccharide containing a functionalized tether. Here, the hydroxyl located on the anomeric carbon is first reacted to acquire the desired functionalized ligand, after which the remaining hydroxyls undergo a series of reactions to acquire carbohydrate end groups. The functionalized tether can be modified to various reactive groups to suite the intended use of the molecule.

In this study, a combination of the first and third classes of glycodendrimer will be synthesized; a galactose-centered PAMAM dendrimer containing carbohydrate end groups.

2.3.4. Polyamidoamine Dendrimers

PAMAM is the most widely studied of all dendrimers. As mentioned previously, Tomalia first synthesized PAMAM dendrimers in the early 1980's. The synthesis of

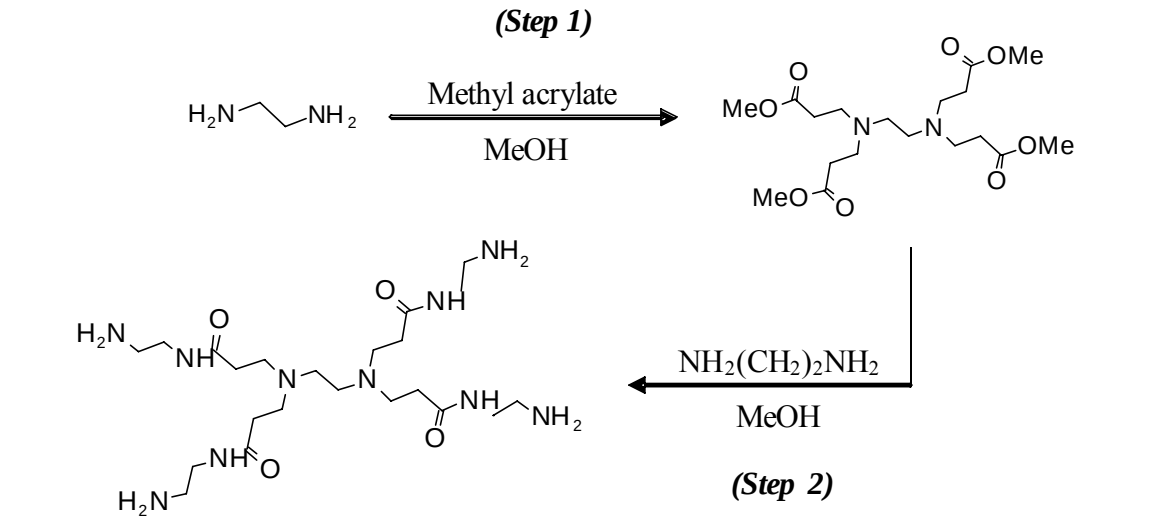

Figure 2-17: The two step iterative synthesis of PAMAM.

these molecules incorporates a repeated two-step sequence. The first step involves an exhaustive Michael addition reaction using methyl acrylate, while the second is reaction with excess ethylenediamine to form the amido-amine linkages (**Figure 2-17**) [78]. They have anionic surfaces in their half-generation form (carboxylate groups) and cationic surfaces in their full generation (amine groups). The 'starburst effect' for PAMAM has been found to occur after the tenth generation [62].

While used successfully in biomaterial studies such as DNA transfer, they have been shown to possess some cytotoxicity. This cytotoxicity is greater in their full generations and increasing with higher generations [79]. This is thought to be the result of interactions between the positive charges on the polymer surface and negative charges found on the cell surface. This effect can be reduced significantly by using the half-generation forms or by adding end groups to help shield the positive charge [80].

2.3.5. Dendrimer Applications

Due to the unique characteristics that dendrimers possess, they have been implemented in a wide range of applications; including sensors, liquid crystals [81], catalysts and gene and drug delivery. Since PAMAM dendrimers are the primary focus in the current study, examples will be directed toward recent studies and applications involving the use of this specific type of dendrimer.

Dendrimer function as sensory devices is enhanced by their ability to possess a large number of end groups, and their versatility allows for their use in varying areas of study. A second generation PAMAM dendrimer modified with sixteen 4-allylamino-1,8-naphthalimide units by Sali et al. [82], for example, has been shown to selectively detect Zn^{2+} cations through fluorescence quenching effects relating to the dendrimers ability to

form complexes with zinc. Detection was also noted to display sensitivities toward changes in pH, similar to Ghosh and Banthia's [83] naphthalene centered G2.5 PAMAM dendrimer, making it a possible pH sensor material. Dendrimer potential for use as biosensors is also documented, as shown by the work of Li et al. [84] in the incorporation of G4 PAMAM dendrimers onto a 2-aminoethanethiol SAM sensor for DNA hybridization analysis. Use of the dendrimer allowed for a major improvement in DNA immobilization capacity, while displaying high sensitivity, selectivity and reproducibility.

Due to their potential for increased sensitivity, dendrimers have also been studied for possible applications in liquid crystal technologies. Work done by Li et al. [85] demonstrated that the light reflection of poly(styrene-methyl methacrylate-acrylic acid) spheres coated with G4 PAMAM dendrimers could be tuned by adjusting pH. This is a result of volume changes that occur in the PAMAM dendrimer at different pH values, with volume observed to increase at lower pH values as the dendrimer becomes more protonated. Similar to Sali's dendrimer, Grabchev et al. [86] synthesized G1-G4 PAMAM dendrimers functionalized with 1,8-naphthalimides for use in liquid crystals displays. The dendrimers were found to emit a yellow-green color with fluorescent maxima at wavelengths of 511-516 nm and absorption maxima at 410-433 nm wavelengths. When introduced into liquid crystal ZLI 1840 as a guest-host binary system they were also found to decrease the phase transition temperatures of the liquid crystal.

Similar to sensor use, dendrimers have been shown to increase catalytic activity primarily due their high surface group density. The advancements being made in dendritic catalysis have recently been summarized by Méry and Astruc [87] and Reek et al. [88]. Metal ions can be introduced within the dendrimer as a core, within the branching arms or as end groups, depending on the intended use. Touzani and Alper [89]

used a silicon centered PAMAM dendrimer with palladium complex end groups to synthesize five- to seven-membered ring lactones and lactams. The regioselectivities obtained were in some cases superior to those found in the homogeneous system and were dependent on reaction conditions. There were also the added benefits of easy separation and re-use of the catalyst (3-7 times). Gong et al. [90] performed hydroformylation of styrene and 1-octene with a G3 PAMAM dendrimer, along variations modified with $PPh_2(CH_2OH)_2Cl$ and 1,3-propane sultone, rhodium complex. Most importantly it was found that such complexes resulted in the selective acquisition of the more important iso-aldehydes when reacted with styrene, in contrast to typical rhodium complexes with diphenyl phosphino ligands, which result in mainly normal aldehydes.

Dendrimers are also beginning to make their way into biological applications such as gene and drug delivery. Dendrimers are being studied as a nonviral gene transfer method for delivering DNA, with full generation PAMAM dendrimers having already been shown to effectively transport DNA into a variety of cell types. This is accomplished by forming complexes with DNA though electrostatic interactions between the positive charges of the dendrimer amino surface groups and the negative charges found on the phosphate groups in DNA. Studies done by Szoka and Haensler [91] found that gene transfer is a function of both the dendrimer size and dendrimer/DNA ratio, with most efficient transfection occurring for G5 PAMAM dendrimer at a dendrimer to DNA charge ratio of 6 to 1. Further studies done by this group demonstrated that higher transfection occurred when there were defects, intentionally made or through degradation, present within the dendrimer than when they were structural perfect. This has been attributed to the increased flexibility of the molecules that results with the presence of the defects [92].

A number of dendrimer conjugates have also been constructed as a way to further improve biocompatibility or gene transfection. Luo et al. [93] conjugated PAMAM dendrimers with PEG and found improved flexibility and decreased overall cytotoxicity, with cytotoxicity noted to increase with increasing dendrimer generations. Arima et al. [94] synthesized PAMAM conjugates with various forms of cyclodextrins and found that the conjugates demonstrated a significant increase in transfection ability over unmodified PAMAM. This was attributed to cyclodextrin's ability to disrupt biological membranes, allowing for an improved release of the DNA from the endosome to the cytoplasm. Antisense oligonucleotides conjugated with PAMAM by Bielinska et al. [95] resulted in a thirty to sixty percent inhibition of specific reporter luciferase gene expression at only picomolar concentrations of dendrimer. Such complexes are important as oligonucleotide stability is needed to successfully inhibit gene expression, and oligonuclotides by themselves undergo degradation in serum and by cellular enzymes.

As previously mentioned, dendrimers possess void spaces within their branching arms that can potentially be used for encapsulating various molecules for drug delivery. PAMAM dendrimer encapsulation ability was demonstrated by Beezer et al. [96] in their encapsulation of acidic hydrophobes. It was suggested that these molecules were forming stable ion pairs with the dendrimers internal nitrogens located within the branching arms, indicating potential, therefore, to encapsulate drugs that are capable of undergoing similar ionic interactions. Indomethacin, an anti-arthritic drug, was recently found capable of encapsulation within PAMAM dendrimers, unmodified and modified with folic acid, by Chandrasekar et al. [97]. It was found that encapsulation efficiency improved and release rates decreased with increases in folic acid moieties. This was explained in that the attachment of the hydrophobic acid molecules on the PAMAM surface create larger void

spaces to accommodate more drug molecules, while simultaneously provide a shielding effect to decrease the release rate of the drugs. Targeting efficiency was also increased for dendrimers with more folic acid surface groups.

Dendrimers can also function as drug delivery vehicles by directly forming conjugates with the drug molecules themselves. 5-aminosalicylic acid was conjugated to G3 PAMAM dendrimers using azo-bond spacers of *p*-aminobenzoic acid and *p*-aminohippuric acid by Wiwattanapatapee et al. [98]. The conjugates displayed colon specific targeting in rats and exhibited prolonged release of the drug (45-57% in 24 hr), exceeding that of the commercial prodrug sulfasalazine (80.2% in 6 hr). In other works, El-Sayed et al. [99] revealed the ability of PAMAM to transport across Caco-2 cell monolayers, with G0 to G2 PAMAM dendrimers found to adequately permeate these cells with nontoxic effects, further demonstrating their potential as drug carriers for oral drug delivery.

The breadth of applications in which dendrimers have been recently applied reveal their diversity as well as highlight their unique characteristics. Still in their infancy, a great deal more is left to be explored and learned about these fascinating molecules. One area of use that has yet to be tackled extensively is incorporation into scaffolds for use in tissue engineering. Studies that have been undertaken typically involve only the use of dendrons as surface modifying agents, such as the PAMAM modified dendrons of Kawase et al.[100, 101] for advancement of hepatoma cell function. In these cases PAMAM dendrons (1 arm) were modified with surface ligands, such as GHK, galactose and fructose, and then attached to the surface of culture plates to study the effect on hepatocyte function. All of the tested ligands provided an enhancement in cellular function over the controls, with a mixture of galactose and fructose providing optimal

conditions for inducing the most significant improvements. However, as was the case in these studies, dendrimers have been mainly applied in supporting roles, with limited cases in which the dendrimer takes on the major material of construct.

Several recent studies do show promise for dendrimers being used in a more prominent tissue engineering role. One study, performed by Söntjens et al. [102], involved the synthesis of a dendrimer with a poly(ethylene glycol) centered core and methacrylated poly(glycerol succinic acid) arms. The intended use for the dendrimer is in cartilage tissue repair. It can be photo-crosslinked with visible light, which allows for crosslinking after filling defects in vivo. The high concentration of end groups also allows for high-density crosslinking, which inhibits swelling after synthesis while supplying an increase in degradation sites. Encapsulated chondrocytes were shown to synthesize neocartilaginous material including type II collagen when seeded within the gels. A second study, undertaken by Duan and Sheardown [103], used a G2 polypropyleneimine octaamine dendrimer as a crosslinking agent for collagen in use as a corneal tissue engineering scaffold. The dendrimer crosslinked collagen was found to possess superior transparency and glucose permeability in comparison to collagen crosslinked with EDC or glutaraldehyde. The resulting gels were capable of supporting corneal epithelial cell growth, while exhibiting no signs of toxicity. These studies may be an indication for the movement of dendrimer application toward more prominent structural and mechanical roles of materials in the future.

The current research intends to expand upon such use by applying dendrimers in a more prominent physical role. The objective is to advance the study of dendrimers in the area of tissue engineering scaffolds using glycodendrimers to form suitable substrates that are capable of supporting liver cell growth as well as maintaining their liver specific

functions. It is believed that the advantageous and versatile properties of dendrimers combined with the biocompatibility of carbohydrates will provide for this type of environment.

CHAPTER 3: MATERIALS AND METHODS

3.1. Polymer Synthesis

3.1.1. Scheme-1 Dendrimer Synthesis

All chemicals used were acquired from Sigma-Aldrich unless otherwise stated. *Step1-glycosylation*: 15 ml of acetyl chloride (Merck) were added to 190 ml of allyl alcohol (99%, Merck) at 0°C. 15 g of D-galactose (99+%, ACROS) were then added and the solution heated to 70° for 2.5 hours under reflux to form **2** [104]. The solution was neutralized with sodium bicarbonate, filtered over a celite bed, and concentrated under vacuum. *Step2-allylation*: Crude **2** was added directly to 300 ml of 33% aqueous NaOH (Merck) solution, followed by the addition of 33 g TBABr (99%, 7.5 equivalents). The

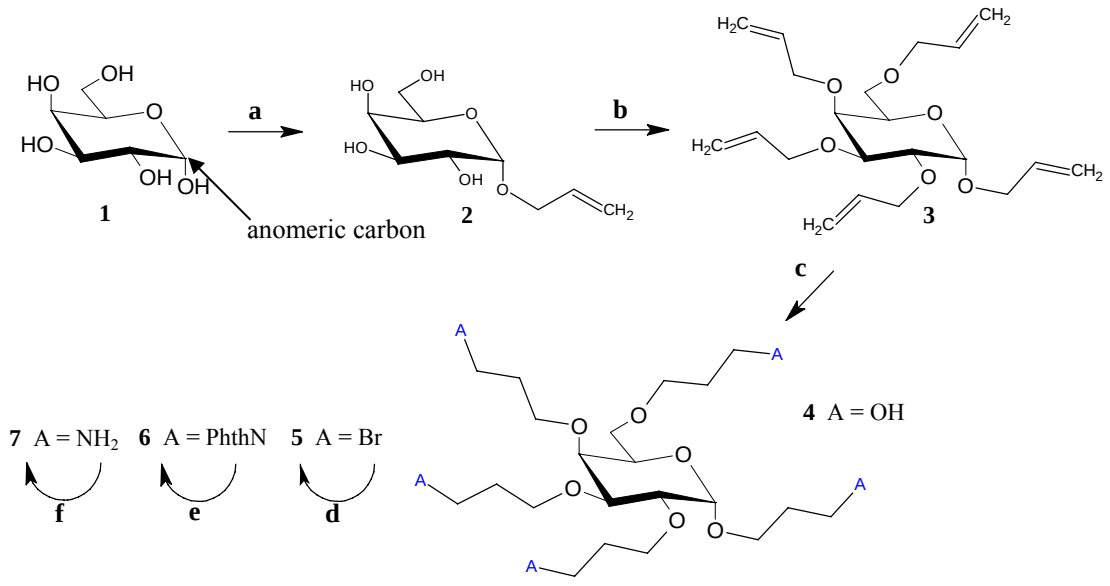

Key: (a) allyl alcohol, acetyl chloride; (b) 33% NaOH, TBABr, allyl bromide; (c) THF, 9-BBN then NaOH, H_2O_2; (d) THF, PPh_3, CBr_4; (e) DMF, KPhthN; (f) THF, NH_2NH_2

Figure 3-1: Dendrimer Core Synthesis 1

solution was heated to 55°C, after which allyl bromide (97%) was added dropwise over a period of one hour. The reaction was carried out for 4.5 hours under reflux at 50-60°C, then at room temperature overnight. 300 ml of toluene were then added to the mixture, mixing for ten minutes, and the phases separated. The organic phase was washed thoroughly with DI water and concentrated under vacuum to get **3**. Product was purified by flash chromatography (toluene-ethyl acetate, 20:1). *Step3-hydroboration-oxidation*: To a solution of **3** in anhydrous THF, 9-borabicyclononane (9-BBN) was added (7.5 molar equivalents) and the reaction ran at room temperature for 1.5 hours under nitrogen. 35% aqueous hydrogen peroxide (Fischer Scientific) and 3M NaOH were then added slowly (12.5 molar equivalents each) and the solution stirred at room temperature overnight. The solution was saturated with potassium carbonate and then an equal volume of diethyl ether (Fischer Scientific) was added. The mixture was stirred for an additional ten minutes, and the phases separated. The aqueous phase was washed three times with equal volume portions of diethyl ether. The organic phases were combined, dried with anhydrous magnesium sulfate (99.5%, Alfa Aesar), filtered, concentrated under vacuum and purified by flash chromatography (ethyl acetate-methanol, 20:1) to get **4**. *Step4-Appel reaction*: Triphenylphosphine (PPh_3, 99%) and carbon tetrabromide ($CCBr_4$, 99%) (7.5 molar equivalents each) were added to a solution of **4** in anhydrous THF. The reaction was carried out in the dark at room temperature overnight, filtered and concentrated. Product was purified using flash chromatography (toluene then methanol). *Step5-Gabriel synthesis (a)*: Potassium phthalimide (PhthN, 98%, 10 molar equivalents) was added to **5** in DMF (ACS, Fischer). The solution was stirred for 5 days at 25-30°C, filtered, and concentrated under high vacuum to get **6**. *Step6-Gabriel synthesis (b)*: **6** was dissolved in anhydrous THF, to which hydrazine (10 molar equivalents) was then added.

The reaction was carried out overnight at room temperature under nitrogen then diluted with methanol, filtered, and concentrated under vacuum to get **7**.

3.1.2. Scheme-2 Dendrimer Synthesis

Step1-ozonolysis: Ozone was bubbled through a solution of perallylated galactose **3** (resulting product of *Step2-Scheme 1*) in dichloromethane (DCM) and sodium bicarbonate at -80°C (dry ice/acetone bath), until the solution was observed to turn blue in color signaling completion of the reaction [105]. An ozone generator (Griffin Technics Corp.) was used to supply the ozone for this reaction. Excess ozone was then removed by bubbling oxygen through the solution until the blue color was observed to dissipate. The solution was then removed from the acetone bath, reacted with triphenylphosphine (6.13

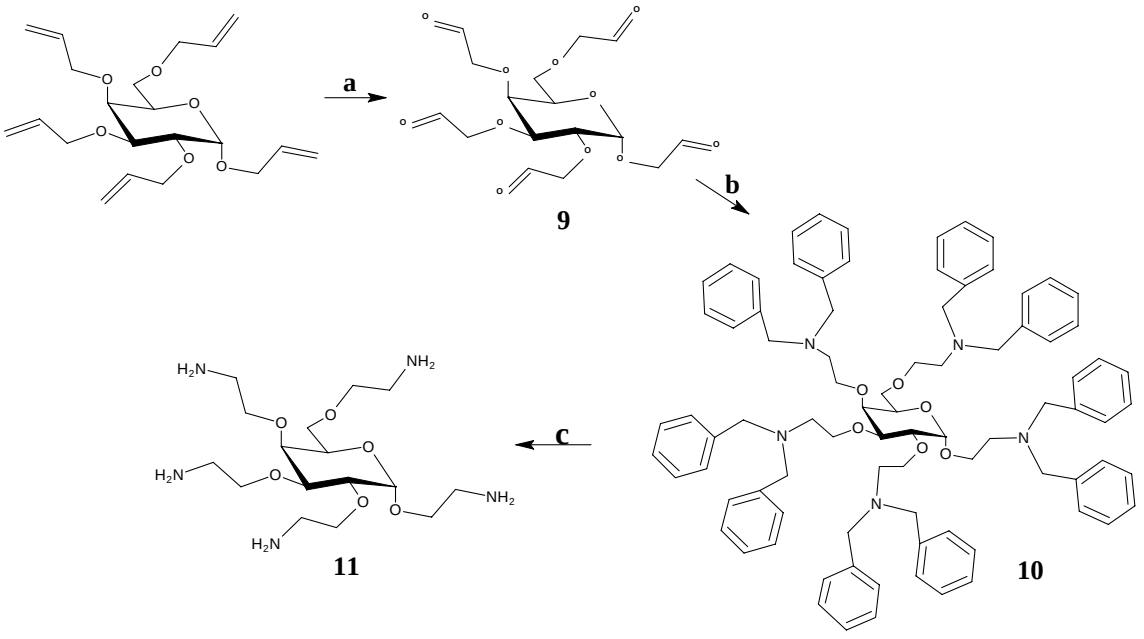

Key: (a) DCM, $NaHCO_3$, Ozone then PPh_3; (b) MeOH, DBA then DCE, $NaBH(OAc)_3$; (c) 10% Pd-C, NH4HCO2

Figure 3-2: Dendrimer Core Synthesis 2

molar equivalents) overnight at room temperature, then filtered and concentrated under vacuum. Product **9** was acquired by dissolving the remaining solids in aqueous solution, then filtering and concentrating again. *Step2-reductive amination*: Dibenzylamine (DBA, 97%, 6.5 molar equivalents) was added to a solution of **9** in methanol, reacted for 24 hours at room temperature, then concentrated under vacuum and dissolved in dichloroethane (DCE, Fisher). Sodium triacetoxyborohydride ($NaBH(OAc)_3$, 9.5 molar equivalents) was then added to the solution and reacted at -10°C for 4 hours. The solution was cooled to -80°C, filtered and concentrated under vacuum to acquire **10**. *Step3-heterogeneous catalytic transfer hydrogenation*: Palladium catalyst (10wt% on carbon, dry powder) was added to a solution of **10** in dry methanol (1.4g in 50mL) under nitrogen. 18 g of ammonium formate (97%) were then added and the reaction ran for 2 hours under reflux, after which an additional 18 g were added and the reaction ran for another 1 hour. Upon completion of reaction the solution was cooled to room temperature, filtered through a celite bed and concentrated under vacuum to acquire **11**.

3.1.3. Polyamidoamine Branching Arm Extension

Step7: Methyl acrylate (99%, 200 molar equivalents) was added to **7** in methanol. The reaction was carried out in the dark for 3 days, and then concentrated and purified with flash chromatography (methanol). *Step8*: **8** in methanol was added to ethylenediamine (99%, 600 molar equivalents) at 0°C, stirred for 5 days at room temperature, and then concentrated under vacuum to give a first generation glycodendrimer [106]. Steps 7 and 8 were repeated sequentially to acquire higher generation dendrimers. In similar fashion, these steps were performed on **11** for dendrimer growth.

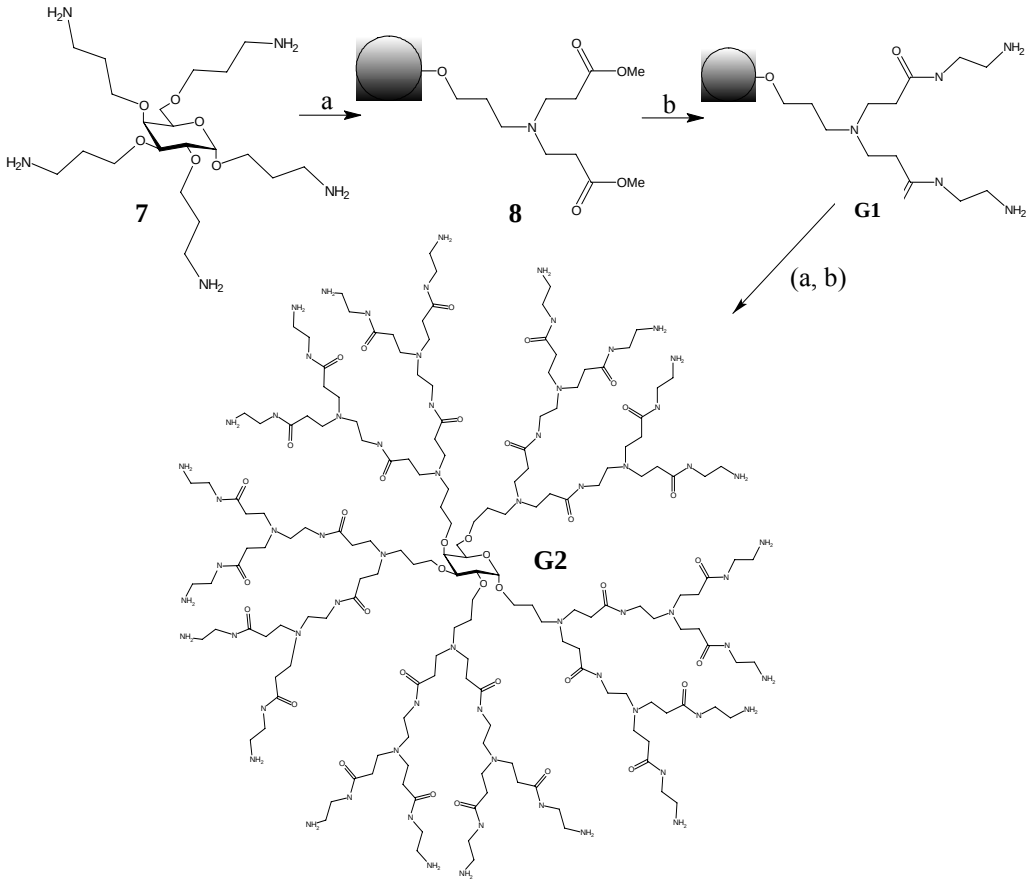

Key: (a) MeOH, methyl acrylate; (b) MeOH, Ethylenediamine

Figure 3-3: PAMAM branching arm extension performed on synthesized glycodendrimer core.

3.1.4. Dendrimer Surface Modification

Galactose was incorporated as a functionalized end group on the dendrimer surface through a zero-length coupling reaction with lactobionic acid (4-O-β-D-galactopyranosyl-D-gluconic acid) (LBA, 97%) using either 1-ethyl-3-(3-dimethylaminopropyl)carbodiimide (EDAC) or N,N'-dicylohexylcarbodiimide (DCC, Fluka 99%) and N-hydroxysuccinimide (NHS, 98+%, Avacado). Use of DCC was the preferred method due to easier product acquisition. When using DCC, coupling was conducted in two steps. First, LBA was reacted with DCC and NHS in DMF for 24

hours. After reaction, the insoluble urea byproduct of DCC (observed as a white precipitate) was filtered off and the solution was concentrated under vacuum. The resulting solid was then dissolved in DI water to which the dendrimer was added for final coupling. After reaction, the solution was filtered to remove excess DCC, then concentrated and washed with THF to remove excess NHS.

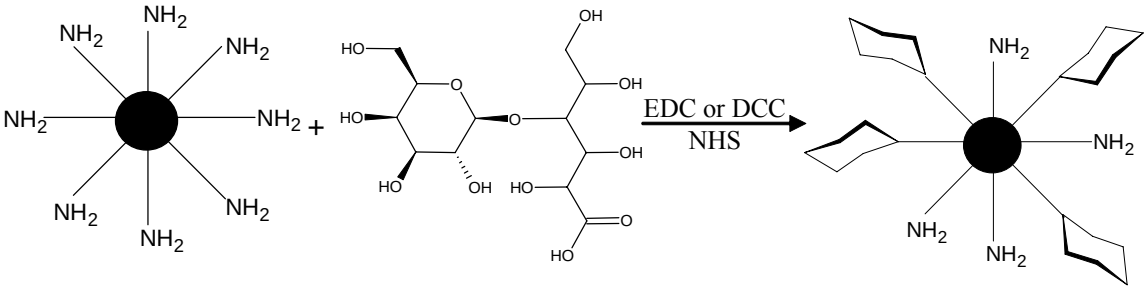

Figure 3-4: Coupling reaction of lactobionic acid using EDC/DCC and NHS.

3.2. Dendrimer Crosslinking/Gel Formation

3.2.1. Glutaraldehyde & Succinyl Chloride

Glutaraldehyde (50% aqueous solution) was added dropwise to prepared aqueous and organic solutions of dendrimer. The solution was stirred vigorously during addition to promote homogeneous reaction. After reaction, the resulting solids were washed with DI water and soaked in aqueous solution overnight to remove unreacted glutaraldehyde. Succinyl chloride (95%) was added dropwise to prepared methanol solutions of dendrimer. Due to the exothermic nature of the reaction, crosslinker addition was performed slowly to avoid overheating. For safety reasons, both of these reactions were performed in a fume hood given the toxicity of the reactants involved.

3.2.2. Poly (ethylene glycol 400 diglycidyl ether) (PEG-DGE) & Poly (ethylene glycol 400 diacrylate) (PEG-DA)

Dendrimer samples were dissolved to form well-mixed aqueous or organic solutions of varying concentrations. The crosslinking agent was then added, (poly(ethylene glycol 400 diglycidyl ether (Polysciences, Inc.) or poly(ethylene glycol 400 diacrylate)), and the solution thoroughly mixed until homogeneous conditions were observed. Samples were then sealed from the atmosphere and placed on an automatic shaker until gelation was complete.

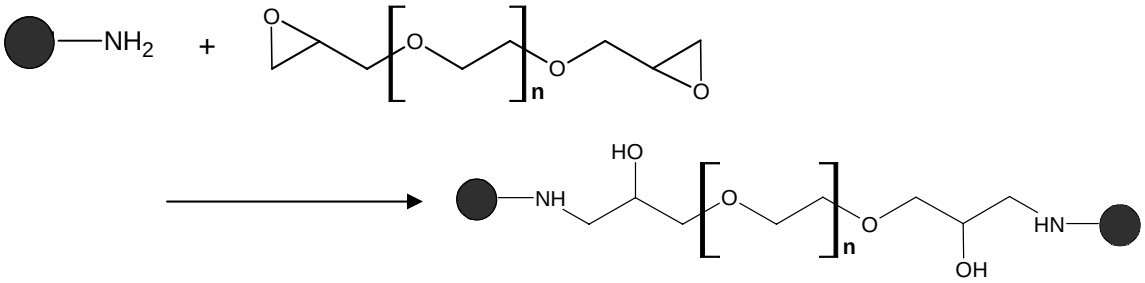

Figure 3-5: Crosslinking reaction between the amine end groups of a dendrimer and an epoxide of a poly(ethylene glycol 400 diglycidylether) crosslinking agent.

3.2.3. Swelling Studies

After initial gelation, hydro- and organogel samples were frozen in liquid nitrogen and then freeze dried overnight. Dry weights of the samples were then recorded, followed by addition of excess DI water or organic media to allow for swelling to occur. To achieve saturated conditions the samples were left submerged for a minimum of 48 hours, or until maximum swelling was observed. Water was exchanged daily to remove any solubles that might have leached from the gels. Upon reaching equilibrium conditions, excess water was removed and the samples patted down with moist filter paper. Weights of the swelled samples were then taken and recorded. The dry and

saturated weights were used to determine the swelling ratios of the gels. This process was repeated on the same samples to determine reproducibility as well as any physical effects such repetition may have on gel structure and performance. Gel swelling ratios (Q) were calculated using **Equation 3.1**, where w_e is the weight of the gel at saturation and w_o is the initial weight of the sample. The soluble fraction of a polymer network was also calculated by using **Equation 3.2**, where w_o is again the initial dry weight of the sample and w is dry weight of the gel after the extraction of solubles [107].

$$Q = \frac{w_e - w_o}{w_o} \tag{3.1}$$

$$S(\%) = 100\frac{w_o - w}{w_o} \tag{3.2}$$

3.3. Polymer/Gel Characterization

3.3.1. Elemental Analyzer

Chemical compositions were acquired through use of an elemental analyzer (Perkin Elmer Instruments, Series II CHNS/O Analyzer 2400). 1 to 2 mg of sample was used for data acquisition. Dendrimer samples were freeze-dried prior to analysis to remove any absorbed moisture, particularly in cases of dendrimer samples, which were found to absorb water quite readily.

3.3.2. Flash Chromatography and Thin Layer Chromatography (TLC)

Sample purification with flash chromatography was carried out with a Personal Flashmaster Plus system (Argonaut). ISOLUTE Flash SI pre-packed silica gel cartridges were used as the separation medium. Flow rates between 1 and 5 mL/min were typically used. Effluent was captured in 5 mL sample tubes. A rotary evaporator (Eyela) or high

vacuum gas manifold was used for solvent removal and product concentration. TLC was used for the determination of product separation. Plates of 1 x 4 inch dimension (Polygram® Sil G/UV_{254} (20 x 20 cm) pre-coated plastic sheets) were prepared and spotted with effluent samples, then placed in a development tank with applicable mobile phase. After developed plates were air dried, they were placed under UV light for spot detection. If fluorescence could not be adequately detected, additional staining methods were used, such as iodine chips or ninhydrin staining solution (1.5g ninhydrin in 100 mL *n*-butanol plus 3 mL acetic acid).

3.3.3. Fourier Transform Infra Red (FTIR) Analysis

FTIR spectra were collected using a Fourier Transform Infrared Spectrometer (Excalibur Series, BioRad Laboratories, FTS 135, USA) equipped with KBr beamsplitter and DTGS detector. Samples that were soluble were analyzed in a zinc-selenide (ZnSe) liquid cell holder, with chloroform used ($CHCl_3$) as the solvent and standard. Insolubles, including crosslinked gel samples, were analyzed in potassium bromide (KBr) pellet form, where KBr was used as the standard. Briefly, 0.1 grams of anhydrous FTIR grade KBr crystals were ground with small amounts of sample using a mortar and pestle. The resulting powder mixture was then pressed into pellet form at 4-6,000 psi of pressure.

3.3.4. Gel Permeation Chromatography (GPC)

Molecular weight analysis was investigated using a WATERS gel permeation chromatography system (isocratic HPLC pump 1515, RI detector 2414, dual wavelength absorbance detector 2487). PEG (for aqueous) or polystyrene (for organic) standards with narrow molecular weight distributions were used for calibration purposes. Both

aqueous (WATERS Ultrahydrogel linear) and organic (WATERS Styragel HR 4E, 5E and 6E (part number dependent on mobile phase)) columns (both 7.8 x 300 mm) were used for analysis. Mobile phases used include HPLC grade THF, ultra pure water (UPW) and UPW with 0.1% TFA. The system was operated at a flow rate of 1 mL/min at 30 ºC. Briefly, 3 mg of sample was dissolved in 1 mL of solvent and then filtered with 0.47 µm PTFE syringe filters (25 mm diameter, Alpha Analytical). An injection volume of 50 µL was used for analysis. Supplied software packages were used for data analysis.

3.3.5. High Pressure Liquid Chromatography Mass Spectrometry (HPLC-MS)

Advanced separation was performed using a Hewlett Packard 1100 HPLC system equipped with a HP quaternary pump (G1354A) and variable wavelength detector (G1314A). A UV detection wavelength of 210 nm was used for analysis. An Agilent Zorbax SB-C18 HPLC (4.6 x 150 mm, 5 µm) column was used. A mobile phase of 40%ACN with 0.14%TFA was used at a flowrate of 1 mL/min. An injection volume of 20 µL was used for sample runs. TFA was added to the mobile phase in order to act as a counterion to the positive charges present in the dendrimers, making dendrimer surfaces more hydrophobic. Previous studies performed by Islam et al. [108] on EDA-core PAMAM dendrimers indicate that no side reactions of the amide groups occur in the presence of excess TFA and that dendrimer particles are stable in solution at this TFA concentration. A mass spectrometer (HP Series 1100 MSD) was used for the acquisition of mass spectra of lower molecular weight samples (<3000 amu). Mass flowrate was reduced to 0.5 mL/min in LC-MS studies, using an injection volume of 5µL. All samples were filtered prior to analysis.

3.3.6. Laser Light Scattering (LLS)

A 90 Plus Particle Size Analyzer (Brookhaven Instruments Corp.) was used in LLS analysis for molecular size determination. Dendrimer samples were dissolved in ultrapure water or methanol at concentrations of 2 to 20 mg/mL and filtered (0.2 μm). Analysis was performed at a temperature of 23 °C and at readings of less than 100 kcps. 90 Plus particle sizing software was used for analysis of data.

3.3.7. Matrix Assisted Laser Desorption Ionization–Time of Flight–Mass Spectrometry (MALDI-TOF-MS)

Mass spectra of positively charged ions were recorded on a **m**atrix-**a**ssisted **l**aser **d**esorption **i**onization **t**ime-**o**f-**f**light (MALDI/TOF) mass spectrometer (Voyager STR by Applied Biosystems or AutoFlex II by Bruker Daltonics). Instruments were operated in the reflector mode for smaller molecules and linear mode for larger molecules. A total of fifty to several hundred single-shot spectra were accumulated from each sample, with acceleration voltage adjusted as necessary depending on the matrix solution used. Briefly, 0.5 μl of the sample solution (10mg/ml; 0.1% (v/v) trifluoroacetic acid (TFA) and 50% (v/v) acetonitrile (ACN) aqueous solution) were mixed with an equal volume of matrix solution (saturated α–cyano-4-hydroxycinnamic acid (CHCA) or sinapinic acid (SA), or 20 mg/ml 2,5-dihydroxybenzoic acid (DHB); in 0.1% (v/v) TFA and 50% (v/v) ACN aqueous solution) and spotted onto a MALDI target plate. Samples were allowed to air dry completely before analysis, allowing for proper crystal formation. A layer-by-layer methodology was performed for dendrimer samples in attempts to improve data acquisition [109]. Software packages provided by Bruker were used for data processing.

3.3.8. Nuclear Magnetic Resonance (NMR) Analysis

A Bruker ACF300 (300MHz) NMR spectrometer was used for ^{1}H and ^{13}C NMR analysis. Deuterated (D)-Chloroform ($CDCl_3$) (99.9 atom %D, Aldrich) was used as the solvent. 10 to 50 mg of sample (higher concentrations needed for ^{13}C analysis) was dissolved in 0.5 ml of solvent. Solutions were filtered with 0.47 μm PTFE syringe filters (25 mm diameter, Alpha Analytical) before being transferred to NMR tubes. Chemical shifts were expressed in parts per (δ) using residual protons in the indicated solvent as the internal standard. Manufacturer provided software was used for the processing of data.

3.3.9. Scanning Electron Microscopy (SEM)

External surface texture of polymer gels was observed using a Scanning Electron Microscope (JEOL, JSM-5600VL). The gels were freeze-dried using a Christ Alpha 1-4 freeze-drying apparatus, and mounted onto brass stubs using black double-sided adhesive tape. The mounted samples were vacuum-coated with a thin layer of platinum prior to examination using an Auto Fine coater (JEOL, JFC-1300) for 40 s.

3.3.10. Transmission Electron Microscopy (TEM)

TEM images were taken with a Jeol's JEM-2010 Transmission Electron Microscope. For sample preparation, dilute solutions of dendrimer were first prepared in DI water and methanol. A tiny droplet of solution was then placed onto a 200 mesh copper grid (formvar/carbon coated, Electron Microscopy Sciences) that was resting in the center of a piece of filter paper. After placement onto the disk, the droplet surface is broken, allowing excess solution to absorb into the filter paper while leaving behind only a thin layer of solution on the disk. The disks were then covered and allowed to dry

overnight. Addition of salts such as sodium and potassium chloride has been shown to improve TEM results by preventing charged dendrimer particles from clumping together [110].

3.3.11. Thermal Gravimetric Analysis (TGA)

Thermal properties of product samples were studied using either a Shimadzu DTG-60AH simultaneous DTA-TG apparatus or a TA instruments machine. Nitrogen was used as the purge gas in both instruments. Sample sizes ranged between 5 and 20 mg and were placed within a cleanly prepared aluminum pan. Analysis was performed using a temperature rise of 10 °C/min up to 750 °C. Data of weight loss and derivative of weight loss versus time were collected. Glass transition temperatures were determined using provided data analysis software of each instrument (Universal Analysis for TA instrument and TGA 60 for Shimadzu).

3.3.12. X-ray Photo Spectroscopy (XPS) Analysis

A Kratos XPS AXIS HSi spectrometer with aluminum K (alpha) x-ray source (1486.71 eV, 15 KV, 10 mA (150w)) was used for XPS analysis. Dried gel samples were carefully placed onto pieces of transparent glass using clear double-sided tape, which were in turn affixed to metal stubs. The laboratory officer in charge carried out further operation of sample analysis. Elemental analysis was carried out for carbon, nitrogen, and oxygen and the data was analyzed and processed using the Kratos software provided.

3.4. Cell Culture

3.4.1. Preparation of Culture Medium

Cell culture medium was prepared using Dulbecco's modified Eagle's medium (DMEM) (Gibco) supplemented with 10% inactivated fetal bovine serum (FBS) (Gibco), 100 mM sodium pyruvate (Sigma), 180 mM calcium chloride (Merck ACS), 1% antibiotic antimycotic solution (100 units/mL penicillin G, 100 µg/mL streptomycin sulfate, and 0.25 µg/mL amphotericin B) (Gibco), 1% non-essential amino acid solution (Sigma) and L-glutamine (Sigma). Prepared medium was stored at 0°C. Medium was heated to 37°C before use.

3.4.2. Human Liver Cell Line (Hep3B)

Human hepatocellular carcinoma cell line Hep3B (Cell Resource Center for Biomedical Research, Institute of Development, Aging and Cancer, Tohoku University) was used for cellular studies of liver functions on scaffolding materials.

3.4.2.1. Thawing & Storage Procedure

Cells stored in liquid nitrogen (cryo-storage tank) or at -80°C (ultra-low freezer) were thawed by placing in a 37°C water bath for thirty seconds. In order to remove the cryopreservative, the cell suspension was added to fresh medium and centrifuged at 1500 rpm for 5 min, after which, the solution phase was aspirated. At this point, fresh medium was added and the cell suspension transferred to T-flasks in appropriate concentrations for culturing.

For storage purposes, the cells were first formed into a pellet by centrifugation. After aspirating the medium, a cryopreservative (10% DMSO solution, or serum free cell

freezing medium) is added to protect the cells from disruption during the thawing and freezing processes. The freezing process is done in a step-wise fashion, 0°C to -20°C to -80°C (Ultra low temperature freezer, Nuaire, NU-6580), to prevent excess shock to the cells. The cells are either kept at -80°C for short term storage, or transferred to liquid nitrogen for long-term storage. Vial concentrations are between 2 and 4 x 10^7 cells/mL.

3.4.2.2. Subculture

Cellular proliferation was observed daily with an inverted microscope. Culture medium was changed on average every three days, unless significant color change of medium was observed (red to yellow). Cells were subcultured upon reaching 90% confluence. First, several milliliters of sterilized PBS solution was used to wash the culture flask. 2-3 mL of a trypsin/EDTA solution (Gibco) were then added, and the flask incubated for 3 min at 37°C. Gentle shaking may be required to fully detach all the cells, which must be done with care to avoid causing excessive cellular damage. 5 mL of fresh medium were then added and the resulting cell suspension transferred into a centrifuge tube for centrifugation at 1500 rpm for 10 min. The supernatant was aspirated to remove the trypsin and 6 mL of fresh medium was added. The resulting cell suspension was mixed thoroughly and divided equally among three new subculturing flasks. The number of cell passage should be noted as a way to keep track of subculture activities.

3.4.2.3. Cell Seeding On/In Polymer Gels

Cells were seeded onto previously prepared gels in 96-well plates at a concentration of 1x10^4 cells per well. For saturated gel samples, 200 µL of media were added to each well. If dried samples were used, 250 µL of media were added on the first

day to compensate for swelling, with 200 µL of media added from the first refreshing of media onwards.

3.4.2.4. Cell Fixation

Cells were affixed to sample/plate surfaces by treatment with 37% formal-calcium or 3% glutaraldehyde solutions. Exposure times of 2-4 minutes for formal-calcium and 1-2 hours for glutaraldehyde were used [111]. Specimens were washed three times with PBS solution before and after treatment.

3.4.3. Cell Viability Tests

3.4.3.1. Hemacytometer Cell Counting

In order to determine cell densities for use in cellular studies, the Hemacytometer method was used. 100 µL of a prepared cell suspension were mixed with an equal volume portion of 0.4% trypan blue solution (Sigma). The trypan blue serves as a means to differentiate live cells from dead cells, with only the dead cells being stained. Viable cells are observed with only a dark outline. 20 µL of this prepared cell mixture were then placed onto the hemacytometer (Hausser Scientific, USA). An inverted microscope (Leica) was used to make the cell counts. The hemacytometer is divided into two large chambers, each consisting of nine large squares that are further subdivided into smaller squares that are used for cell counting (see **Figure 3-6**). Four of the nine large squares are used for cell counting with an additional fifth square, not

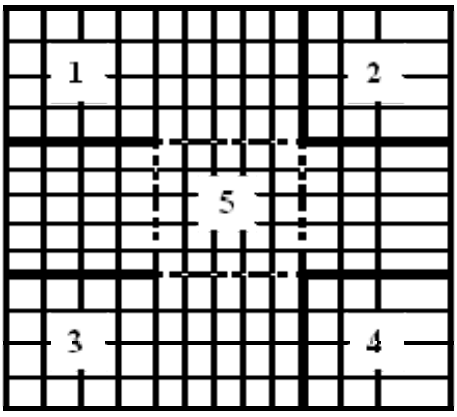

Figure 3-6: Layout of a single hemacytometer chamber

utilized in these studies, also available for use. The total number of cells is counted for each large square and the average number for each chamber is determined. If the averages differ by more than 20% the test is performed again. Percent viability and viable cells per milliliter of suspension were calculated [112]. For the performed methodology, a dilution factor of 2 was used in **Equation 3.4**.

$$\%Viability = \frac{number\ \ of\ \ live\ \ cells}{total\ \ number\ \ of\ \ cells}\ \ x\ \ 100 \tag{3.3}$$

$$\frac{Viable\ \ cells}{mL} = \frac{average\ \ live\ \ cells}{mm^2}\ \ x\ \ 10^4\ \ x\ \ dilution\ \ factor \tag{3.4}$$

3.4.3.2. MTT Assay

To assess cell proliferation and cell viability in response to external factors, an MTT (3-(4, 5-dimethylthiazolyl-2)-2, 5-diphenyltetrazolium bromide) assay was performed. This assay measures dehydrogenase activity of viable cells, which reduce the yellow tetrazolium MTT to purple formazon. Starting from a cultured 64-well plate of test samples (including control wells), the cells (Hep3B) were washed twice with PBS solution, followed by addition of 200 µL serum-free DMEM solution. 20 µL of MTT solution (5 mg MTT (Duchefa 98.5%)/ ml PBS) were then added to each well, and the plate incubated for 2 to 4 hours at 37°C and 5% CO_2. As MTT is light sensitive, this process should be carried out as quickly as possible. After reaction, unreacted MTT along with the medium was aspirated from the wells and the wells washed twice with PBS solution. 200 µL of DMSO were then added and the plate gently shaken in the dark for 15 minutes. This serves to lyse the cells as well as dissolve the formed formazon crystals. A microplate reader (GENios, XFluor4 software) was used to take

spectrophotometric readings of the wells, using a test wavelength of 570 nm and a reference of 620 nm. DMSO was used as a blank [113]. The average of the blank readings was used as a zero standard and subtracted from all other sample readings.

3.4.4. Direct Contact Cytotoxicity Test (ISO 10993-5)

3.4.4.1. Material Preparation

Polymer gels were crosslinked in 64-well plates and then freeze-dried to acquire circular-shaped samples. A 2 mm thick polyethylene (PE) film was used as a negative control, and a 0.5 mm thick polyurethane (PU) film containing 0.25% zinc butyldithiocarbamate (ZDBC) as a positive control. The gels were washed with 70% ethanol, DI water, and PBS five times each, and sterilized overnight under UV light.

Required solutions include culture medium, neutral red solution and formal-calcium solution. The culture medium used consisted of DMEM supplemented with 10% FBS, 1% non-essential amino acid solution (Sigma), 100 mM sodium pyruvate, 2 mM L-Glutamine and 1.5 g/L sodium bicarbonate. Neutral red solution was prepared by diluting neutral red dye (CI 50040) to a concentration of 50 μL/mL of medium. The solution was allowed to stand for 24 hours in the dark and then centrifuged at 1500 rpm for 5 minutes to remove undissolved crystals before use. Formal-calcium solution was prepared by mixing 10 mL of 10% calcium chloride and 10 mL of 37% formaldehyde (J. T. Baker) into 80 mL of DI water.

3.4.4.2. L929 Cell Line

Mouse fibroblast cell line L929, NCTC clone 929 of strain L, (ATCC, CCL-1, USA) was seeded in 6-well culture plates at a suspension density of 1 x 10^5 cells/well in 3

mL of medium. Cells were incubated at 37°C and 5% CO_2 until 90% confluence was reached. Medium was changed daily. Once subconfluency was reached the medium was removed and material test samples placed in the center of the wells, directly on top of the cell monolayer. Samples should cover approximately 10% of the well surface area [114]. Care should be taken in sample placement so as not to cause significant cell damage or displacement. Cells were cultured under conditions of sample exposure for a period of 2 to 7 days.

3.4.4.3. Analysis

After culturing for the designated time period, the medium and samples were removed from the culture plate and inhibition zones marked on the bottom side of the plate with permanent marker. The cells were washed with PBS and then subjected to 4 mL of prepared neutral red solution, incubating for an additional 3 hours. NR solution was then aspirated and the cells washed with 4 mL of formal-calcium solution for 2-3 minutes. Formal-calcium was used as a fixative to fixate the cells onto the culture plate. Exposure time is kept to a minimum to avoid excessive cellular damage. Culture plates were then left to air dry for final analysis. Cytotoxicity was calculated using **Equation 3.5**, where S is the diameter of the sample inhibition zone and N is the diameter of the negative control inhibition zone, taking the average of triplicate samples.

$$\%Cytotoxicity = \frac{S - N}{N} x100 \tag{3.5}$$

3.4.5. Functionality Tests

3.4.5.1. EROD Assay

The EROD (7-ethoxyresorufin-*o*-deethylase) assay serves to determine cytochrome P450 activity within cells. This enzyme undergoes deethylation in the presence of NADPH produced by the cell, and oxygen. Pre-sterilized samples were placed in a 64-well culture plate and seeded at $1x10^4$ cells/well. After predetermined cultivation times were attained, medium was aspirated and the wells washed twice with PBS solution. 100 µL of PBS containing 5 mM 70ethoxyresorufin and 10 mM dicumerol (3,3'-methylene-bis(4-hydroxycoumarin)) was added to each well, and the culture plate incubated for 4 hours. 100 µL of 1M sodium hydroxide solution was then added and the culture plate placed in the dark for 30 minutes to lyse the cells. A microplate reader (GENios or Tecan infiniteM200) was used to take readings of the enzyme fluorescence, using a test wavelength of 530 nm and a reference of 590 nm. A resorufin standard curve was used to determine the P450 activity of the cells. For preservation of cells involved in longer-term studies, no sodium hydroxide solution was added. Medium was instead taken directly as is for analysis.

3.4.5.2. Human Albumin ELISA Assay

The enzyme-linked immunosorbent assay (ELISA) (Human albumin ELISA quantitation kit, Bethyl Laboratories, Inc., E80-129) is used to quantitatively measure albumin secretion, in this case by Hep3B cells. Test samples are samples of medium aspirated from wells during incubation periods. The samples were centrifuged at 15,000 rpm for 5 min and filtered with 0.45 µm PTFE filters to remove any remaining solids

from solution. Samples were stored at -20°C until use. The assay consists of 5 steps. *Step1*: 1 µL capture antibody (goat anti-human albumin-affinity purified) was diluted to 100 µL of coating buffer (0.05 M bicarbonate solution) for each well (96-well plate) to be used and incubated for 60 minutes. After incubation, the coating solution was aspirated and the wells washed three times each with wash solution (50 mM Tris, 0.14 M NaCl, 0.05% Tween 20, pH 8.0). *Step2*: 200 µL of blocking solution (50 mM Tris, 0.14 M NaCl, 1% bovine serum albumin (BSA), pH 8.0) were added to each well and incubated for 30 minutes. After incubation the blocking solution was removed and the wells were washed three times each with washing solution. *Step3*: Standards were prepared by diluting calibrator (human reference serum) in sample diluent (50 mM Tris, 0.14 M NaCl, 1% BSA, 0.05% Tween 20, pH 8.0) to concentrations of 400, 200, 100, 50, 25, 12.5 and 6.25 ng/mL. 100 µL of standards and samples were then added to treated wells and incubated for 60 minutes. After incubation solutions were aspirated and wells washed five times each with washing solution. *Step4*: 100 µL of HRP conjugate (goat anti-human albumin-HRP conjugate) in sample diluent (1:70,000) was added to each well and incubated for 60 minutes. After incubation the conjugate solution was removed and the wells washed 5 times each with washing solution. *Step5*: 100 µL of [3,3',5',5-tetramethylbenzidine] (TMB) (Sigma) was added to each well and incubated for 30 minutes. TMB reaction was terminated by addition of 100 µL of stopping solution (2 M H_2SO_4). A microplate reader was used to take absorbance readings using a test wavelength of 450 nm and a reference of 620 nm.

3.4.6. Live/Dead Assay

Hep3B cells were cultured on test samples at a seeding density of 1 x 10^4 cells/mL. Medium was refreshed prior to the assay. 100 µL of live/dead solution were added to each well and the culture plate kept in the dark for 1 hour at room temperature. Two different live/dead solutions were used over the course of study; 1. 20 µL of ethidium homodimer (EthD) and 10 µL of calcein AM in 10 mL of PBS; 2. 2 µL each of DEAD Red stain and SYTO 10 nucleic Acid stain (Molecular Probes Live/Dead Reduced Biohazard cell viability kit #1) per mL of HBSS. In the latter case, samples were washed three times each with HBSS prior to and after the addition of staining solution. HBSS was also used in place of sample medium. An inverted Leica microscope fitted with a halogen lamp and appropriate filters was used to view live (green) and dead (red) cell fluorescence.

3.5. Additional Studies

3.5.1. One-Pot Conversion of an Alcohol to Amine – Carbohydrates

Carbohydrate (D-(+)-Galactose), PPh_3, and sodium azide (99%, Merck) were added to a solution of DMF-CCl_4 (carbon tetrachloride) (4:1). The solution was heated to 70°C under reflux for 4 hours. DI water was then added to complete the reaction. An equal volume of diethyl ether was added and the solution mixed thoroughly for an additional ten minutes. The ether layer was then removed and concentrated to obtain crude product. [115]

3.5.2. End-Group Modification of Trehalose – Reaction with Hydroxyls

Fmoc-glycine-OH (Nova Biochem) was reacted with D-(+)-trehalose (α-D-glucopyranosyl-α-D-glucopyranoside) in a coupling reaction using DCC (5.5 molar equivalents) in DMF for 48 hours. NHS can also be added in addition to DCC to speed up reaction times. After reaction, the solution was filtered to remove precipitated byproduct. Piperidine was then added to cleave protecting groups, mixing for 30 min. The final product was concentrated under high vacuum and mass spectrum taken (MALDI-TOF-MS).

3.5.3. Glycodendrimer Reaction with a Peptide-Based Dendron

The zero generation galactose-centered PAMAM dendrimer was reacted in a coupling procedure using DCC and NHS with G2 dendrons of lysine-lysine-glycine-Fmoc structure in DMF. The solution was allowed to react for 24 hours under vigorous mixing (vortex mixer). Upon completion of reaction, piperidine was added to cleave the protecting groups. Product was then concentrated under high vacuum and mass spectra taken (MALDI-TOF-MS).

CHAPTER 4: DENDRIMER SYNTHESIS

4.1. Introduction

The advance and modification of polymer chemistries is an ongoing science to develop materials with ever superior properties and performance. Dendrimers are a unique family of polymers that have displayed a number of advantageous properties over conventional linear and hyperbranched polymers; while having only been first discovered about thirty years ago and still being a fairly new area of materials study. These materials consist of tree-like branching units with a central core; offering a high degree of control over their size and shape, large numbers of end groups for reaction or modification, as well as additional characteristics such as encapsulation ability as a result of their spherical/globular tending structures. Such properties have already demonstrated usefulness in the areas of sensory devices [116, 117] and as gene and DNA [118, 119] transfer agents. Given the current use of dendrimers in the biological fields, there is also believed to be great potential in utilizing their properties in the area of tissue engineering. Here, a galactose-centered PAMAM dendrimer is synthesized for future use as a scaffold material for culturing liver cells. The dendrimer is synthesized to generation four and then surface modified with a galactose moiety for improved biocompatibility in cellular applications.

4.2. Results

4.2.1. Scheme-1 Dendrimer Synthesis

4.2.1.1. Glycosylation & Allylation

In order to acquire like chain ends on all five arms of galactose, Fischer glycosylation was first utilized to react the more stable hydroxyl located off the anomeric carbon, which is stabilized by its bonding to two oxygen atoms. This reaction takes advantage of the carbocation forming ability of the anomeric carbon by reaction with an acid. A color change in solution of clear to yellow was observed over the course of reaction, with a yellow syrup acquired as the final product. Crude product was used directly in further reaction.

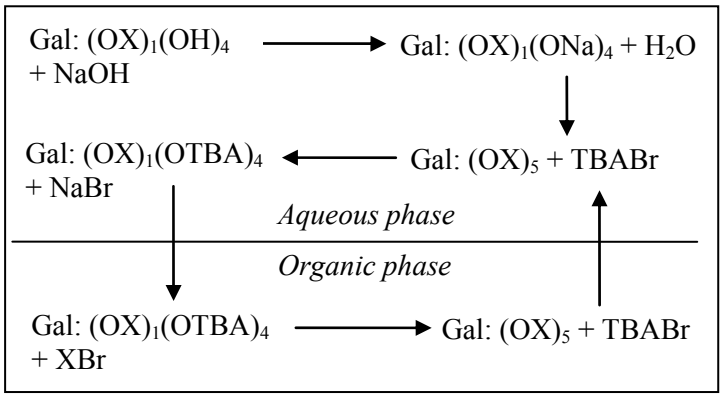

Figure 4-1: Allylation mechanism. Galactose is the core containing five end groups (X = allyl).

The remaining hydroxyls were then reacted in a phase transfer catalysis reaction (allylation) with allyl bromide, using TBABr as the catalyst (see **Figure 4-1**). Temperatures were kept in a moderate range in order to prevent degradation of the carbohydrate. Incomplete conversion of end groups resulted in reactions ran at temperatures lower than 50 °C. Adequate washing of the organic phase with water was necessary to ensure complete removal of TBABr salts from the product. An overall yield

of 74% was found for *Steps 1* and *2*. An FTIR spectrum of allylated product reveals vinyl C=C peaks at 1647 and 3086 and the absence of an OH band, indicating that complete conversion of galactose hydroxyl groups had been obtained. A mass peak of 377 (calc. 380.47) was obtained in MALDI-TOF-MS. Acquired elemental analysis data supports theoretically calculated values [calculated: C, 66.29; H, 8.48; O, 25.23, found: C, 64.02; H, 8.34; O, 27.64]. NMR: δ_H 300 MHz, $CDCl_3$; 5.8-6.0 (5H, $-OCH_2C\mathbf{H}CHO_2$), 4.9-5.4 (10H, $-OCH_2CHC\mathbf{H_2}$, 1H, $-CHC\mathbf{H_2}O-$), 3.8-4.4 (10H, $-OC\mathbf{H_2}CHCH_2$), 3.5-3.7 (2H, $-C\mathbf{H_2}OCH_2CHCH_2$, 2H from sugar ring) Additional 3H from sugar ring are predicted to be at 3+, 4+, and 5+ positions but are not distinguishable in spectra. δ_C; 134-136 (5C, $-OCH_2\mathbf{C}HCH_2$), 116-118 (5C, $-OCH_2CH\mathbf{C}H_2$), 96 (1C, anomeric), 68-80 (10C; 5C, $-O\mathbf{C}H_2CHCH_2$, 1C, $-\mathbf{C}H_2OCH_2CHCH_2$, 4C from sugar ring).

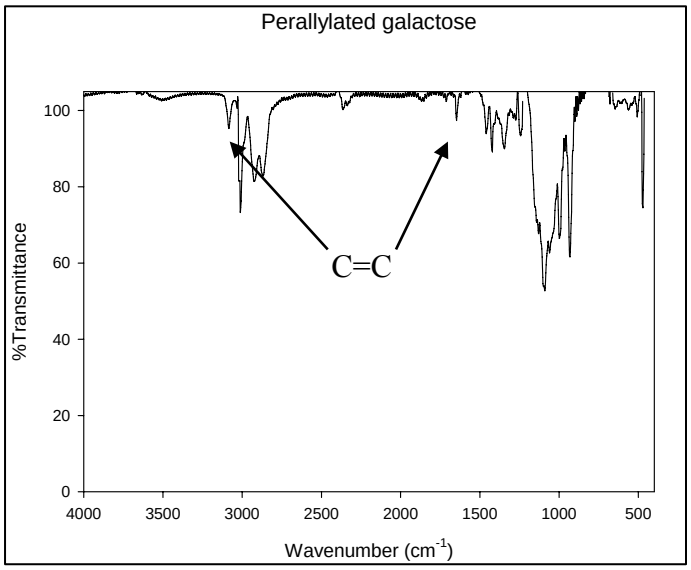

Figure 4-2: FTIR spectrum of perallylated galactose

4.2.1.2. Hydroboration/Oxidation

A borane-THF complex was initially used for hydroboration reaction, but it was observed to form an organogel when reacted with **3** in THF. As an alternative, 9-BBN was used. **3** was freeze dried prior to use to ensure maximum removal of water, as both

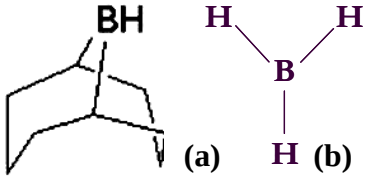

Figure 4-3: Structures of (a) BBN and (b) borane

borane and 9-BBN are moisture sensitive, which also required the reaction to be run under nitrogen. Due to the exothermic nature of the oxidation reaction, the temperature was monitored and kept below 40°C using an ice bath during the addition of H_2O_2. Light yellow syrup was attained as the final product in 65% yield. A crystalline solid was found as the major byproduct that was determined to be 1,5-cyclooctanediol through elemental analysis [calculated: C, 66.63; H, 11.18; O, 22.19, found: C, 66.64; H, 11.71; O, 21.65]. FTIR spectra of the product displayed a large hydroxyl peak from 3200-3600 and the loss of the C=C peaks. MALDI: [calculated: 470.5; found: 475.1863] Elemental analysis: [calculated: C, 53.60; H, 8.90; O, 37.40, found: C, 55.25; H, 9.73; O, 35.02] NMR: δ_H 300 MHz, $CDCl_3$; 1.5-2.0 (10H, -$OCH_2C\mathbf{H_2}CH_2OH$, 5H, - $OCH_2CH_2CH_2O\mathbf{H}$), 3.4-3.9 (10H, - $OC\mathbf{H_2}CH_2CH_2OH$, 10H, - $OCH_2CH_2C\mathbf{H_2}OH$, 3H from sugar ring), 4.2-4.3 (1H from sugar ring), 5.0-5.1 (1H from sugar ring). MS spectra can be found in **Appendix A**.

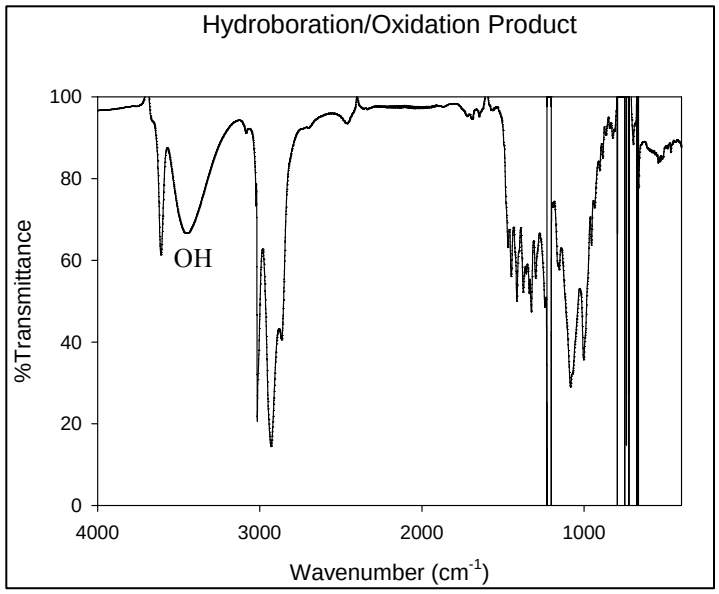

Figure 4-4: FTIR spectrum of hydroboration/oxidation product.

4.2.1.3. Appel Reaction & Gabriel Synthesis

Halogenation was accomplished through the Appel reaction [120] with product attained in 70% yield. As this reaction is exothermic, carbon tetrachloride was added in a stepwise fashion to avoid overheating of the solution. Orange colored syrup was found as

the final product. Triphenylphosphine oxide was separated out as a white crystalline byproduct [elemental analysis: calc. – C, 77.69; H, 5.43, found – C, 76.98; H, 5.27]. A loss of the hydroxyl peak and the emergence of an HBr peak at 540 were observed in FTIR spectra and MALDI-TOF-MS gave a mass peak at 784.1 (calc. 785) (see **Appendix A.1**).

The final conversion of bromine to amine was performed in two steps [121]. The first step was nucleophilic substitution of bromide with phthalimide (PhthN), resulting in a light yellow solid at 92% yield. FTIR spectra showed a strong C=O peak at 1750 as well as an amine peak at 3450. [Elemental analysis: calc. – C, 65.64; H, 5.15; N, 6.27, found – C, 67.70; H, 4.30; N, 5.94] NMR: δ_H 300 MHz, $CDCl_3$; 1.8-2.0 (10H, -$OCH_2C\mathbf{H_2}CH_2N$-), 3.6-4.0 (10H, -$OC\mathbf{H_2}CH_2CH_2N$-, 10H, -$OCH_2CH_2C\mathbf{H_2}N$-, 3H, sugar ring, 2H, -$CHC\mathbf{H_2}O$-), 4.2 (1H, sugar ring), 5.0 (1H, sugar ring), 7.4-7.9 (20H, aryl)]. The second step was hydrazinolysis, which replaced PhthN with an amine group. Again, yellow syrup was found as the final product at 60% yield. A broad medium intensity amine peak is observed in FTIR spectra at 3400 as well as the loss of the C=O peak. A mass peak at 463.88 (calc. 465.64) was obtained in mass analysis.

4.2.2. Scheme-2 Dendrimer Synthesis

4.2.2.1. Ozonolysis

Upon completion of ozonolysis, the product was concentrated, dissolved in aqueous solution and filtered to remove excess triphenylphosphine and triphenylphosphine oxide. The product was observed to be a transparent, slightly yellow solid. Crude product was used directly in subsequent reactions.

4.2.2.2. Reductive Amination

Reductive amination was performed in two steps due to encountered solubility constraints. The second step involving the addition of $NaBH(OAc)_3$ had to be carefully maintained at -10 °C, as the solution was observed to foam at warmer temperatures. The final product was observed to be a light yellow syrup at 76% yield. FTIR spectra revealed aromatic peaks at 698, 3020 and 1600 as well as an –NH– peak at 1500. MALDI-TOF-MS gave a mass peak at 1295.22 (calc. 1296) (see **Figure A-5** in Appendix A). Elemental analysis [calculated: C, 79.66; H, 7.54; N, 5.40, found: C, 80.97; H, 7.30; N, 6.09] NMR: δ_H 300 MHz, $CDCl_3$; 7.0-7.5 (50H, benzene rings), 3.3-3.9 (20H, -$N(C\mathbf{H_2}C_6H_5)_2$, 10H, -$OC\mathbf{H_2}CH_2N(CH_2C_6H_5)_2$, 2H, -$C\mathbf{H_2}OCH_2CH_2N(CH_2C_6H_5)_2$, 5H from sugar ring), 2.5-2.9 (10H, - $OCH_2C\mathbf{H_2}N(CH_2C_6H_5)_2$).

4.2.2.3. Heterogeneous Catalytic Transfer Hydrogenation

In the heterogeneous catalytic transfer hydrogenation reaction, addition of palladium catalyst to methanol was performed carefully under nitrogen. Cooling water temperature was adjusted appropriately, as temperatures too low resulted in the solidification of ammonium formate in the condenser. Upon completion of reaction the solution temperature was allowed to cool, resulting in the crystallization of ammonium

formate which was then removed by filtration. After concentrating the filtrate under vacuum, the remaining product was dissolved in THF and again filtered to remove any remaining ammonium formate. The final product was a yellow colored crystalline solid (72% yield). FTIR spectra showed an amine peak at 3500 and the loss of the aromatic alkene peaks. MALDI-TOF-MS gave a mass peak of 396.36 (calc. 395.5) (see Appendix A, **Figure A-7**).

4.2.3. PAMAM Synthesis

Increasing dendrimer generations resulted in thick syrupy materials. Full generations were found to be thick yellow syrups, with color intensities observed to decrease at higher generations. Half-generation products were observed to be more fluid, while possessing a much darker color. Yields were taken to be quantitative. Mass peaks were difficult to obtain for many of the dendrimers using MALDI-TOF-MS. For this reason, mass gains after reactions and the full removal of solvent in conjunction with other analytical methods such as LLS were used to help ascertain degrees of reaction.

FTIR spectra of a G4 dendrimer revealed a broad amine peak from 3100-3300 cm^{-1} as well as a strong carboxyl peak at 1650 cm^{-1}. These peaks are representative of the large number of amine end groups and the numerous carboxyl groups present within the branching arm units of the dendrimer. A slight increase in amine versus carboxyl peak ratio was observed for increasing dendrimer generations.

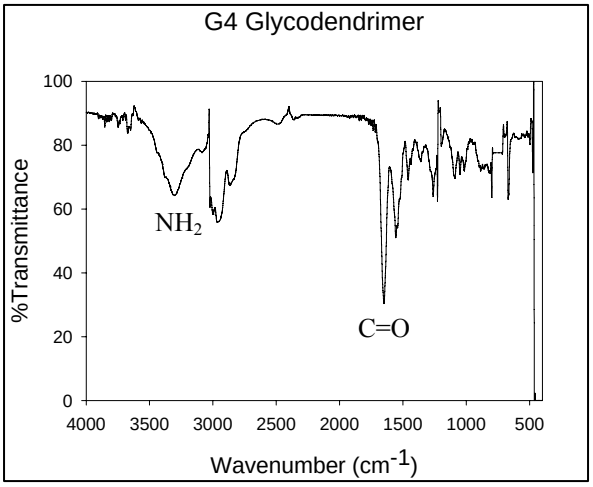

Figure 4-5: FTIR spectrum of G4 glycodendrimer

NMR analysis performed on different dendrimer generations illustrated distinctive and recurring peaks between half and full-generation materials. Strong 1H peaks at 7.0-7.5 (–0-CH_3–) and 13C peaks at 75-80 (–CH_3–O–CO–) were observed for half generation particles, and 1H peaks at 3.1-3.3 (-NH_2) and 13C peaks at 40-43 (R–CH_2–NH_2) for full generations.

As seen **Table 4-1**, TGA analysis revealed increasing glass transition temperatures (T_g) for higher generations of both half and full generation dendrimers, with values appearing to begin leveling off at higher generations.

Table 4-1: TGA analysis of full and half-generation glycodendrimers

Sample	Tg (°C)	Sample	Tg-2 (°C)
G2.5	217	**G3**	276
G3.5	231	**G4**	284
		G5	286

4.3. Surface Modification

Introduction of galactose onto dendrimer surfaces resulted in yellow to orange colored solids that were more solid in nature in comparison to the syrupy states unmodified dendrimers. These solids were observed to absorb a considerable amount of water over time, signified by samples becoming more liquid in nature. 25 and 50% reaction of dendrimer surface groups were conducted, with actual conversions of 23 and 46% calculated from collected DCU and NHS byproduct. These materials will be referred to as GXM25 and GXM50, where X is dendrimer generation. Modified dendrimers were also found to be insoluble in organic solutions of methanol, a further indication that the desired reaction did take place; as unreacted dendrimers would be soluble in methanol, the solvent in which they were originally synthesized.

The emergence of a large hydroxyl peak from 3000-3500 cm^{-1} was observed in FTIR analysis. An increasing hydroxyl to carboxyl peak ratio was also exhibited for increasing levels of surface modification. This is representative of the increasing carbohydrate presence on the dendrimer surface.

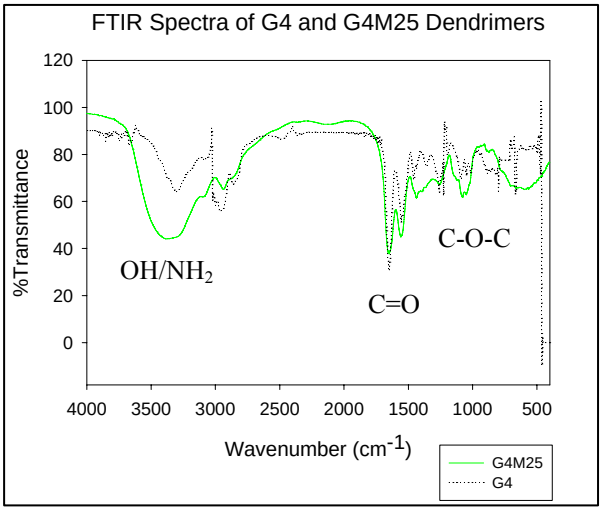

Figure 4-6: FTIR spectra comparison between un/modified G4 glycodendrimers

TGA analysis on surface modified dendrimers found two major slopes of degradation. T_g values were found to range between 200 and 400 °C, with values increasing for higher concentrations of surface modification. Percent weight loss

corresponding to the lower of the two values was also observed to increase for enhanced surface modification (see **Table 4-2**), indicating that these values most likely relate to the surface sugar groups.

Table 4-2: TGA data of G4 surface modified dendrimers

Sample	Tg-1 (°C)	Tg-2 (°C)	Weight Loss Ratio (T_g-1:T_g-2)
G4M25	227	399	1.42
G4M50	234	403	1.07
G5M25	231	406	1.74
G5M50	229	408	1.16

4.4. Additional Analysis

Laser light scattering results on dendrimer particles indicate a slight increase in particle size for increasing generations and surface modification. Average sizes of full generation dendrimers and selected surface modified dendrimers can be found in **Table 4-3** below.

Table 4-3: LLS data for dendrimer particles

Sample	Particle size (nm)	Sample	Particle size (nm)
G3	1	**G5M25**	5
G4	2	**G5M50**	5
G5	4		

*acquired in aqueous solution

TEM visualization of unmodified dendrimers revealed sample particles clumped together into large masses, making individual particle identification difficult. A large

number of spherically shaped bodies do appear within the clumped masses. This clumping problem did not initially appear as prevalent in modified dendrimer samples, where a number of spheres were observed (see **Figure 4-7**). Given the size of the observed particles however (20-100 nm) even these should consist of a number of grouped particles.

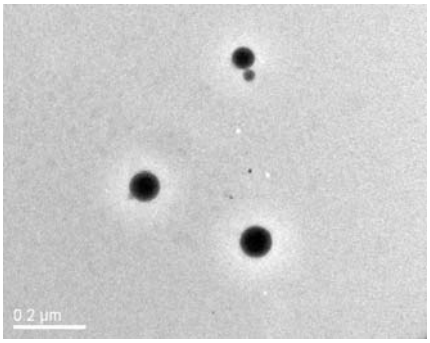

Figure 4-7: TEM image of G4-M50 dendrimer particles

Advanced separation and mass analysis by means of HPLC-MS was performed on selected lower molecular weight sample products, mainly of those involved in core preparation syntheses. Selected data is shown in **Table 4.4** below. The acquired MS data matched quite closely to that obtained in MALDI-TOF-MS, particularly for products **4** and **11**.

Table 4-4: HPLC-MS data for low MW products

Sample	Elution Time (min)	Mass Peak
Product 4	15.5	475.2
Product 7	11.0	455.0
Product 11	12.0	398.2

4.5. Discussion

Galactose-centered cores containing five amine terminated branching arms were obtained using both methods of synthesis. *Scheme 2* methodology, however, was found to be superior in terms of obtained yields (~40% vs. ~20% for *Scheme 1*) and overall reaction time, with less intensive purification requirements. *Scheme 2* was therefore

chosen as the pathway of choice and was used for all further product synthesis for experimentation and analysis.

Both reaction pathways possessed their own positive and negative features. *Scheme 2*, for example, although shorter involved a higher degree of hazardous materials and more extreme reaction conditions in terms of temperature requirements. *Scheme 1* on the other hand, consisted of reactions that were mainly run at room temperature but required longer reaction times and a few more steps. The most limiting aspect of *Scheme 1* however, was the purification that was needed in each step, including the evaporation of more difficult solvents such as DMF.

The crosslinking that occurred between borane-THF complex and **3** is thought to result from both molecules being multifunctional, having 3 and 5 reactive sites respectively. This could allow for a number of interconnecting bonds to arise between adjacent particles. Use of excess solvent may have prevented crosslinking from occurring, but accomplishing complete reaction would be difficult due to the steric hindrance that would arise upon two carbohydrates reacting with the same borane molecule. For this reason a large excess of reactant would also be necessary to ensure complete reaction, resulting in low efficiency in terms of use of reactant. As an alternative, crosslinking was prevented through the use of 9-BBN, which is a monofunctional molecule and thus capable of forming only a single bond. The obtained organogel and would have basically been boron crosslinked sugar molecules. The gel was observed to be translucent and spongy.

Analysis of dendrimer products proved to be somewhat difficult. Higher generations, in particular, were found to be somewhat ineffective in terms of mass analysis, with only broad peaks obtained in MALDI analysis. This may be due to several

factors, including the presence of impurities in the product samples that may interfere with the ionization process, particle fragmentation or matrix compatibility issues. Of particular difficulty was getting matrix components to crystallize with dendrimer samples. PAMAM type dendrimers are also noted to become protonated in and have been previously reported to form complexes with water, which can further complicate their analysis [122]. Although synthesized beyond G4, mass peak were not acquired for larger particles.

As reported in other studies on various dendrimer molecules [123, 124], these synthesized glycodendrimers displayed a similar trend of higher glass transition temperatures for increasing generations. T_g values indicate a leveling off between G4 and G5 dendrimers. Additional data performed on higher generation particles must be collected to confirm this. The observed increase in T_g values (for both full and half-generation dendrimers) can also be taken as an indicator that the dendrimer particles were in fact undergoing reaction and increasing in size. The observation of a single transition in TGA analysis also indicates a fairly uniform product, with multiple degradation peaks expected for a product consisting of different or unreacted products (unless they are of the same components and structures of the main product).

Particle size data from LLS analysis is comparable to that found in studies performed on EDA centered PAMAM dendrimers, which have reported sizes of 1.7 to 3.0 nm for G4-G6 dendrimer particles [125]. The slightly larger acquired particle sizes of 1.3 to 4 nm for G3-G5 dendrimers are feasible given that these dendrimers consist of a larger core and a larger number of end groups which leads to a faster growth rate. Sizes for dendrimers smaller than G3 were not obtained due to instrument limitations. A comparison between numbers of endgroups present in different generations of

conventional and synthesized glycodendrimers is found in **Table 4-5**. As viewed from this table, conventional dendrimers run slightly over 1 generation behind the glycodendrimers in terms of the number of endgroups they possess.

Table 4-5: Endgroups comparisons between dendrimers

Convention (EDA core)		*Glycodendrimer*	
Generation	**Number of Endgroups**	**Generation**	**Number of Endgroups**
G4	32	**G3**	40
G5	64	**G4**	80
G6	128	**G5**	160

4.6. Conclusions

A galactose-centered PAMAM glycodendrimer was synthesized through a series of chemical reactions. Dendrimer core molecules were prepared using two different reaction pathways, with the second scheme found to be more simplistic in terms of necessary purification work, required less overall reaction time as well as resulted in a higher overall yield. The obtained dendrimer nanoparticles were surface modified with a galactose moiety using a zero-length crosslinking reaction to improve material biocompatibility for future use. Size and thermal behavior were found comparable to and in accordance with properties of similarly reported dendrimers. Synthesized particles are intended for future use in scaffold materials for cell culture support. Possessing large numbers of reactive end groups, these materials are thought to be able to induce significant cell-scaffold interactions to enhance and sustain cell survival and function.

4.7. Future Work and Recommendations

- As is the case in all dendrimer syntheses, a large number of reactions were required for polymer preparation. It is recommended that additional reaction sequences be studied in order to decrease the total number of necessary reactions as well as total reaction times. Several possibilities will be discussed in future chapters of this work.

- One alternate method considered for core preparation was through utilization of 'click chemistry' [126]. Although not attempted, it is theoretically feasible. Similar to *scheme-1* and *2*, the initial two reaction steps would be identical to those of glycosylation and allylation, with the exceptions of replacing allyl alcohol with propargyl alcohol and allyl bromide with propargyl bromide. The final step would involve reaction with an azide-amine using copper sulfate and sodium ascorbate in a butanol-water (1:1) solution. This would allow for the attainment of amine end groups on a galactose core in only three steps. The main obstacle would be finding a cost-effective azide-amine reactant for the final reaction.

- These synthesized glycodendrimer nanoparticles will be further used in the construction of scaffold materials for use in Hep3B hepatocyte cultures. This work will be discussed in subsequent chapters.

- Alternative ligands could also be used in place of or in addition to lactobionic acid for dendrimer surface modification. Of particular interest would be small peptide groups, such as RGD and YIGSR that have also been shown have positive effects on cellular interactions and function.

CHAPTER 5: GEL FORMATION

5.1. Introduction

Scaffold design is an intrinsic part of developing materials for use in tissue engineering. This is particularly true when involving anchorage dependent cells such as hepatocytes, which exhibit a loss of function and survival when detached from a surface for even a short period of time. Material makeup, surface properties, as well as dimensional shape (i.e. flat film versus gel or sponge) have all been shown to affect cellular behavior and function. Several properties that have demonstrated more prominent influence on cell-scaffold interactions include hydrophobicity, ionic charge, and surface roughness, making the choice of scaffold material critical.

Due to their unique physical properties and the specific control that is able to be employed in their shapes and sizes, dendrimers are thought to make favorable materials for use in tissue culture support systems such as scaffolds. PAMAM dendrimers, in particular, have demonstrated diversity in applications within the fields of biological science, including use as gene transfer agents and in drug delivery systems. Of more particular interest, is the demonstrated ability of dendrimers to induce increased cellular interactions through 'cluster effects' in cell culture systems. It is envisioned that incorporating dendrimers as a major material in a solid scaffold support system will thus lead to improved cell function and survival as a result of such interactions. In the present study, previously synthesized galactose-centered PAMAM dendrimers were formed into solid support materials through the use of several crosslinking agents, including PEG-DGE, PEG-DA and glutaraldehyde. Analytical analysis including swelling and thermal

studies were performed on synthesized materials, which are intended for use in future studies as liver cell support materials.

5.2. Results

5.2.1. Poly (ethylene glycol 400 diglycidyl ether)

The crosslinking of galactose-centered PAMAM dendrimers with a PEG-DGE crosslinking agent resulted in gels of varying physical properties. These properties were found to be dependent on and controllable with the quantities of (a) crosslinking agent, (b) dendrimer and (c) solvent used in the gelation process. Final synthesized gels were observed to be transparent in swollen states, with varying intensities of yellow as a color.

Higher concentrations of PEG-DGE (Φ_{PEG}) combined with less solvent content resulted in strong, harder materials of increased densities. These materials exhibited a significant bounce property when dropped onto a solid surface, and were observed to break into smaller fragments upon the exertion of substantial force. Softer, less physically structured, more fluid gels were synthesized with increased solvent content and lower Φ_{PEG}. These materials exhibited a stickier surface characteristic at higher dendrimer concentrations. Gels formed with surface modified dendrimers were found to require higher percentages of dendrimer in order to undergo gelation versus those that were unmodified. Gelling times varied between several minutes to a number of hours, with faster gelation occurring for mixtures consisting of higher Φ_{PEG}.

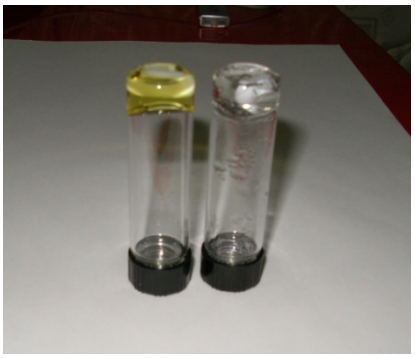

Figure 5-1: Image of crosslinked PEG-DGE glycodendrimer gels

The swelling properties of G3 to G6 unmodified dendrimer gels are depicted in **Figure 5-2**. Properties for G4 and G5 surface modified dendrimer gels are found in **Table 5-1**. Swelling ratios ranged between values of 3 and 8 for gels of unmodified dendrimers and between 3 and 12 for modified dendrimers. As revealed in the graph and table, higher PEG-DGE content led to lower swelling ratios, while a higher dendrimer to crosslinker ratio and higher solvent content resulted in an increase in swelling abilities. For a majority of samples, swelling ratios were also observed to increase on the second set of runs, particularly for gels formed with higher generation dendrimers and higher dendrimer to crosslinker ratios.

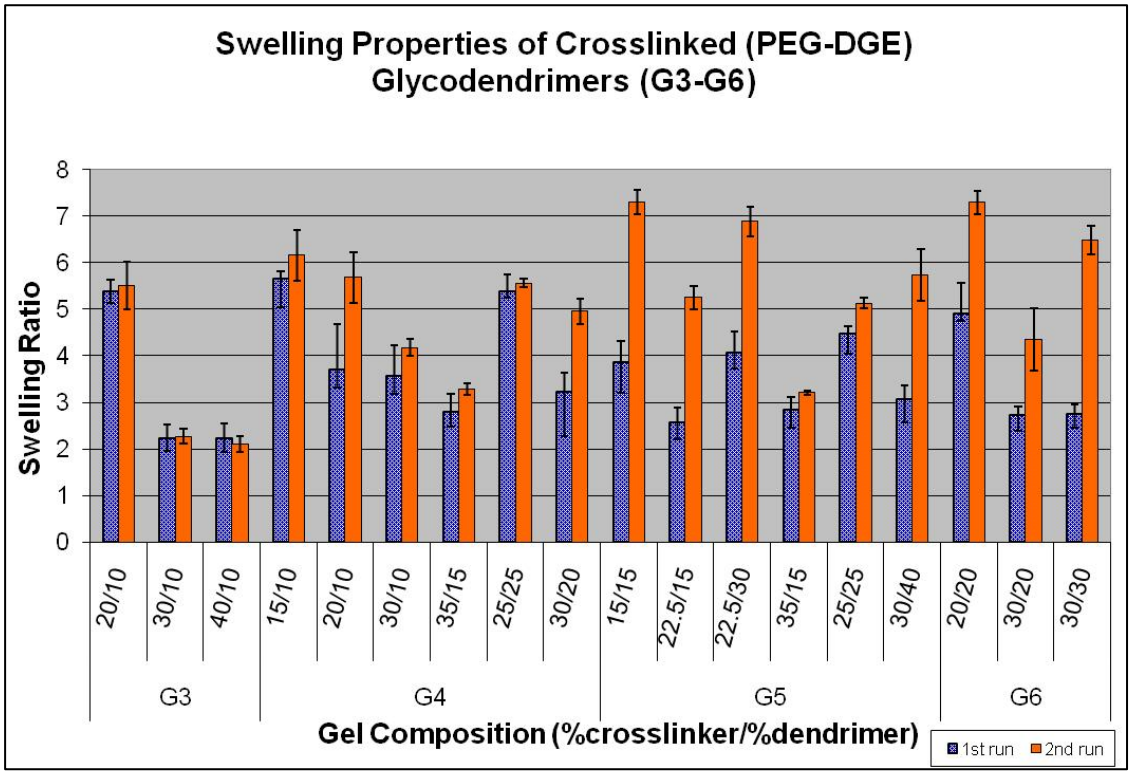

Figure 5-2: Swelling properties of PEG-DGE crosslinked glycodendrimers

Of the gels consisting of surface modified dendrimers, those composed of G4 dendrimers with higher degrees of surface modification displayed higher swelling. Little

variance in swelling was observed between gels made with G5 modified dendrimers of different coverage, with exception to samples with high dendrimer contents.

Table 5-1: Swelling properties of PEG-DGE crosslinked surface modified glycodendrimers

Gel Samples	Conc. (%C:%D)	Run 1 Swelling Ratios		Run 2 Swelling Ratios	
		AVG	STD	AVG	STD
G4-M25	20:20	5.7	0.370	**4.8**	0.527
	30:30	3.6	0.374	4.2	0.328
	30:20	3.6	0.607	5.1	0.227
	20:40	**3.0**	0.079	7.1	2.229
G4-M50	20:20	5.9	0.741	**9.1**	0.493
	30:20	6.2	2.023	8.4	1.424
	30:30	4.2	0.235	6.2	0.388
	20:40	**7.2**	1.068	10.5	0.834
G5-M25	20:20	4.4	0.340	7.3	0.246
	30:20	2.5	0.473	4.1	0.201
	30:30	3.7	0.107	5.7	0.299
	20:40	3.8	0.189	8.4	1.322
G5-M50	20:40	4.5	1.288	8.9	0.497
	40:40	2.9	0.354	4.0	0.467
	30:40	2.4	0.060	3.2	0.581

where C=crosslinker and D=dendrimer

SEM images of freeze-dried materials were taken to observe material surface morphologies, see **Figure 5-3** below and **Appendix B.1**. Materials generally showed smooth surfaces. Gels formed with higher dendrimer content displayed a visual increase

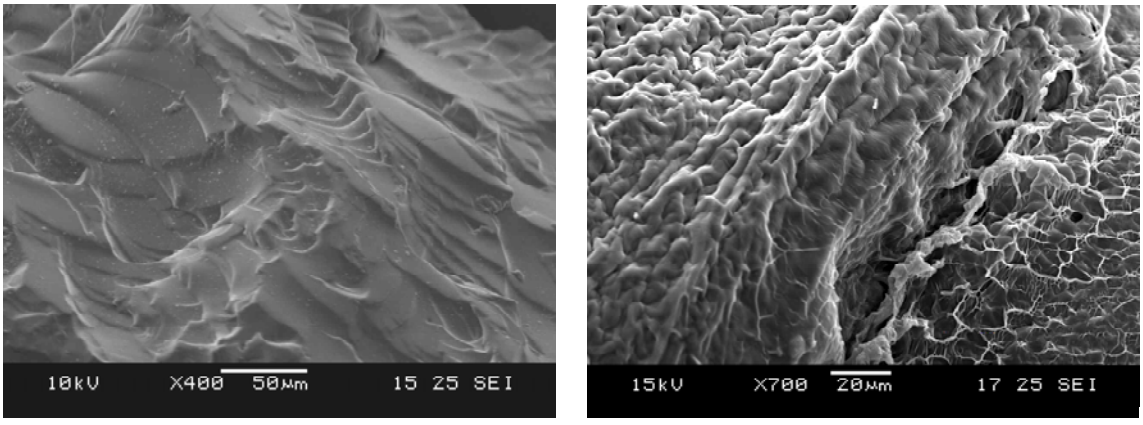

Figure 5-3: SEM images of PEG-DGE crosslinked G5 (30:10) (left) and G4 (30:40) (right) dendrimer gels

in surface roughness, with pores and irregular cavernous morphologies even observed in some instances. Gels composed of modified dendrimers also exhibited an increase in surface roughness in comparison to gels consisting of like concentrations of unmodified dendrimers.

An increase in the ether peak at a wavenumber of 1100 cm^{-1} and the emergence of a broader more prominent peak in the hydroxyl/amine region are visible in FTIR spectra of crosslinked gels. A decrease in strength of the carboxyl and amine peaks of amides at 1650 and 1555 cm^{-1} as well as the C-H peaks at 3000 cm^{-1} are also observed in comparison to uncrosslinked dendrimers. These peak trends become more pronounced in gels of higher crosslinker compositions. Increasing PEG-DGE content also resulted in an observed increase in ether verses carboxyl peak ratio (see **Appendix B.1**; spectra depicting (a) PEG-DGE vs. PEG-DGE crosslinked G4 dendrimers, and PEG-DGE crosslinked (b) G4-M25 and (c) G4-M50 gels of varying concentrations).

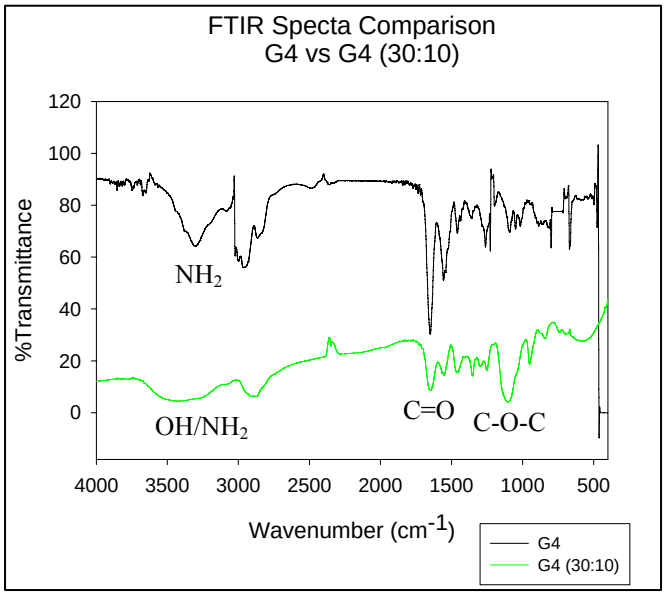

Figure 5-4: FTIR spectra of unmodified G4 and PEG-DGE crosslinked G4 (30:10) dendrimers

TGA analysis was performed to study the effect of crosslinker composition on thermal degradation (see **Table 5-2**). Samples generally produced one to two main degradation peaks, with values ranging between 250 and 400 °C. Higher crosslinker composition resulted in increased values of T_g. An increase in dendrimer surface

modified end groups also resulted in an increase in observed T_g values. Corresponding weight loss to lower T_g values was observed to increase for higher crosslinker content. Additional TGA data can be found in **Appendix B.1**.

Table 5-2: TGA analysis of PEG-DGE crosslinked G4 dendrimers

Sample (%C:%D)	T_g-1 (°C)	T_g-2 (°C)	Weight Loss Ratio (T_g-1:T_g-2)
G4 (30:20)	354	--	--
G4M25 (30:20)	279	393	0.45
G4M25 (20:40)	260	352	0.27
G4M50 (30:20)	391	--	--
G4M50 (30:30)	300	382	0.88

where C=crosslinker and D=dendrimer

To study the elemental surface environments of the gels, XPS analysis was carried out. A larger nitrogen signal was observed in gels containing higher dendrimer concentrations. This would be expected given the larger presence of surface amines. An increase in oxygen levels was found in gels of higher crosslinker concentrations as well as gels synthesized with surface modified dendrimers. Multiple carbon peaks were clearly observed in XPS spectra, with peak areas found to be proportional to the concentrations of crosslinker and dendrimer found in the gel (see **Figures 5-5** to **5-7** below). An impact on carbon peak ratios was observed for the degree of dendrimer surface modification as well. XPS data of selected gel samples, including atomic ratios of carbon, nitrogen and oxygen surface elements are tabulated below. Sensitivity factors of 0.25, 0.42, and 0.66 for C 1s, N 1s and O 1s peaks were used for atomic ratio determinations in all XPS data results.

Table 5-3: Selected XPS data of PEG-DGE crosslinked gel samples

Sample (%C:%D)	Peak	Position BE (eV)	Area	FWHM (eV)
G4 (30:20)	C 1s 1	285.00	1815.05	1.05
	C 1s 2	286.29	778.17	1.53
	N 1s 1	399.51	454.69	1.52
	O 1s 1	532.50	1421.70	2.11
G4M25 (30:20)	C 1s 1	285.00	1465.38	1.06
	C 1s 2	286.50	1150.47	1.40
	N 1s 1	399.76	310.01	1.48
	O 1s 1	532.59	1841.99	1.58
G4M25 (20:40)	C 1s 1	285.00	1719.27	1.11
	C 1s 2	286.43	1817.43	1.31
	C 1s 3	288.22	145.89	1.16
	N 1s 1	399.64	1453.90	1.55
	O 1s 1	532.48	2493.01	1.78
G4M50 (30:20)	C 1s 1	285.00	510.97	1.05
	C 1s 2	286.35	471.88	1.40
	N 1s 1	399.65	179.78	1.65
	O 1s 1	532.51	820.83	1.66

Table 5-4: Elemental ratios present on gel surfaces

Sample (%C:%D)	Atomic Ratios		
	C:N	C:O	N:O
G4 (30:20)	9.58	4.82	0.50
	(5.52	*1.95*	*0.35)*
G4M25 (30:20)	14.18	3.75	0.26
	(7.51	*1.66*	*0.22)*
G4M25 (20:40)	4.26	3.90	0.92
	(4.39	*1.79*	*0.41)*
G4M50 (30:20)	9.18	3.16	0.34
	(9.49	*1.53*	*0.16)*

*Theoretical atomic ratios in italics

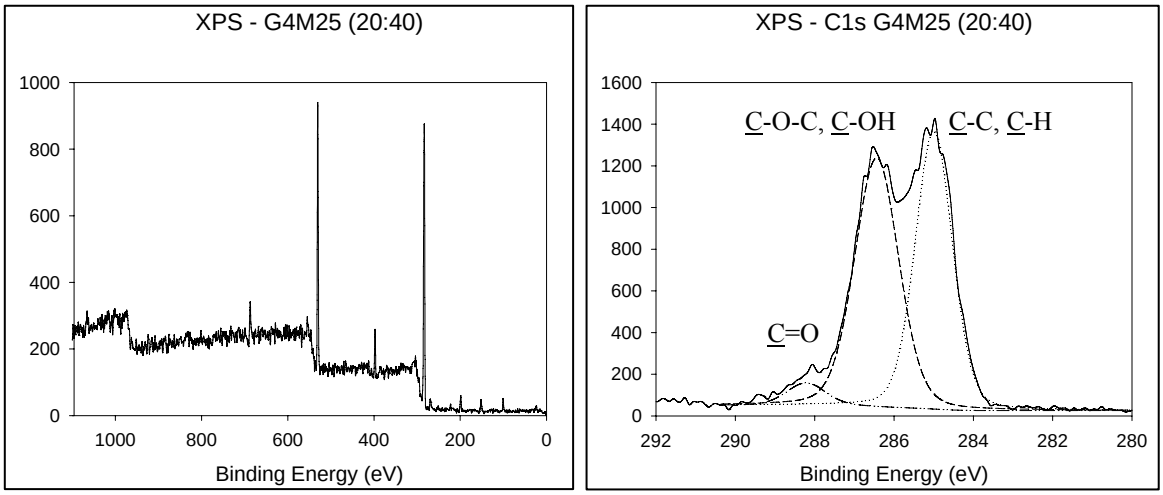

Figure 5-5: XPS wide scan (left) and C 1s Peak (right) for G4M25 (30:20) gel

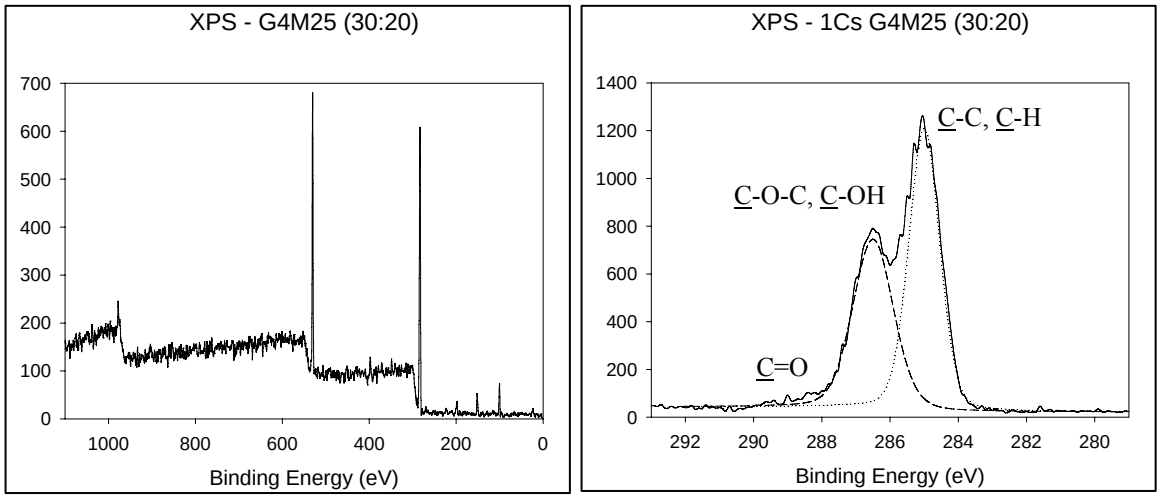

Figure 5-6: XPS wide scan (left) and C 1s Peak (right) for G4M25 (20:40) gel

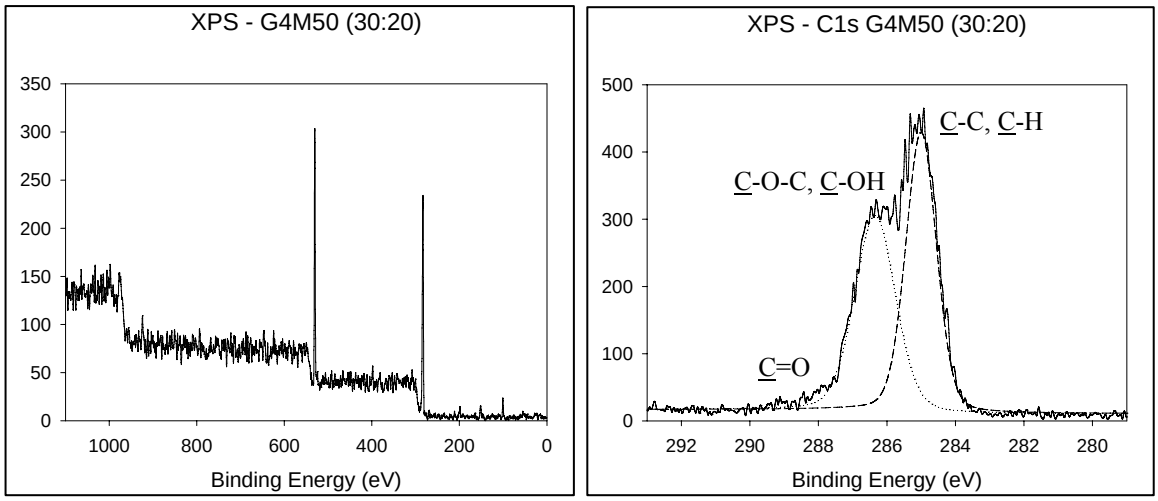

Figure 5-7: XPS wide scan (left) and C 1s Peak (right) for G4M50 (30:20) gel

Attempted solid phase MALDI-TOF-MS on gel samples provided little information. For this case a small sample of the solid gel was fixed to the target plate at which the laser was directly fired upon, with no use of a matrix solution. Several low molecular weight peaks were obtained that could possibly correspond to fragmented PEG or dendrimer segments (see **Appendix B.2**).

5.2.2. Glutaraldehyde

Two distinct outcomes were acquired when using glutaraldehyde as a crosslinking agent for unmodified dendrimer samples. Product properties were dependent on crosslinker concentration as well as mixing speed.

(1) *Method G-1*: If the dendrimer solution mixture was not mixed thoroughly during the addition of glutaraldehyde or the added glutaraldehyde solution was too concentrated, a yellow precipitate was witnessed to immediately precipitate out of solution. This precipitate was opaque in nature and was observed to turn a purple/reddish color over the course of several hours. Upon visual inspection, it was also observed that the crosslinked material contained areas of varying color intensities, indicating a fairly unhomogeneous product.

(2) *Method G-2*: If the dendrimer solution was mixed vigorously during or immediately upon the addition of glutaraldehyde, gelation of the entire solution was typically able to be achieved, resulting in a more gel-like substance. In this case, a vortex mixer was utilized for achieving greatest mixing in a timely fashion. Resulting materials were observed to be translucent, with colors turning from an initial orange to similar shades of purple that were characteristic of the products obtained in the previous method.

Even with increased mixing speeds, unhomogeneous areas were still witnessed within the gels, marked by visible swirls of more opaque material.

Crosslinking of dendrimer particles in organic solutions of methanol was also achieved. Products looked to be more homogeneous in color and spongier in texture than those prepared in aqueous solutions using identical methods. Upon drying however, the materials became hard flaky solids that exhibited little if any swelling upon submersion back into solvent. These materials were not used in further experimentation.

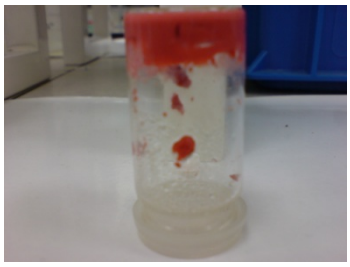

Figure 5-8: Method G-2 gel

Swelling studies performed on aqueous phase crosslinked glycodendrimers revealed a limited ability to take in aqueous solution in comparison to PEG-DGE crosslinked materials, with swelling ratios ranging between 3.5 for *Method G-1* Glut G4 (13:16) and 12 for *Method G-2* Glut G4 (8:33) materials. Gels synthesized using *Method G-1* techniques displayed decreased swelling ratios compared to those using *Method G-2*. Gel stabilities, however, were more unpredictable for products of *Method G-2* synthesis with reswelling after drying proving ineffective. Mass loss was observed in all samples upon placement in excess solvent for swelling, with a number of *Method G-2* samples found to dissociate completely.

SEM images of dried gel samples revealed considerably rough surfaces with a large numbers of porous structures. *Method G-2* gel samples displayed an increased surface roughness over *Method G-1* samples. Additional images can be viewed in **Appendix B, section B-2**. Gels formed in organic solution were also found to exhibit similar degrees of surface roughness.

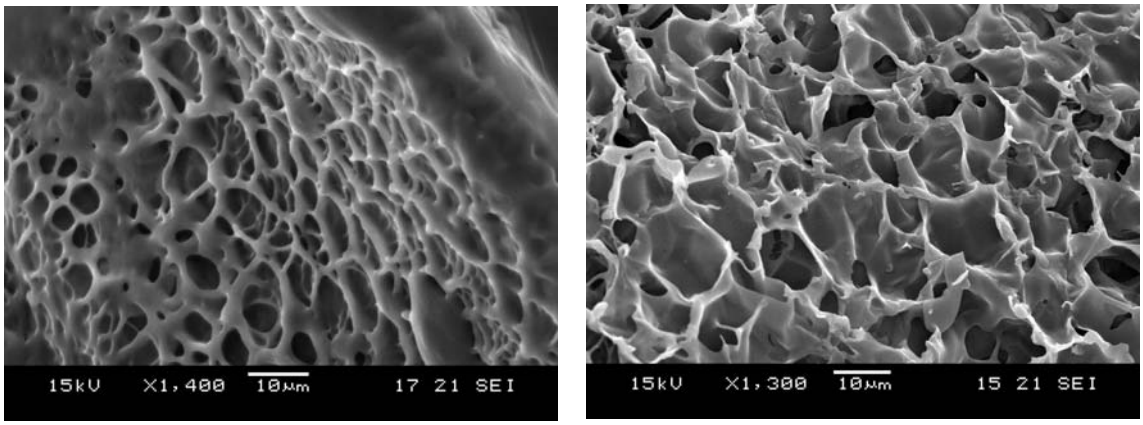

Figure 5-9: SEM images of dried glutaraldehyde crosslinked G4 (left) and G4-M50 (right) glycodendrimers

Crosslinking of modified dendrimer samples under conditions of vigorous mixing resulted in transparent, purple colored gels. Dilute solution mixtures with low concentrations of glutaraldehyde resulted in very fluid gels. These materials were found to dissociate almost completely in excess water over a period of 24 hours. SEM images of dried materials revealed an increase in surface roughness and pores in comparison to those prepared with unmodified dendrimers.

FTIR spectra of glutaraldehyde crosslinked dendrimers appear quite similar to those of PEG-DGE crosslinked gels, with exception to the ether peak. There is once again a broadening and increase in peak intensity in the hydroxyl/amine region in comparison to the carboxyl and C-H peaks of unmodified dendrimers. The relative carboxyl peak intensity is not affected as significantly as that observed in PEG-DGE gels.

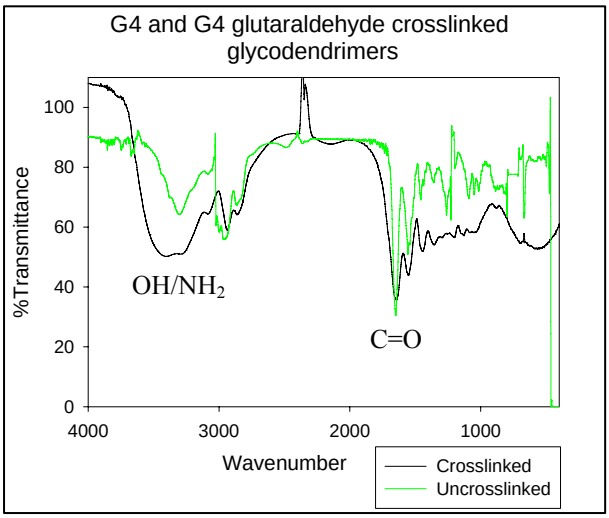

Figure 5-10: FTIR spectra comparison between glutaraldehyde crosslinked G4 and uncrosslinked G4 glycodendrimers

This may be an indication of unreacted aldehyde end groups deriving from the glutaraldehyde crosslinking agent still being present in the materials.

T_g values for glutaraldehyde crosslinked samples were found to range between 270 and 440 °C, being largely independent of crosslinking method used for synthesis. Multiple degradation peaks were observed in TGA spectra. XPS analysis on *Method G-1* glutaraldehyde crosslinked G4 (13:16) and G4M50 (13:16) samples revealed a larger nitrogen surface presence in comparison to PEG-DGE crosslinked gels, particularly for materials consisting of unmodified dendrimers. The carbon peak is observed to trail on the back end (unsymmetrical), indicating several peaks in close proximity. A larger carbon peak at 283 eV was also identified for the G4 glutaraldehyde crosslinked sample.

Table 5-5: XPS data for selected glutaraldehyde crosslinked dendrimer gels

Sample (%C:%D)	Peak	Position BE (eV)	Area	FWHM (eV)	Atomic Ratios		
					C:N	C:O	N:O
G4 (13:16)	C 1s 1	285.00	2847.47	1.07	6.55	5.52	0.84
	C 1s 2	286.02	1692.06	1.30	*(4.15*	*2.52*	*0.61)*
	C 1s 3	287.95	271.71	1.28			
	N 1s 1	399.52	1234.03	1.61			
	O 1s 1	531.90	2301.02	2.28			
G4M50 (13:16)	C 1s 1	285.00	1270.47	1.18	12.55	4.09	0.33
	C 1s 2	286.19	155.56	1.71	*(7.06*	*1.71*	*0.24)*
	N 1s 1	399.93	190.90	2.03			
	O 1s 1	532.36	919.71	2.28			

*Theoretical atomic ratios in italics

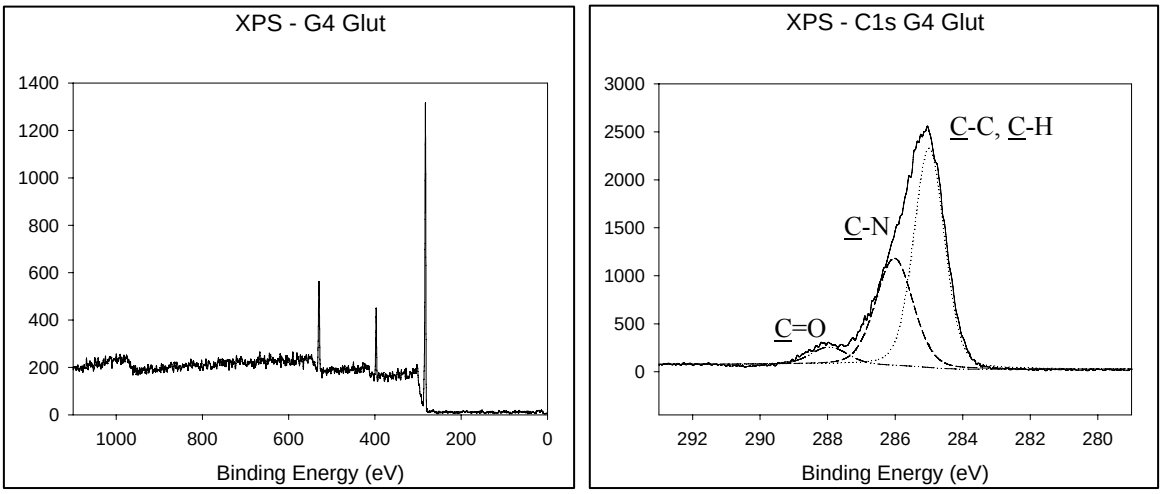

Figure 5-11: XPS wide scan (left) and C 1s Peak (right) for glutaraldehyde G4 (13:16) gel

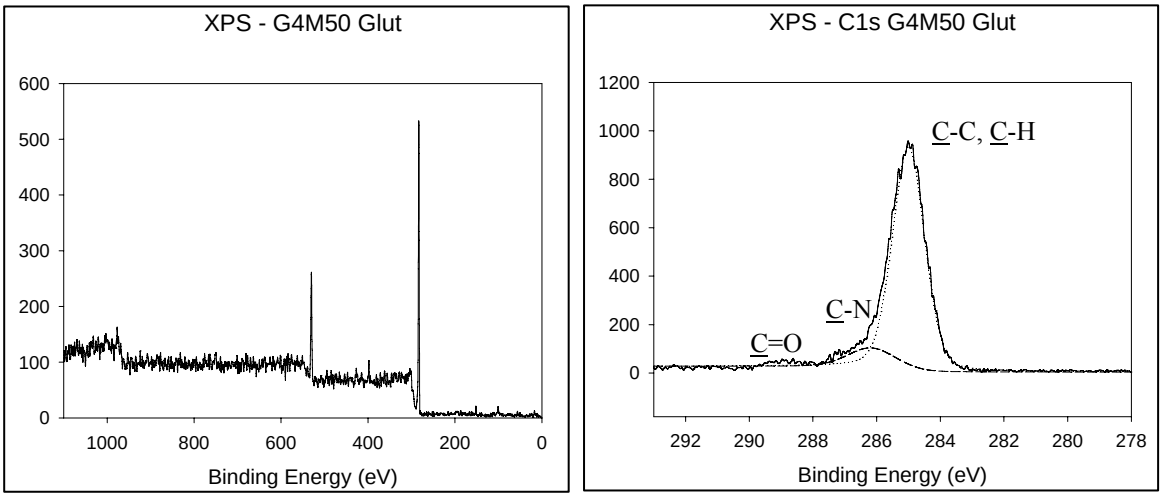

Figure 5-12: XPS wide scan (left) and C 1s Peak (right) for glutaraldehyde G4M50 (13:16) gel

5.2.3. Poly (ethylene glycol 400 diacrylate)

Permanent gelation of dendrimers using a PEG-DA crosslinking agent was not attained in aqueous solution mixtures. Initial crosslinking *was* observed to occur, with the solution mixture attaining a solid form that could be handled and transported without loss of structure. These materials however, disassociated back into liquid form over a

period of several days. A permanent gelation was acquired through use of organic solvents. Both methanol and 2-propanol were successfully used as solvents in achieving gelation. 2-propanol, however, was found to perform as a better solvent in terms of attaining desired crosslinked product properties and was therefore selected as the solvent of choice for gel preparation. The attained crosslinked gels were transparent and yellow in color, similar to those of PEG-DGE crosslinked dendrimers. A majority of gel samples were noted to lose significant mass when immersed in excess organic solvent for a period of 24 hours, with some gels dissolving completely. Dried gels that were synthesized in organic solution mixtures and subsequently maintained their form when submerged in excess organic solvent were still found to dissolve completely when placed in aqueous solution.

Swelling ratios of PEG-DA crosslinked gels ranged between 2 and 4 for G4 and G5 dendrimers, significantly lower than those prepared with PEG-DGE. A significant increase in the standard deviations for second run test data was also noted for gels composed of lower crosslinker to dendrimer ratios. No studies were performed for gels synthesized with surface modified dendrimers due to their insolubility in the organic solvents used.

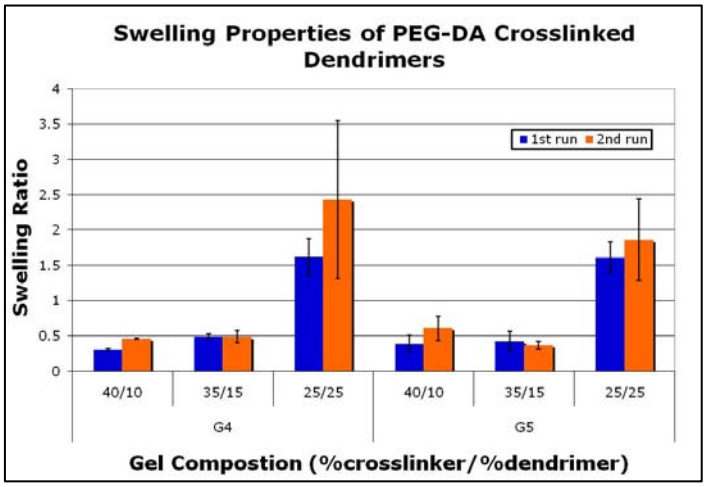

Figure 5-13: Swelling Properties of PEG-DA crosslinked G4 glycodendrimers

FTIR spectra of the gels again reveal increased peak intensities in the hydroxyl and ether regions, corresponding to the addition of PEG. An increase in carboxyl to amine peak ratios is observed in gels of increased crosslinker concentrations. An additional peak at 1732, corresponding to C=O stretch, emerges in samples of higher PEG-DA content.

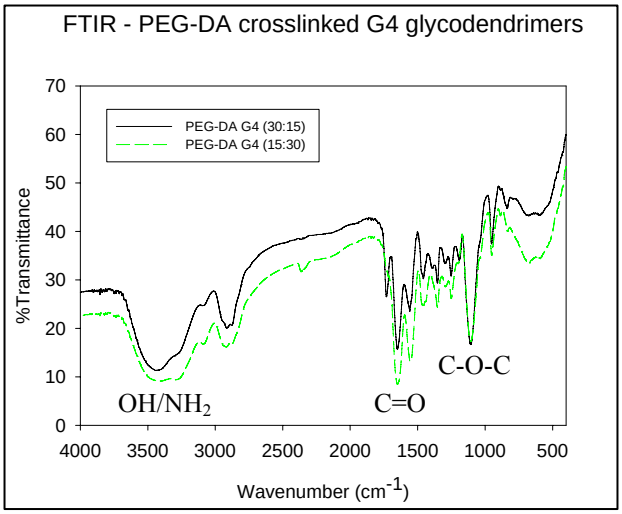

Figure 5-14: FTIR spectra comparison between PEG-DA crosslinked glycodendrimers of differing compositions

Smooth surfaces with no visible pores were observed in SEM images of dried gel samples. Thermal analysis on selected gels found Tg values of 334.26 and 291.61 °C for PEG-DA G4 (30:15) and (25:25) samples respectively. These values range between those for PEG-DA and G4 dendrimers, increasing for higher PEG-DA content. XPS surface analysis revealed a significant nitrogen surface presence in comparison to previously discussed gels. Multiple nitrogen and oxygen peaks were also observed in higher dendrimer concentrated samples (see **Appendix B.3**).

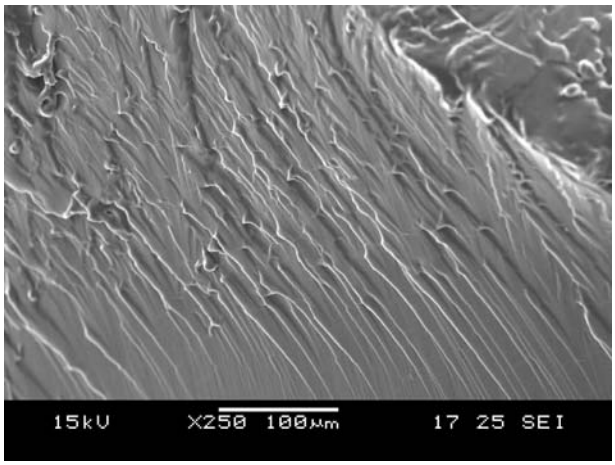

Figure 5-15: SEM image of PEG-DA G4 (15:30) gel

Table 5-6: XPS data for selected PEG-DA crosslinked dendrimer gels

Sample (%C:%D)	Peak	Position BE (eV)	Area	FWHM (eV)	Atomic Ratios		
					C:N	C:O	N:O
PEG-DA G4	C 1s 1	285.00	1640.96	1.12	14.26	4.34	0.30
(40:10)	C 1s 2	286.33	1100.31	1.47	*(11.21*	*1.69*	*0.15)*
	C 1s 3	289.14	90.98	0.90			
	N 1s 1	399.40	333.69	1.50			
	O 1s 1	532.64	1724.76	1.80			
PEG-DA G4	C 1s 1	285.00	476.01	1.11	3.27	2.76	0.84
(35:15)	C 1s 2	286.26	1653.23	1.35	*(7.43*	*1.81*	*0.24)*
	C 1s 3	288.32	134.18	1.77			
	N 1s 1	399.25	1022.88	1.43			
	N 1s 2	401.12	141.64	1.60			
	O 1s 1	530.65	230.32	1.14			
	O 1s 2	532.46	1935.44	1.60			
PEG-DA G4	C 1s 1	285.00	2386.54	1.12	3.95	4.08	1.03
(25:25)	C 1s 2	286.35	1494.85	1.36	*(4.42*	*2.11*	*0.48)*
	C 1s 3	288.19	256.60	1.64			
	N 1s 1	399.64	1217.24	1.35			
	N 1s 2	400.50	542.96	4.05			
	O 1s 1	530.99	299.00	1.20			
	O 1s 2	532.54	2377.91	1.72			

*Theoretical atomic ratios are in italics

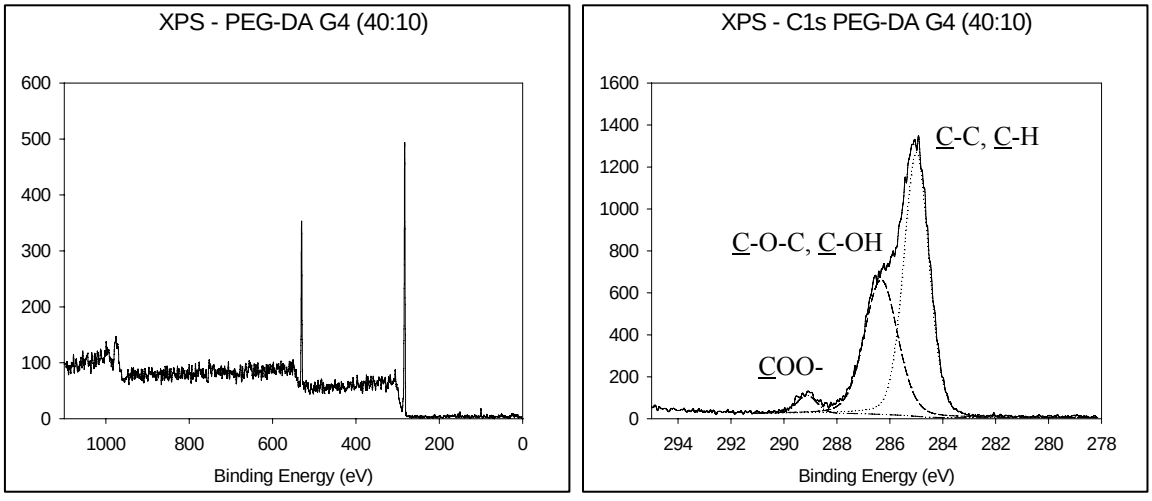

Figure 5-16: XPS wide scan (left) and C 1s Peak (right) for PEG-DA G4 (40:10) gel

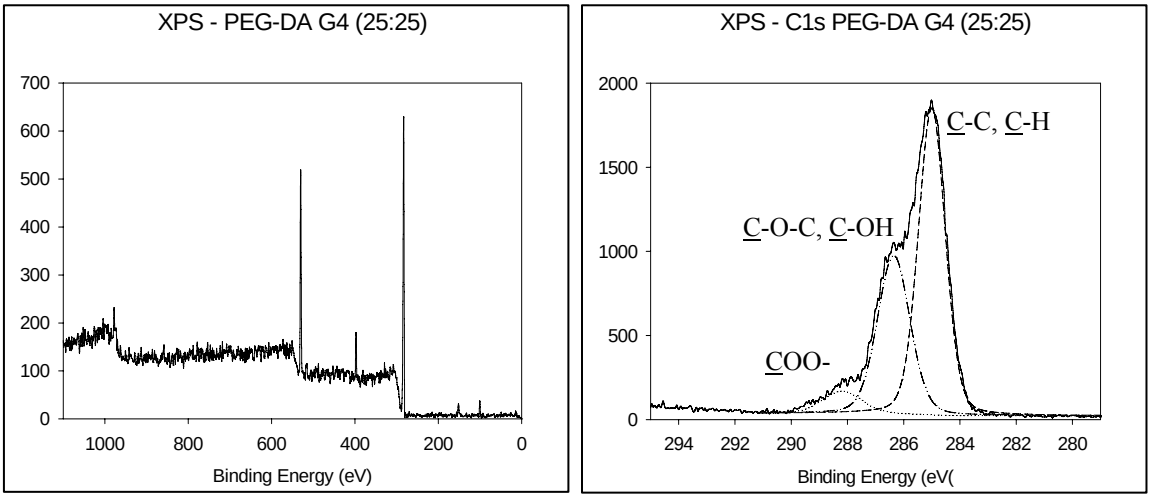

Figure 5-17: XPS wide scan (left) and C1s Peak (right) for PEG-DA G4 (25:25) gel

5.2.4. Succinyl chloride

No gelation was able to be attained in the attempted use of succinyl chloride as a crosslinking agent with the dendrimers. Aqueous solutions could not be used in the gelation process due to succinyl chloride's extreme reaction with water. Due to the instability of this reagent in water, it will rapidly react to form its corresponding acid [127]. Attempts at crosslinking within organic solvents such as methanol resulted in the formation of a brown syrup precipitating from solution. No material was acquired that would be physically suitable for future use in cell cultivation.

5.3. Discussion

5.3.1. Poly (ethylene glycol 400 diglycidyl ether)

PEG-DGE consists of an extended PEG group with epoxide end groups. Epoxies have been used in a large range of applications that include industrial uses in paints, adhesives and composites, as well as biomedical uses in the areas of tissue scaffolding [128, 129] and drug release [130]. Upon reaction (nucleophilic addition) with an amine,

the epoxide ring breaks open resulting in the formation of a C-N bond and a hydroxyl group (see **Figure 3-4**) [70]. Each primary amine end group is capable of reacting with two epoxides. Intramolecular secondary amines present within the branching arm units are also capable of reaction. Steric hindrance and hampered accessibility present in higher generation dendrimers should, however, considerably limit if not prevent such reactions from occurring. The emergence of the hydroxyl peak in FTIR spectra of PEG-DGE crosslinked gels, as well as the variance in T_g values attained is an indication that the intended reaction between amine and epoxide has occurred.

Thermodynamically, gels are crosslinked polymer networks that are capable of absorbing solvent in which they are insoluble in. Experimentally, swelling abilities of crosslinked materials have been directly linked to crosslinking density, with higher degrees of crosslinking resulting in decreased swelling [131,132]. Theoretically this makes sense, as the more highly crosslinked a material is the more tightly bound are the individual particles, resulting in a tighter matrix. This will restrict flexibility and movement, which in turn reduces the amount of water that can be absorbed and retained by the material. This supports the reported findings of decreased swelling ratios for gels formed with higher Φ_{PEG}. Decreased swelling was also observed for gels synthesized in overall lower water content. Dilution of sample solution reduces crosslinking density by limiting the number of particles in close proximity to each other, thereby reducing the number of inter-particle reactions each particle can undergo. In such scenarios there may be a number of unreacted crosslinker end groups or a high occurrence of looping present in the system, depending on the concentrations employed.

A parameter that is often used to describe the reaction stoichiometry of gelation is the *r* value, which represents the ratio of reactive polymer end groups to reactive

crosslinker end groups. Studies have shown that there is a minimum and maximum value of *r* for which a given system will undergo gelation [133]. An in-depth study of *r* values was not undertaken due the limited supply of dendrimer particles. Instead, gelation conditions were concentrated around those which were expected to produce desired results. A table of *r* values corresponding to selected PEG-DGE crosslinked gel samples is shown below in relation to component weight percents of crosslinking agent and dendrimer used during the gelation process. In this case *r* = 2 x (moles of amine endgroups)/(moles of epoxide endgroups).

Table 5-7: Calculated *r* values for PEG-DGE crosslinked dendrimer gels

Sample	*r*	Sample	*r*	Sample	*r*
G4 (30:10)	0.81	**G4M25 (30:20)**	0.86	**G4M50 (30:20)**	0.44
G4 (35:15)	1.04	**G4M25 (20:20)**	1.29	**G4M50 (20:20)**	0.67
G4 (25:25)	2.42	**G4M25 (20:40)**	2.48	**G4M50 (20:40)**	1.33

Referencing the previously reported swelling ratios for dendrimer gels, it can be noted that an increase in *r* value leads to an increase in swelling ability, which can again be linked to crosslinking density. The *r* value also explains why a larger percentage of surface modified dendrimers were required to achieve the same gelling effects as unmodified dendrimers. The affects of dilution on increasing swelling ratios can also be clearly observed between gels possessing the same *r* value but different weight percentages of gelling agents, taking G4 (15:10) versus G4 (30:20) as one example.

The increased values of Q that were observed during second run swelling experiments are likely an effect resulting from the soluble fraction of the polymer networks, w_{sol}. As swelling was calculated using initial weight versus saturated weight,

first run swelling analysis doesn't take into account this soluble weight fraction. This will result in a lower calculated swelling, as the actual weight of swelled gel is lower than that used for the calculation. This is supported by larger increases in second run swelling being associated with gels that possess higher soluble weight fractions.

Soluble weight fractions for selected gels are shown in **Table 5-8** along with corresponding *r* and Q values. It can be seen from the data that increasing *r* values and increasing solvent content result in higher values of soluble mass fraction for the gels. Gels synthesized with surface modified dendrimers are found to possess particularly high values for w_{sol}, even for lower values of *r*. This implies that either (i) the modified surface groups are interfering in crosslinking reactions between particles and/or (ii) having larger but fewer particles significantly effects network formation.

Table 5-8: Weight soluble fractions of PEG-DGE crosslinked dendrimer gels

Sample	*r*	Q	w_{sol}	Sample	*r*	*Q*	w_{sol}
G4 (30:10)	0.81	4.18	2.54	**G4M25 (20:20)**	1.29	4.81	24.21
G4 (35:15)	1.04	3.29	6.10	**G4M25 (30:30)**	1.29	4.15	16.43
G4 (25:25)	2.42	5.56	23.24	**G4M25 (20:40)**	2.48	7.13	23.65

It has been previously reported that high values of *r* can lead to smaller clusters of reacted material that are unattached to the major gel framework, which would then leach from solution during swelling [133]. Additionally, a higher percentage of intramolecular reaction (loop formation) occurs for more highly diluted conditions as a result of particles being spaced further apart. Loop formation is also more probable in particles containing large numbers of reactive endgroups in close proximity, such as higher generation dendrimers. The combination of larger but fewer particles and the significant number of

reaction sites per molecule that are present in gelation conditions of higher generation dendrimers, may therefore conceivably result in such scenarios from occurring. This could partially explain the large increases found in soluble fractions for materials containing increased dendrimer concentrations.

Since these conditions would have significant effects on system flexibility and overall matrix structure, they would in turn also affect the degrees of swelling attainable. Other factors that could affect network structure of the gels include natural degradation, although this is far more unlikely taking into account the materials in question and given the relatively short time periods of testing, or structural changes that may have occurred during the freeze-drying process, but this is also quite unlikely given that the materials are quite flexible.

Increased swelling abilities for samples of higher dendrimer content may also be partly due to the dendrimers natural ability to contain small molecules within its void spaces. The dendrimer generation and size of its void space as well as the overall reaction conditions present in the system, such as solvent used, may both affect how much solution or how many particles the dendrimers can successfully 'absorb'[134, 135]. Solution pH may also affect the gels aptitude for swelling given the possible presence of surface charges within the materials brought about from the dendrimers [136].

The observed surface morphologies of dried gels ranged from smooth to wrinkled to possessing pore-like voids. Increased surface roughness for gels synthesized with higher water content would be expected as there is less solid material covering a larger area of space, which would lead to a more drastic change in structure between dry and swollen physical states. This would result in a more wrinkled surface appearance in the dry state in comparison to more tightly bound, higher crosslinked samples. In addition to

naturally occurring network formation, observed void spaces could also be a result of entrapped air bubbles during gelation or inhomogeneities resulting in small microgels leaching from the main gel network during swelling.

XPS surface analysis generally determined C to N atomic ratios in the range of theoretical values, which were based on the assumption of complete reaction of all materials. Some degree of variation from theoretically determined values are expected due to actual incomplete reaction of the gelation process as witnessed from the varying soluble weight fractions determined for the gel materials during swelling studies.

The dendrimer, PEG crosslinking agent and the crosslinked dendrimer gels are all hydrophilic materials. The hydrophilic nature of the gels is demonstrated by their attained swelling ratios and their readily absorption of aqueous solution. Since hydrophilic materials have been demonstrated to support cell adhesion, it is thought that these dendrimer constructs will make suitable substrates for use in cell culture systems. Although the gels are hydrophilic, full-generation dendrimers also contain a significant positive surface charge due to the large number of amines present. This surface charge has been shown to exhibit negative effects on cytotoxicity but should be alleviated to a degree through crosslinking. The extent to which this charge is dampened will be dependent upon the *r* values (crosslinking density) of the gels.

As previously discussed, additional molecules can be added to the dendrimers surface to further shield against undesired or harmful positive surface charges. In this study, lactobionic acid was used as a surface-modifying agent. The zero length coupling reaction used presents a galactose moiety at the outermost position, which is also a known asialoglycoprotein receptor for hepatocytes. The incorporation of specific cell-interacting ligands onto a material surface is also a common technique to improve cell-scaffold

compatibility [137, 138]. The sugar therefore plays a dual role of shielding the positive surface charge as well as improving cell-scaffold compatibility through direct interaction with the cells.

5.3.2. Glutaraldehyde

Glutaraldehyde is one of the most commonly used homobifunctional bisaldehyde crosslinking agents for reaction with amines. It has been used as a coupling agent for surface modification and is commonly used as a tissue fixative in cell culture studies for the acquisition of visual images such as SEM [139, 140]. As with PEG-DGE, each glutaraldehyde molecule is capable of reacting with two amines, enabling it to couple molecules together. Unlike with PEG-DGE however, each amine is only capable of reacting with a single glutaraldehyde molecule. The coupling reaction between one of the aldehyde groups of glutaraldehyde and an amine results in what is known as a Schiff's base (see **Figure 5-18**) [141]. This molecule can undergo further reduction to a more stable secondary amine. No reduction was performed in the synthesis of gels in this study; however, as it has been shown that reduction of Schiff's base is unnecessary under normal conditions [142].

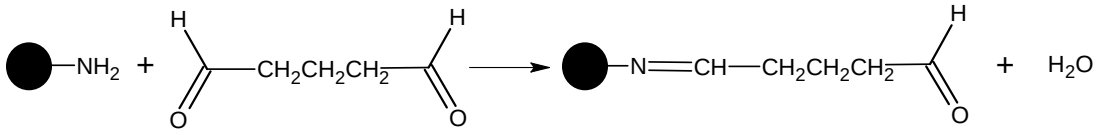

Figure 5-18: Coupling reaction of a primary amine with glutaraldehyde resulting in a Schiff's base

The reduced swelling abilities obtained for glutaraldehyde crosslinked gels may primarily be a result of the smaller chain length of the crosslinking agent and its affect on gel network structure. First, smaller crosslinker chain lengths would result in a more

tightly bound solid, reducing the amount of solvent that the material could absorb and retain. Due to the smaller size of glutaraldehyde, intramolecular bonding is also more likely to occur between sidearm chains and end groups within a single dendrimer particle. A considerable number of these reactions could occur in systems involving higher generation dendrimers where large numbers of end groups are present in closer proximity to each to other. These intramolecular reactions are expected to be numerous in the more solid products obtained in *Method G-1* synthesis, where fast reaction times combined with more concentrated crosslinker addition or slower mixing speeds would give rise to conditions allowing for increased bonding of this type to occur.

Gelation of unmodified dendrimers was noted to be more difficult to achieve than with surface modified dendrimers. Again, this may be an indication that intramolecular reactions were curbed by the presence of the added surface moieties, limiting crosslinking to a higher extent between molecules. This would counteract the rapid reaction times while allowing for more adequate mixing to take place, enabling for gel formation to occur. However, given the small size of glutaraldehyde in comparison to the galactose containing surface ligands, adequate crosslinking may also be hindered as a result of these shielding effects. This could lead to an increase in microgel formation, resulting in the high soluble weight fractions (or complete dissolution) observed in *Method G-2* surface modified gels.

As previously mentioned, the crosslinking reaction of glutaraldehyde with dendrimer amines was found to proceed at a significantly high reaction rate, with solid formation observed almost immediately upon addition to still solutions of dendrimer. For this reason, a completely homogeneous product was difficult to attain, even when vigorous mixing was employed. This was especially true for unmodified dendrimers.

Dilution of the glutaraldehyde before addition to dendrimer solutions helped to a certain extent, but limited dilution was available due to the reaction conditions employed (generally calling for about 50% aqueous solution). As the dendrimer is also solid or syrupy in nature, it must also be dissolved to allow for proper reaction to occur, further limiting the dilution available toward glutaraldehyde.

Soluble weight fractions and *r* values of selected glutaraldehyde crosslinked dendrimers are found in **Table 5-9,** where *r* = (moles of amine endgroups)/(moles of aldehyde endgroups). Due to the reactions involved in *Method G-1* synthesis, values of *r* for these materials should merely be referenced to describe initial reaction conditions and not final product characteristics. Products precipitating from solution while exhibiting network inhomogeneities indicate that regions of relatively high dendrimer concentration or crosslinker agglomeration were present within the materials. Soluble weight fractions for *Method G-2* materials were calculated based on weights of initial reactants used (assuming complete reaction and retention of weight) instead of undergoing swelling/drying cycles as a result of their inability to regain their swollen states after drying. Significant amounts of microgel formation are expected to have formed, indicated by the visual loss of mass and significant leeching of color into solution. As viewed in the table *Method G-2* materials experience extensive mass loss, with remaining mass observed to experience large swelling (indicating very low crosslinking densities).

Table 5-9: Swelling data for glutaraldehyde crosslinked dendrimers

Sample	*r*	Q	w_{sol}
G4 (13:16)	0.28	3.51	12.85
G4 (3:27)	2.05	3.43	29.09
G4M50 (14:36)	0.57	5.04	64.32
G4M50 (8:33)	0.23	12.61	92.68

A significant amount of unreacted aldehyde may also be present in the gels due to entrapment or lack of bonding sites as a result of low *r* values or spacial and orientation limitations. For example, due to the short range of the glutaraldehyde molecule, once the initial network is set a number of additional bounded molecules may not be in reach of any other reactive sites. The presence of excess aldehyde is supported by the significant carboxyl peak still present in FTIR spectra of crosslinked gel samples.

The effects of unreacted aldehydes present within the materials on cell culture cytotoxicity are not known. Additional problems associated with the presence of excess aldehyde groups however, include non-specific binding of proteins such as antibodies [143]. Reaction of free aldehydes located within a solid construct with free proteins may impair cellular studies that aim to measure specific cell function, specifically the production of various proteins such as albumin and p450 in the case of Hep3B hepatoma cells.

Excess unreacted glutaraldehyde entrapped within the gel will present a toxicity problem if not completely extracted from the materials, as glutaraldehyde itself is a known toxin. Fürst and Banerjee (2005) illustrated the toxicity issues of using glutaraldehyde-based materials by demonstrating that even the medically used surgical

adhesive, Bioglue, releases amounts of glutaraldehyde that can induce cytotoxic effects. To remove the presence of unreacted crosslinker, samples were soaked in excess water that was changed daily. Initially, the solution was witnessed to turn pinkish in color, similar to that of the reacted solid product. The color change was thus presumed to be a result of small, reacted molecules unbound from the primary crosslinked network, leaching from the samples into solution. This process was continued until the solution was observed to remain colorless. This in itself, however, does not guarantee absence of further leeching when subjected to a cell culture environment.

5.3.3. Poly (ethylene glycol 400 diacrylate)

Similar to PEG-DGE, PEG-DA consists of a central extended PEG unit, only possessing acrylate end groups instead of epoxides. Acrylates are common reactive groups that are often used in polymer synthesis. Polyacrylates are found in a number of industrial products; including diapers (as super absorbents), Plexiglass and superglue to name a few. Reaction between an acrylate and an amine results in the breaking of the double bond on the acrylate to give a C-N bond with the amine. Just as in the methyl acrylate reaction of PAMAM synthesis, each primary amine is capable of reacting with two acrylate groups. The primary difference in gel network in comparison to that of PEG-DGE is the added presence of carboxyl groups instead of hydroxyl groups.

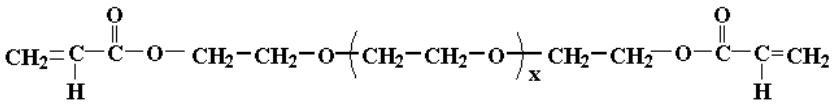

Figure 5-19: Structure of poly(ethylene glycol 400 diacrylate); x=400

Swelling ratios for PEG-DA crosslinked gels in 2-propanol were minimal for low values of *r*, with a moderate increase for values around 2. The most structurally perfect gel networks were observed more clearly for *r* values approaching 1 than with the previously tested crosslinkers. This is expected as a one to one ratio of endgroups is optimal. This is due to too high a value resulting in looping and 'microgel' formation that is unbound from the primary network. while too low a value will result in a large number of crosslinker reacting on only a single side with no available reaction sites to complete the 'linking' with its other side.

Larger Q values could be expected at even higher values of *r*. Given that values of w_{sol} already reach approximately 25% at values just over 2, higher values of *r* may not be attainable while maintaining the structural integrity of the gels; at least at tested solvent concentrations (i.e. values may already be nearing r_{max}). The solvent itself could be one cause for the low values of Q observed, possibly resulting from the lower organophilicity of long chain –PEG– units present within the gels [144]. This would limit organic solvent absorption into the gel in comparison to an aqueous solvent.

Table 5-10: Swelling data for PEG-DA crosslinked glycodendrimers

Sample	*r*	Q	w_{sol}	Sample	*r*	*Q*	w_{sol}
G4 (40:10)	0.60	0.47	10.66	**G5 (40:10)**	0.63	0.61	15.37
G4 (35:15)	1.03	0.49	3.87	**G5 (35:15)**	1.08	0.37	9.23
G4 (25:25)	2.40	2.43	26.01	**G5 (25:25)**	2.51	1.87	19.28

Again, the increase in standard deviations found for second run swelling studies most likely resulted from the mass loss of samples, w_{sol}, noted between runs, which could affect the swelling capability and network structures of the samples during

drying/swelling cycles. Soluble mass fractions of PEG-DA crosslinked gels were found to be comparable to those of PEG-DGE crosslinked gels of like concentrations. This indicates that similar gelation networks with the dendrimers were obtained for each of these crosslinking agents. This would be somewhat anticipated given that each are similar in molecular weight and involve similar reactions with the dendrimer amine endgroups.

The instability of the PEG-DA gels most likely arises from the presence of ester linkages present in the crosslinked matrix. There will be potential for hydrolysis of these esters to occur in aqueous solution, with the matrix breaking down into carboxylic acid and alcohol components. Another possibility is reaction between the ester linkages and endgroup amines, which would break down into amides and alcohols. As materials are stable in organic solutions, such interactions with water molecules are believed to be the cause for the observed rapid gel dissociation. Although these organogels are not particularly suitable for aqueous environments, they may be useful in circumstances that call for the use of organic solvents. Given that these gels dissociate fairly quickly in aqueous solution, they could also be applied in applications that require quick release of a particular entrapped molecule.

5.4. Conclusions

Several crosslinking agents were studied for the purpose of crosslinking glycodendrimer nanoparticles into materials suitable for future use as scaffolds in liver cell support. Of the materials investigated, PEG-DGE resulted in what is believed to be the most suitable materials for application in such cell culture systems. Physical traits such as gel density and swelling ratios can be directly controlled though variations in

dendrimer and crosslinker concentrations during the gelation process. Actual swelling ratios ranged between 2 and 8 for unmodified dendrimers and 3 and 11 for surface modified dendrimers. These values were found to increase for higher ratios of amine to epoxide reaction sites as well as for synthesis with more dilute samples incorporating higher water contents. Resulting materials also have the advantage of being transparent, which would allow for easy visualization of desired cellular studies. The gels should also be biodegradable through enzymatic reaction with ether and amide groups present within the material.

5.5. Further Work & Recommendations

- One recommendation would be to further investigate alternative crosslinking agents, such as those containing PLA or PLGA, which at present are commonly used biocompatible materials for tissue engineering scaffolds. More biocompatible crosslinking agents may allow for easier introduction of cell material during the gelation process itself, which would enable for a more disperse and homogeneous encapsulation of the cells. Additionally, crosslinkers that are more conducive to cell adhesion, unlike PEG which has been shown to decrease cell and protein adhesion [145], could serve to improve scaffold performance. Crosslinking with combinations of larger molecules such as chitosan or gelatin would also be feasible. Preliminary attempts at crosslinking mixtures of gelatin and dendrimer and chitosan and dendrimer did result in gel formation.
- Depending on desired gel properties, crosslinker chain length could also be varied to acquire gels with higher swelling capabilities. Unal et al. (2006) recently synthesized superabsorbent dendrimer gels capable of reaching swelling ratios of

as high as several hundred. Similarly, longer crosslinker chain lengths could also be used to increase the fluidity of the gels, creating a more natural environment for cell suspension.

- In addition, these gels could be further studied for use in drug encapsulation or delivery. The gels would have two modes of encapsulation; the dendrimers themselves, as well as within the gel during the gelation process. Release profiles would therefore behave in a dual manner as well and could potentially, to a certain extent, be controlled by varying crosslinking density or through further surface modifications.
- It is also recommended for further review on possible applications of the acquired organogels. A couple current biomaterial applications being researched for the use of organogels include topical drug delivery [146] and cosmetics [147].

CHAPTER 6: Cell Culture

6.1. Introduction

Tissue engineering is a rapidly evolving field with immense potential for technological advances directed toward the betterment of human life. Liver disease, in particular, is an ever-present problem in modern society, with statistics revealing that worldwide affliction is on the rise. The number of acquired organ donations is not sufficient to handle this growing health problem, evident by the thousands of individuals who currently find themselves on waiting lists to receive such organs. These shortages are creating a demand for alternative tissue sources. The culturing of tissues on engineered scaffold materials may offer one such alternative to donor organs.

Hydrogels are water-swollen polymer networks that have received significant attention in the area of tissue scaffold materials. A number of different materials, from both natural and synthetic origins, have been applied toward hydrogel formation for research in such applications [148, 149, 150]. Dendrimers are monodisperse polymers with layered tree-like branching units. Polyamidoamine (PAMAM) dendrimer-containing networks have been previously studied for various biomedical applications including drug delivery systems [151], gene transfer agents [152], and tissue engineering scaffolds [153]. Thus far no dendrimer-composed hydrogel system has been studied for use as a tissue scaffold material, specifically for use in support of liver cell growth. In this work, synthesized glycodendrimer hydrogels were studied for use as liver cell scaffold support materials. Standard cytotoxicity studies were conducted on glycodendrimers and glycodendrimer-composed hydrogels, as well as cell functionality tests to determine cell behavior during Hep3B culture on hydrogel and material samples.

6.2. Results

6.2.1. Cytotoxicity

6.2.1.1. Dendrimers

Effects on L929 cell morphology in solution phase cytotoxicity tests for G4, G4-M25 and G4-M50 dendrimers at varying concentrations are shown in **Figures 6-1** and **6-2**. Additional photos can be found in **Appendix C** for other dendrimer samples. As shown, higher dendrimer concentrations (0.1 and 0.05 g/ml) resulted in significant changes in cell morphology after only three hours. Cell structure was observed to contract in size while taking on a more spherical shape. Less significant effects resulted

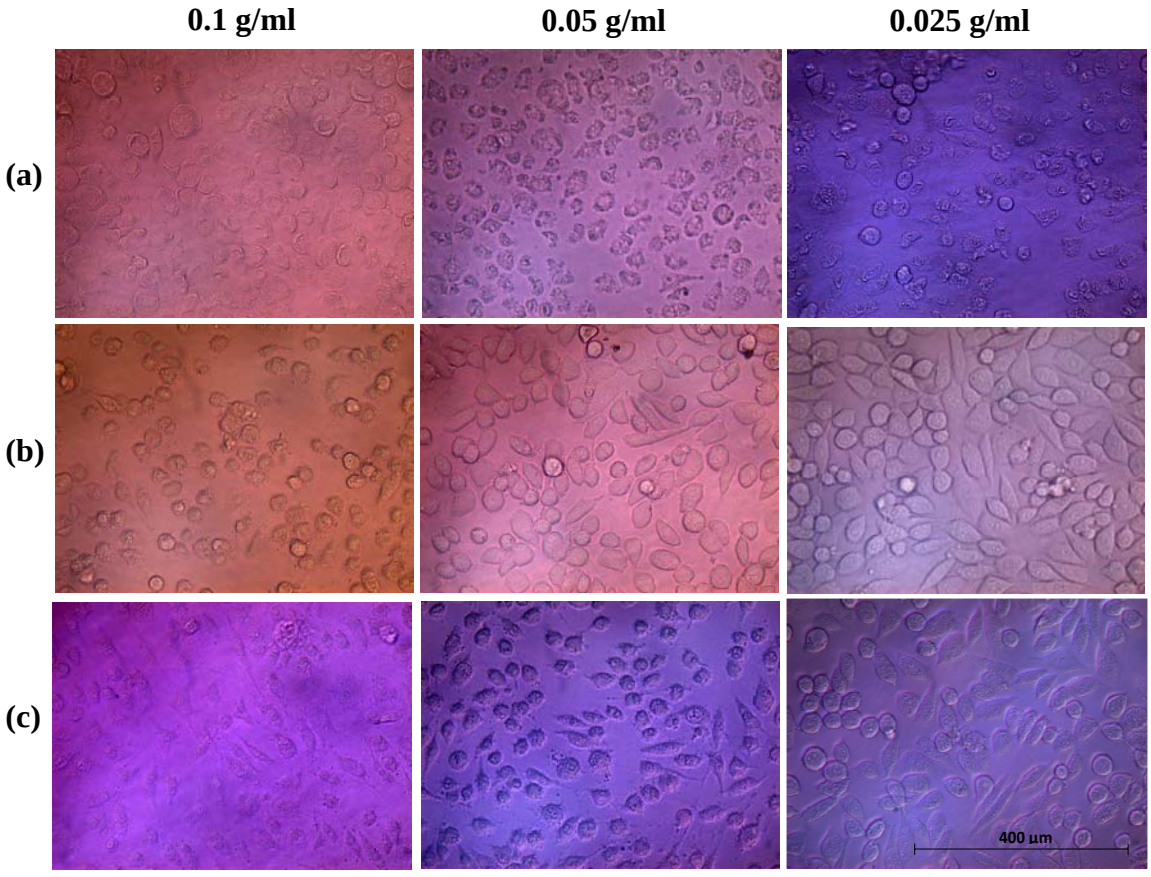

Figure 6-1: Solution phase cytotoxicity tests of (a) G4, (b) G4-M25 and (c) G4-M50 dendrimers. Photos were taken after 3 hours (x20 magnification).

at the lower concentration of 0.025 g/ml, with severity decreasing for dendrimers with higher ratios of carbohydrate end group modification. After 28 hours in sample solutions, almost all cells were observed affected at higher dendrimer concentrations, exhibiting shrunken structures and a loss of proliferation. Cells exposed to G4-M50 and G4-M25 at concentrations of 0.025 g/ml displayed a continuing ability to proliferate during the test period while showing minimal signs of physical damage. A limited number of healthy cells were observed for G4-M25 and G4-M50 dendrimers at a concentration of 0.05 g/ml as well.

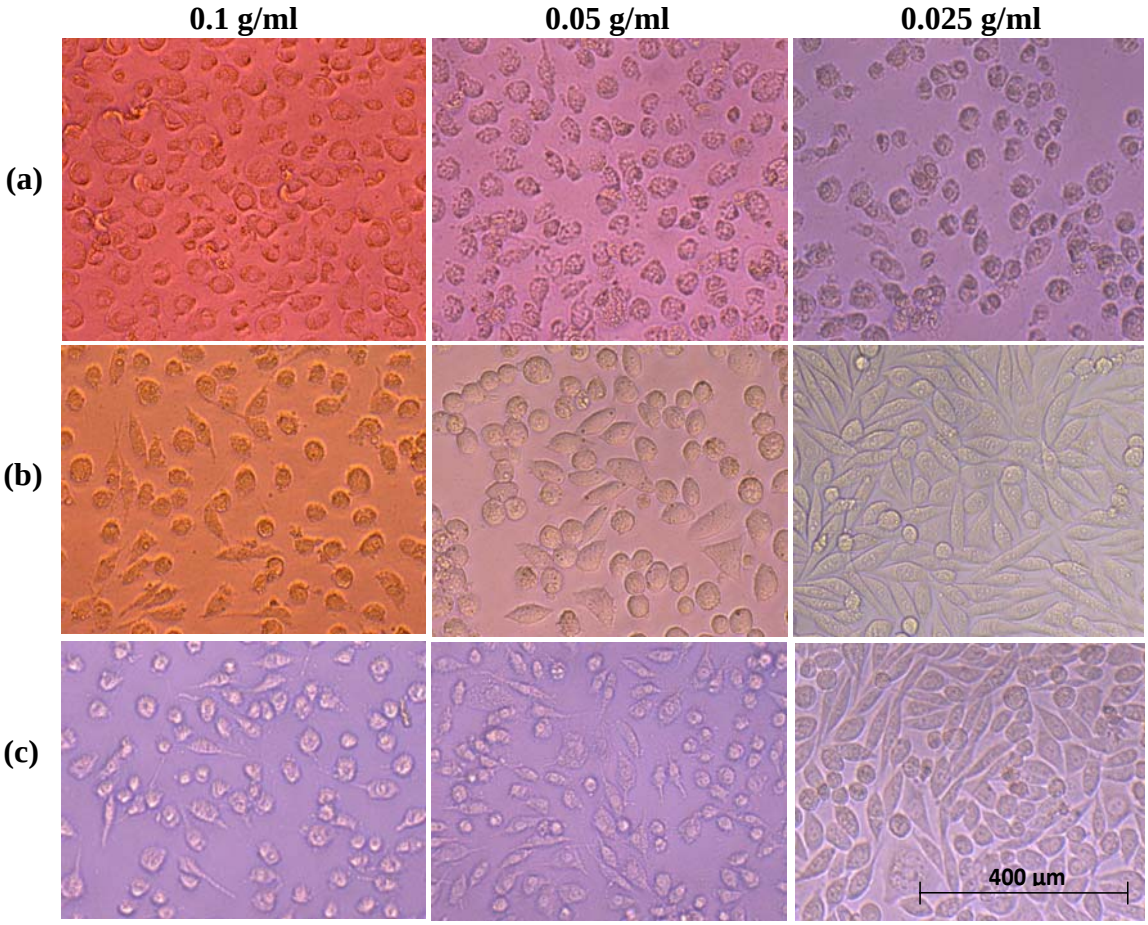

Figure 6-2: Solution phase cytotoxicity tests of (a)G4, (b) G4-M25 and (c) G4-M50 dendrimers. Photos were taken after 28 hours (x10 magnification).

6.2.1.2. PEG-DGE Crosslinked Dendrimer Gels

A majority of PEG-DGE crosslinked dendrimer gels of varying compositions exhibited minimal to no cytotoxic effects on the L929 cell line. In most cases no change in cell morphology was detected, with cells observed to proliferate and spread along the culture plate surface while in direct contact with the hydrogels, as illustrated in **Figure 6-3** below. In some cases cells were even observed to attach to the gels themselves while displaying initial signs of spreading onto and over the gel. This is depicted below for a PEG-DGE crosslinked G4 dendrimer (30:30). PEG-DGE crosslinked G5 dendrimer (20:40) samples did result in detachment of L929 cells from the culture plate surface. Large numbers of cells were observed clumped together, with a significant amount seeming to 'stick' to the gel surface.

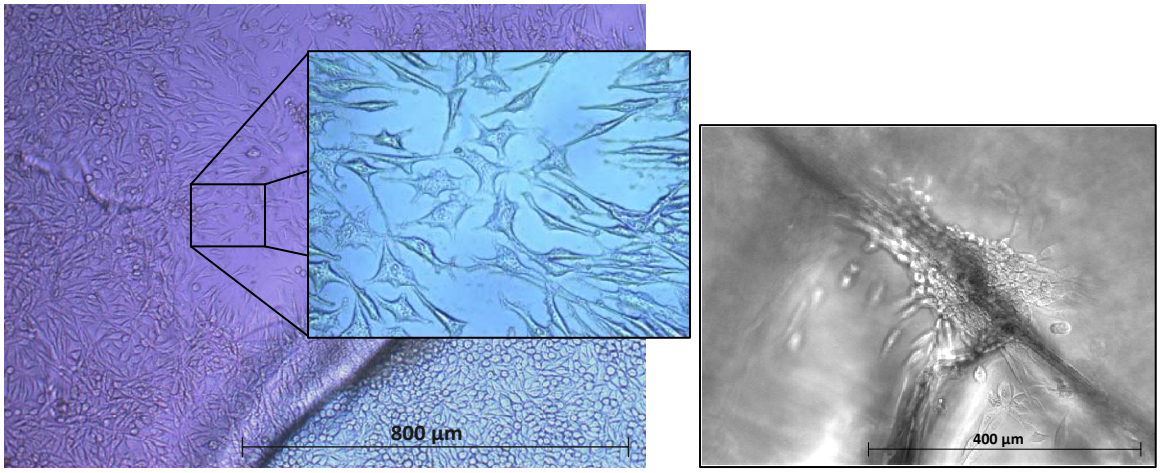

Figure 6-3: Direct contact cytotoxicity test of PEG-DGE crosslinked G4 gel (10:20) (left) and G4-M50 (30:30) (right).

6.2.1.3. Glutaraldehyde Crosslinked Dendrimer Gels

As shown in **Table 6-1,** initial tests of glutaraldehyde crosslinked dendrimer materials (*Method G-1*) resulted in significant signs of toxicity in comparison to PEG-DGE crosslinked gels,. Cytotoxic effects were still observed over significant areas even

after extended submersion of samples in aqueous solution in attempts to remove any unreacted or unbound toxic materials, exceeding even that of the positive control.

Table 6-1: Cytotoxicity of Crosslinked Dendrimers

Sample	Area of Effect (cm^2)
NC	0
PC	6.61
PEG-DGE G4 (30:10)	0
Glut G4 (13:16)	11.60

where NC = negative control
PC = positive control

6.2.2. Hep3B Cell Culture

6.2.2.1. PEG-DGE Crosslinked Dendrimer Gels

Hep3B cells cultured onto various PEG-DGE crosslinked dendrimer gels displayed several different characteristics dependent on the seeding method used; (a) onto the flat surface of dried gels, (b) onto the broken surface of dried gels or (c) onto the surface of swollen gels. Cells seeded onto the surface of dry flat gels were observed to congregate along formed cracks found on the gel surface. The cells then either remained in these long chain formations along the surface imperfections or separated out into larger spheroids (see **Figure 6-4)** that were observed to expand in size over time. Cells seeded onto the broken surfaces of dried gel materials were primarily observed to congregate into a number of spheroids that were spread out over the surface of the gel. The number and size of these cell masses varied from sample to sample, while growing in size over extended lengths of culture. This particular seeding method was found to be most

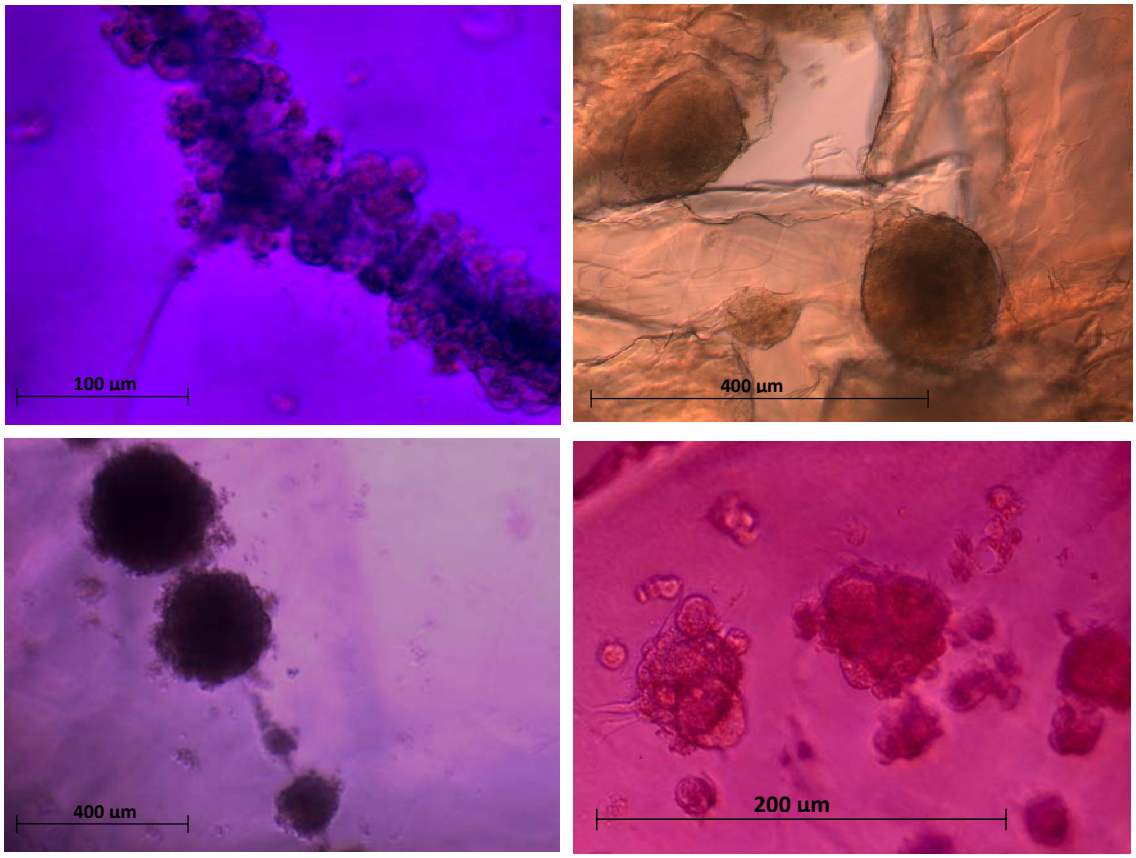

Figure 6-4: Hep3B cells seeded onto a dry flat gel surface (upper left = G4 (30:10), lower left = G4 (40:10) and a dry broken gel surface (upper right = G5 (40:20), lower right =G4M50 (20:20)).

effective in achieving cell attachment to gel surfaces. Seeding onto gels already in their swollen states did result in slight cell attachment, but this was significantly less than that attained when seeding onto gels in their dry state.

Upon close ispection, individual cells taking on more elongated spreading morphologies can be seen attached and spreading onto gel surfaces. These cells typically extend out from the main cell mass. An increase in gel dendrimer content resulted in improved initial cell attachment. Gels containing galactose surface groups exhibited an increased number of spheroid formations in comparison to those that didn't. Increased PEG-DGE content and lack of galactose surface moieties resulted in fewer more highly spaced spheroids. Complete breakdown of the most gel-like substances resulted within 7

days of culture. No significant degradation of more highly crosslinked materials was noted. Samples *were* observed to continuously expand over the course of cell culture however, indicating some breakdown of scaffold networks may have been taking place.

6.2.2.2. Glutaraldehyde Crosslinked Dendrimer Gels

Due to their previously observed cell toxicities in direct contact experiments, cell culture results for glutaraldehyde crosslinked materials were expected to be less promising than the previously discussed PEG-DGE crosslinked gels. As somewhat anticipated, cells were observed to die out quickly in a number of seeded culture wells, with prolonged attachment predominantly failing. A number of *Method G-1* synthesized materials, however, were also observed to support cell growth in segmented areas as can be seen in **Figure 6-5**. These results were rather inconsistent, varying from sample to sample. Once successfully attached, however, cells did appear to proliferate and spread over a specific area. In most instances cell growth was witnessed over an 'edgy' or

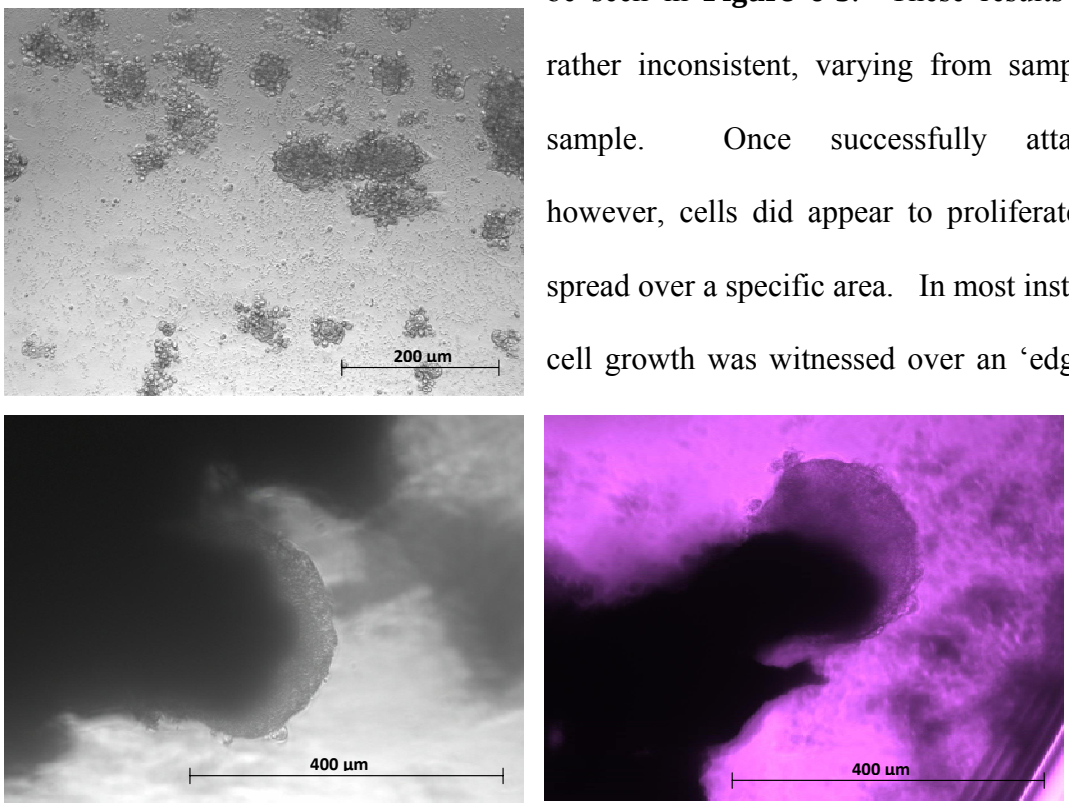

Figure 6-5: Hep3B culture onto glutaraldehyde crosslinked dendrimers; Upper left – G4 *Method G-2*, *Lower Left/Right* – G4M50 *Method G-1*.

protruding area of the material, such as those seen in the cell culture photos. Over time the cells were observed to expand into the pictured globular cell masses. Culture onto *Method G-2* synthesized gels resulted in the initial formation of smaller spheroid clusters along the gel surface. Proliferation, to a large degree, was observed to be limited on these materials. Prolonged cell survival was typically not attained on these materials, with significant decreases in cell number occurring after approximately one week of culture.

6.2.3. Functional Assay

6.2.3.1. PEG-DGE Crosslinked Dendrimer Gels

EROD assays performed on cells cultured on various glycodendrimer-composed hydrogels produced a range of results. Cultures with gels comprised of surface modified dendrimers and higher crosslinker content produced higher P450 production readings. Only cells seeded onto gels consisting of G4M50 dendrimers resulted in higher P450 production readings than blank (flat cellular sheet) cultures. Cells were noted to maintain at or near their maximum production levels through the end of cell culture experiments (7 days in the case of culture of **Figure 6-6)**. Additional culture studies demonstrated continued function of up to 16 days for selected G4M50 containing gel samples.

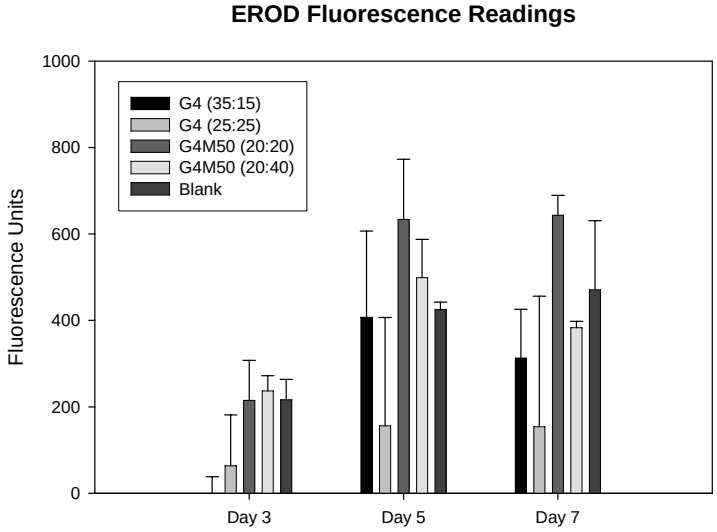

Figure 6-6: EROD assay results

Accurate results for MTT analysis proved difficult as a significant number of undissolved formazon crystals were found within a number of the gels even after extended exposure times in DMSO. This will have considerable effects on data accuracy, with produced results being lower than the actual values that would otherwise be attained. Regardless of the concerns on accuracy, the results still indicate cellular proliferation was occurring within gel sample systems, with moderate increases observed for G4M50 containing gels from Day 3 to Day 7 of cell culture. Highest proliferation was still observed in blank culture systems.

Table 6-2: MTT cell culture results

Sample	Day 3	Day 7
G4 (35:15)	0.22±0.02	0.18±0.03
G4 (25:25)	0.30±0.02	0.20±0.02
G4M50 (20:20)	0.29±0.02	0.57±0.06
G4M50 (20:40)	0.35±0.03	0.47±0.10
Blank	0.74±0.08	1.60±0.13

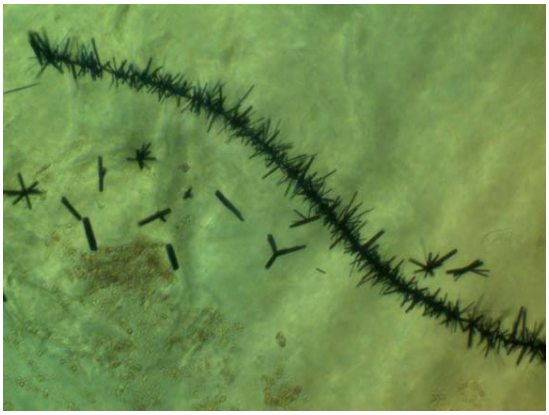

Figure 6-7: Undissolved formazon crystals in (G4M50 (20:40)) sample

6.2.3.2. Glutaraldehyde Crosslinked Dendrimer Gels

Despite the poor overall performance in initial cell attachment, several glutaraldehyde crosslinked material samples did display the support and maintenance of adequate cellular growth and function. In fact, through nine days of culture, cells seeded onto certain prepared samples of glutaraldehyde crosslinked G4 and G5 dendrimers

showed higher P450 production at comparable stages in PEG-DGE crosslinked culture studies.

Table 6-3: EROD assay results for glutaraldehyde crosslinked materials

Sample	Day 3	Day 6	Day 9
G4 (13:16)	128±35	629±95	913±224
G5 (13:16)	158±83	530±291	997±197
G4M50 (15:35)	129±53	1092±177	464±279
Blank	115±13	88±64	169±172

Table 6-4: MTT assay results for glut. crosslinked materials

Sample	Day 3	Day 7
G4 (13:16)	1.23±0.28	0.80±0.12
G4 (13:16)	1.19±0.57	0.80±0.19
G4M50 (15:35)	0.23±0.00	0.31±0.02
Blank	0.74±0.08	1.60±0.13

MTT analysis also indicates extensive proliferation within the first several days of culture for *Method G-1* materials, with culture systems still maintaining a fairly moderate level of proliferation in comparison to blank systems up to a period of one week. As expected from culture observations, proliferation on *Method G-2* gels was the most limited.

6.3. Discussion

6.3.1. PEG-DGE Crosslinked Dendrimer Gels

Dendrimer hydrogels synthesized with a PEG-DGE crosslinking agent were found to exhibit little to no visible signs of direct contact toxicity, with exception to a few samples containing high dendrimer contents. As solution phase toxicities of all dendrimer particles induced cytotoxic effects, crosslinking has then been shown to be adequate in most cases for negating or shielding any negative effects arising from

dendrimer surface charges. The fact that addition of galactose moieties to dendrimer surfaces was shown to reduce solution phase cytotoxic effects is an indication that they will adequately perform their hypothesized dual role of shielding surface charges and increasing interactions with Hep3B cells.

Gel scaffold materials were shown to support the culture and survival of Hep3B cells up to a period of two weeks with maintenance of cellular functions. Bio/degradability was displayed by the fairly rapid breakdown of the more fluid, low crosslinking density gels. As the materials were previously stable after extended submersion in aqueous solution prior to culture, degradation is believed to be the result of the culture environment; possibly a combination of chemical hydrolysis [154] and enzymatic breakdown derived from the cells themselves.

Similar to previously reported materials containing or modified with galactose surface moieties [155, 156], cells were observed to form into segmented spheroids on synthesized gel surfaces. Enhanced cellular function was found for culture onto materials containing dendrimers of greater surface modification. This indicates that the galactose surface moieties did affect cellular function as to their intended role. Increased cellular function was also observed for higher crosslinker concentrations. This can be linked to the increased proliferation that was observed to take place on the harder, more solid surfaces. This increased proliferation should eventually translate into the subsequent performance of cellular functions.

Acquired MTT and EROD results also indicate a higher level of per-cell function for cells cultured onto gel samples, as proliferation (translating to number of cells) was observed to be significantly lower than blank cultures yet production levels of P450 were higher. This would be expected given the reported increase in cell functions for liver cell

spheroid morphologies [157] and typical mammalian cell proliferation versus function behavior [7].

6.3.2. Glutaraldehyde Crosslinked Dendrimer Gels

Cell culture onto materials synthesized using glutaraldehyde as a crosslinking agent displayed some signs of success, even though moderate cytotoxic effects were observed in L929 fibroblast and most Hep3B cell cultures. The observed high toxicity is believed to be linked to the toxic nature of glutaraldehyde itself. As previously mentioned, even medically applied glutaraldehyde crosslinked materials have been reported to induce cytotoxic effects due to leeching. For materials synthesized under conditions of high *r* values, as in these studies, there is an increased probability for the presence of free glutaraldehyde molecules within the materials. Despite the toxicity issues, once cells were successfully attached to material surfaces, proliferation and expansion into larger cell masses was witnessed to proceed fairly well.

The highest levels of initial proliferation were encountered on *Method G-1* materials, which continued to display significant cell support through nine days of cell culture. Similar to PEG-DGE materials, proliferation occurred at higher levels on materials offering a more solid support. Maximum cellular function was obtained for *Method G-2* materials on Day 6 but dropped dramatically by Day 9, at which point significant quantities of the gels had dissociated into solution. *Method G-1* materials hit their maximum at Day 9, reaching twice the levels of blank systems. This indicates the possibility for extended culture of Hep3B cells with support of function and survivability on these materials. No degradation of these materials was observed throughout the designated culture periods.

6.4. Conclusions

Hep3B hepatoma cells were successfully cultured onto PEG-DGE crosslinked glycodendrimer gels. These materials maintained cell survival while enhancing specific cellular function of cytochrome P450 production. Increased crosslinker to dendrimer ratios and presence of galactose surface ligands resulted in improved cellular attachment, survival and function. These findings demonstrate the potential use for such materials in the application of engineered scaffolds for purposes of cell culture support, in this specific case for support of liver cells.

Cells cultured onto glutaraldehyde crosslinked materials displayed higher toxic effects with a more limited effectiveness for supporting initial cell growth, most likely deriving from the toxic nature of the crosslinking agent. Upon successful attachment, however, these materials supported high levels of cell function while maintaining adequate cell survivability. With improved and cleaner synthesis methods to increase reproducibility and decrease initial toxicity; these materials could also make suitable scaffold materials for cell support.

6.5. Future Work & Recommendations

- Future work could include further in-depth culture studies. One recommendation would be to try and encapsulate the cells within the gel during the gelation process. This may a problem, however, due to the longer gelation times required to get the more fluid gels that are desired. One way around this may be cell introduction at the later stages of crosslinking, at a point where the gel is still very fluid but not yet fully crosslinked. The main limitation will be that the cells cannot survive for a long period of time

without culture medium, and if medium is added before crosslinking is complete the gel may simply dissociate into solution. Initial use of serum-free culture medium as the reaction solvent in place of water may be one way to help alleviate this problem.

- As suggested in the text, given the initial culture results for *Method G-1* glutaraldehyde crosslinked materials, improved synthesis methods may allow for acquisition of more homogeneous and less toxic inducing materials that could be reasonably implemented as scaffold support materials. Due to the lack of degradation, application would most likely be limited to *in-vitro* use in temporary support devices.

- The culture of actual hepatoma cells, instead of cancer cell lines could also be undertaken. This would give a better insight into how these materials would perform in real-life applications in respect to supporting actual liver growth and function.

- As discussed previously in **Chapter 2**, the study of coculture systems may also be employed as a means to further improve scaffold performance. This would most likely be performed with the introduction of an epithelial cell line in conjunction with the already studied Hep3B cell line.

CHAPTER 7: Additional Studies

7.1. Introduction

One of the more central areas of concern in these studies was the number of reactions needed to reach the desired end product. This includes synthesis of the carbohydrate core along with actual dendrimer growth. For this reason, a number of alternate routes were studied in an attempt to decrease the total number of reactions required, focusing specifically on core molecule preparation and the overall conversion of the carbohydrate hydroxyls to amines.

7.2. One-Pot Conversion of Alcohol to Amine

Reddy et al. (2000) had previously demonstrated a one-pot synthesis of converting an alcohol to an amine for linear chain alcohols. This reaction has a similarity to *step-4* of *scheme-1*, in that it involved reaction of hydroxyls with triphenylphosphine. Further reaction, however, involved sodium azide and reduction with water, instead of the use of CBr_4. This one-pot method was found unsuccessful for the conversion of carbohydrate hydroxyls to amines, however. The main reason for this is thought to be that the reaction conditions required are just too harsh for use with carbohydrates, and simply results in the degradation of the sugar molecules. No discernable products were identified through analytical means. This method was therefore deemed unsuitable for use as an alternative reaction pathway in the production of amine endgroups for these studies.

7.3. Peptide Coupling onto a Trehalose Core

Direct coupling of a peptide onto the hydroxyls of a trehalose molecule was attempted as another alternate reaction route to attaining amine end-groups on a

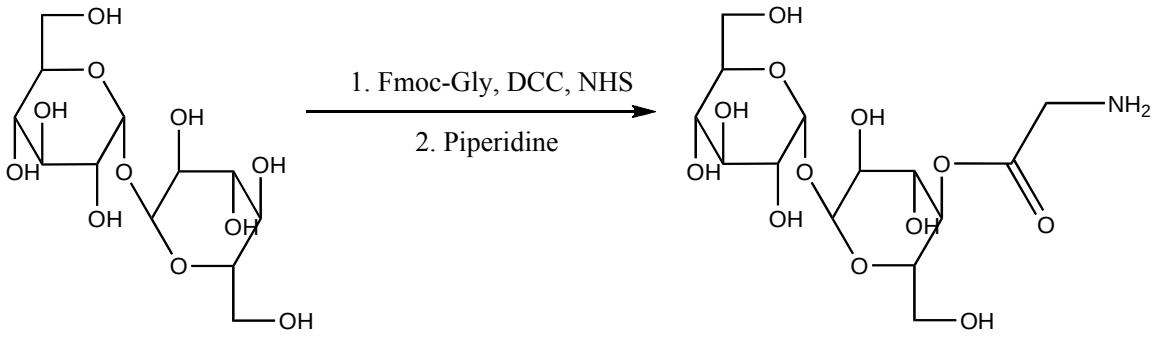

Figure 7-1: Coupling reaction of trehalose with Fmoc-glycine using DCC and NHS.

carbohydrate core. This was performed through a zero-length crosslinking reaction while utilizing 9-fluorenylmethyl carbamate (Fmoc) protecting group chemistry. The coupling procedure was identical in nature to that used in the surface modification of dendrimers, except in this case reaction was between an activated carboxylic acid and the carbohydrate hydroxyl instead of an amine. A single glycine coupling is depicted in **Figure 7-1**. Since the coupling reaction with hydroxyls is slower than with amines, the reaction was run for several days to allow for the highest attainable levels of conversion. N,N'-dicyclohexylurea (DCU) byproduct was seen to precipitate from solution over the course of reaction. Filtered DCU byproduct was used as an indicator towards extent of reaction in cases not using NHS, as it will only be formed upon successful coupling of the amine and hydroxyl and is mostly removed through the filtration process.

Fmoc protecting-group chemistry is commonly used in solid phase peptide synthesis (SPPS) procedures, allowing for the coupling of two particles while preserving the desired active end groups, which in this case is the amine. Mild basic conditions presented by piperidine after coupling removes Fmoc, leaving open amines. After deprotection and product concentration, Fmoc-piperidine byproduct (see **Figure 7-2**) was removed from aqueous solution through filtration. The Fmoc-piperidine complex was

observed to be a yellow colored solid. Carbon dioxide is the other byproduct produced in this reaction, which thermodynamically drives the whole process [158].

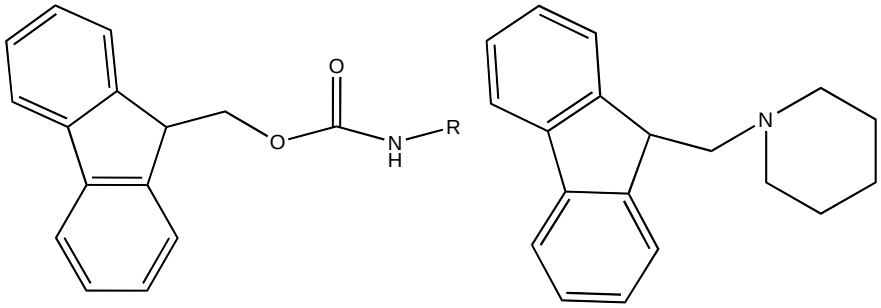

Figure 7-3: Fmoc protecting group on a terminal amine (left), and Fmoc-piperidine byproduct (right).

Final concentrated product was found to be a clear to white colored sticky solid. Mass peaks of up to six glycine substitutions were clearly identified in MALDI-TOF-MS spectra of the material, with six substitutions displaying the largest signal (see **Figure 7-3**). This suggests that crowding and steric hindrance became too high for further reaction after six substitutions were attained. A minor peak that would represent complete end group conversion (seven substitutions) was observed in one spectrum (see **Appendix D**, **Figure D-1**), but this peak could not be *clearly* obtained and reproduced in subsequent testing. Mass peaks were observed to be

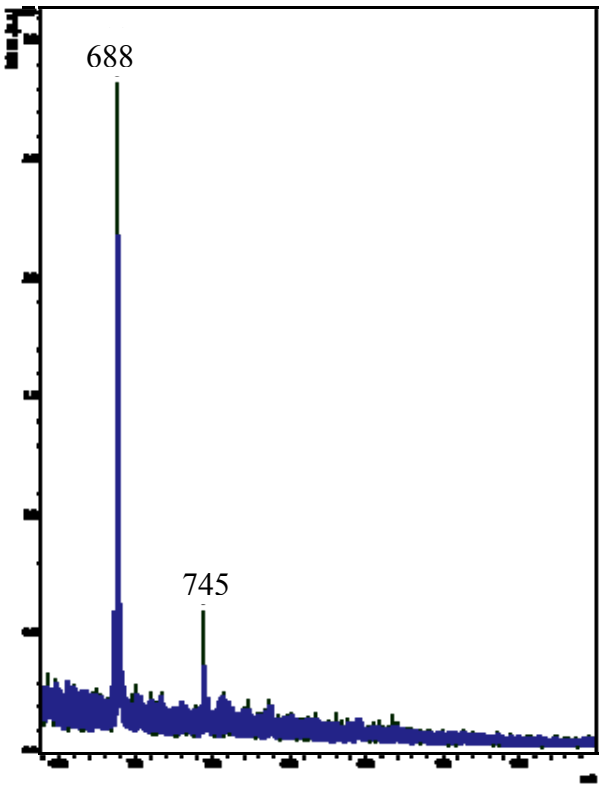

Figure 7-2: MALDI-TOF-MS spectra for products of glycine to trehalose coupling.

slightly off from actual values (+4 amu in one set of spectra and -5 amu in another). Increments of exactly 57 mass units, however, were identified between major peaks (688, 745), signifying increasing glycine group substitution. Instrument calibration or ionic effects may have caused the errors in mass peak values for the particles.

Product TGA analysis revealed two main degradation peaks (see **Appendix D**, **Figure D-2**). The first peak is believed to result from moisture absorbed by the product before analysis, with weight loss observed to begin at approximately 100 °C. The second peak, belonging to the main product, was calculated to have a Tg value of 283.03 °C. This value is higher than degradation temperatures for both glycine (240 °C) and trehalose (~200 °C). The shape of this peak is also quite smooth, indicating product should be fairly uniform in nature; consisting of a majority of the six glycine-substituted product form based on mass analysis.

In conclusion, although complete coupling of all trehalose hydroxyls was unable to be achieved in good yield, this reaction could still be used for possible dendrimer synthesis in cases where geometric symmetry is not of utmost importance. The reaction was shown to produce a trehalose core with up to six reactive branching arms in good yield, which will allow for fast growth in terms of size and number of end groups. Most importantly, however, is that this reaction allows for the acquisition of amine end groups on a carbohydrate core in one relatively simple step. This would be a significantly less intensive reaction scheme than either of the previously discussed and utilized galactose-core preparation pathways of *scheme-1* or *scheme-2*. One potential limitation with these molecules is that the starburst effect may occur at a much smaller generation as a direct result of the number of arm units in conjunction with the relatively small core size. This

may considerably limit the size of dendrimers maximum growth, and therefore may be unsuitable for applications that require larger particle sizes.

7.4. Peptide Coupling onto a G0 Galactose-Centered Dendrimer Core

Similar to the reaction discussed with peptide coupling to a trehalose core, here a coupling reaction was attempted between the amine endgroups of a zero generation galactose-centered PAMAM glycodendrimer and a G2 peptide dendron of the form Fmoc-lysine-lysine-glycine as seen in **Figure 7-4**. The bold glycine unit depicted in the figure will be the point of reaction for coupling. Fmoc protecting group chemistries were implemented in similar fashion, with Fmoc groups present on end lycine units (not pictured in the figure) during coupling. The peptide dendron itself was synthesized using SPPS procedures through utilization of a peptide synthesizer (MultiPep, Intavis AG Bioanalytical Instruments). The core glycodendrimer is the G0 dendrimer acquired using *scheme-2* in this research, possessing five reactive endgroup amines. This reaction could also be thought of as the final step of a convergent dendrimer synthesis.

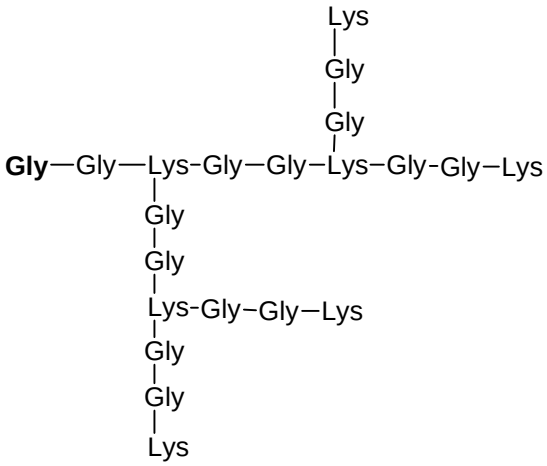

Figure 7-4: G2 peptide dendron of the form Gly-Gly-Lys

Clearly visible peaks corresponding to the peptide and a single dendron coupling onto the dendrimer core (peak A) were observed in MALDI-TOF-MS spectra of dendrimer-peptide reaction product. A broad peak and a weak intensity broad hump that would represent second (peak B) and third (peak C) couplings can also be seen. **Figure**

7-5 depicts a MALDI-TOF spectrum covering the mass range of coupled products. Calculated versus acquired mass data for dendron-dendrimer couplings can be viewed in **Table 7-1**. MALDI-TOF mass peaks for peptide as well single-coupled product (a specific peak within a broad peak) correspond well with calculated values. No specific peaks were observed for further couplings; however the apex of peak B still matches closely to the expected calculated value for that of two couplings. The apex of peak C is difficult to precisely determine due to its weak intensity and broad nature, but the mass range over which the peak is observed does cover the calculated mass for a three coupled product.

Table 7-1: Mass data for peptide-dendrimer coupling

Molecule	Molecular Wt. MALDI	Calc.	#endgroup amines
1-coupling	2107	2109	12
2-couplings	~3800	3822	19
3-couplings	~5600	5535	26
Peptide	1712	1713	8

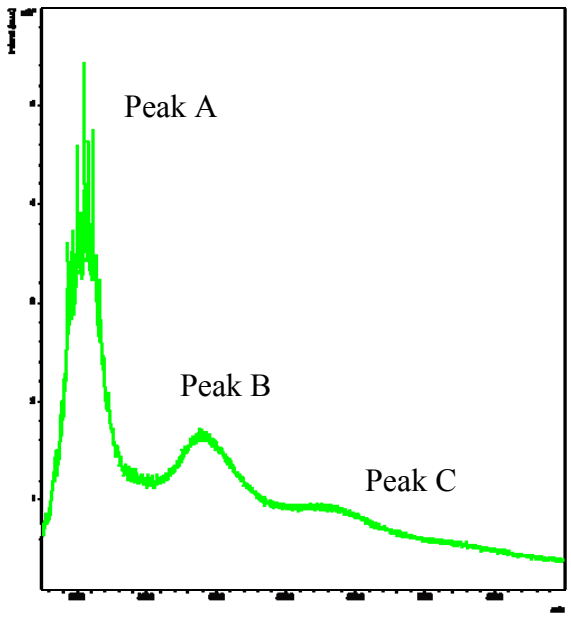

Figure 7-5: MALDI-TOF-MS for G2 peptide coupling to a G0 glycodendrimer core

The acquisition of broad mass peaks is most likely a result of minor defects present within the molecules in combination with other salt peaks. The presence of impurities could also affect clean peak acquisition. Additional peaks that were considered but not found are those for dimer dendron particles (resulting in peaks at twice the dendron molecule weight) and double charged molecules (resulting in peaks at half the molecular weight). One reason for the

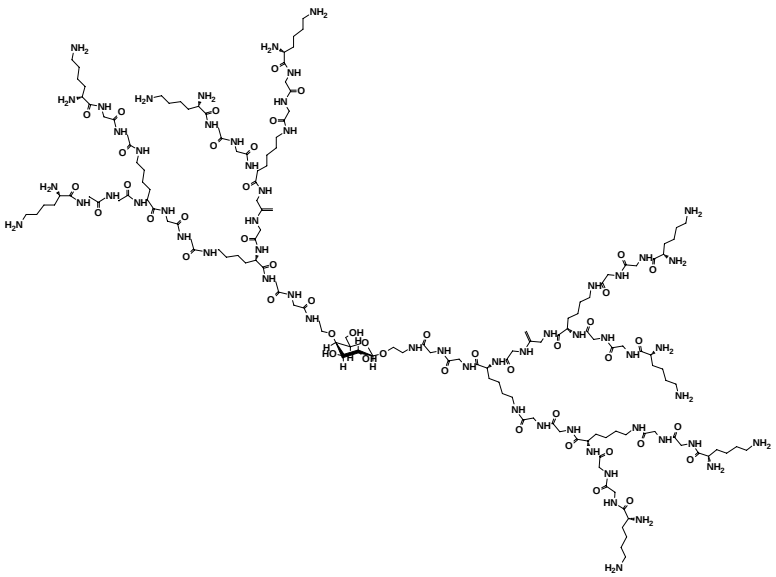

Figure 7-6: G0 dendrimer with two coupled peptide dendrons

limited number of coupling reactions observed could be attributed to the large size of the peptide dendrons in comparison to the smaller dendrimer core. This disparity in size would create significant steric hindrance after several dendron couplings onto the core molecule, which is a common problem encountered in convergent dendrimer synthesis. From a purely visual perspective it would seem that up to three substitutions should be able to adequately couple without much problem, so there may be additional factors contributing to the lack of reaction such as solvent or mixing conditions. In addition to steric issues, proper alignment of the larger peptide dendrons for reaction with remaining core amines will also become a major limitation. Extending spacer arms onto the core reactive groups might be one way to help alleviate steric concerns and increase coupling yields.

In conclusion, indication is that a successful zero length coupling reaction of up to three couplings of a G2 peptide dendron onto a G0 glycodendrimer core was achieved. Steric effects in conjunction with other unknown factors most likely contributed to the

lack of additional or complete coupling. Resulting products should be biocompatible as well as biodegradable, given that their composition is made entirely of amino acid chains and a carbohydrate core. Mechanical SPPS synthesis for dendron production on a solid support is beneficial in terms of reducing the physical requirements otherwise needed for sidearm chain synthesis. Increased coupling will be needed in order to acquire more applicable products possessing higher numbers of reactive endgroups with additional ability such as encapsulation.

CHAPTER 8: CONCLUSIONS

In conclusion,

- An amine terminated galactose core for extended PAMAM dendrimer synthesis was constructed through two reaction pathways. Dendrimer synthesis was then extended up to generation four where dendrimer particles were surface modified with a galactose moiety to improve biocompatibility of the dendrimers for use in scaffold materials to be applied in Hep3B cell culture systems.
- Glycodendrimer particles were crosslinked into solid form using crosslinking agents of PEG-DGE, PEG-DA and glutaraldehyde. Increased gel swelling ratios were found for materials formed under gelation conditions of lower *r* values and higher solvent content, as well as for materials synthesized with surface modified dendrimers.
    - PEG-DGE formed stable hydrogel materials ranging from fluid gels to stiff solids. These materials exhibited the highest swelling capabilities of the materials studied.
    - PEG-DA crosslinked materials were found to form stable organogels, but dissociated within 24 hours as hydrogels.
    - Glutaraldehyde reaction was found to proceed very quickly, primarily resulting in solid inhomogeneous products. Gelation of surface modified dendrimers was attained under reaction conditions of high mixing speed and diluted crosslinker addition.

- Cytotoxicity and cell culture studies of PEG-DGE and glutaraldehyde crosslinked materials were conducted.
    - PEG-DGE materials were primarily found to be nontoxic, with selected materials found to support the survival and maintenance of enhanced cellular function up to periods of two weeks. Increased surface modification along with higher gel crosslinker contents resulted in improved displays of cell function.
    - Glutaraldehyde crosslinked materials induced a fair degree of cytotoxic effects. Upon successful initial cell seeding, however, cells were observed to proliferate and exhibit sustained enhanced function for periods of up to nine days.

Synthesized galactose-centered PAMAM dendrimers were successfully applied as major components in a hydrogel scaffold material. Allowing for easy property manipulation through control of gelation conditions while displaying low signs of cytotoxicity and promising Hep3B cell culture result, PEG-DGE crosslinked glycodendrimers are considered to have the highest potential for future use as cell scaffolding materials.

CHAPTER 9: REFERENCES

[1] Hepatitis and Liver Disease in the United States, http://www.liverfoundation.org/images/articles/1008/generalLD.pdf, *The American Liver Foundation*. 2005.
[2] Facts at a Glance Liver and Liver Disease, http://www.liverfoundation.org/images/articles/1104/FactsAtAGlanceTheLiver.pdf, *The American Liver Foundation*. 2002-2003.
[3] ALF Transplant Fund, http://www.liverfoundation.org/db/articles/1029, *The American Liver Foundation*. 2002-2003.
[4] Gray, H. Anatomy of the Human Body. Philadelphia: Lea & Febiger. 1918; Bartleby.com, 2000. www.bartleby.com/107/.
[5] Guyton, A. C. and Hall, J. E. Textbook of Medical Physiology. W. B. Saunders Company, 2000.
[6] April, E. W.; Erickson, A.; Montano, S. Anatomy. New York: Wiley; Media, Pa: Harwal Pub. Co. 1984.
[7] Arias, I. M. The Liver: Biology and Pathobiology. New York: Raven Press. 1982.
[8] Surrenti, C.; Casini, A.; Milani, S.; Pinzani, M. Fat-storing cells and liver fibrosis: proceedings of the 71st Falk Symposium held in Florence, Italy, July 1-3, Kluwer Academic Publisher. 1993.
[9] LeBouton, A. V. Molecular and Cell Biology of the Liver. Boca Raton: CRC Press. 1993.
[10] Michalopoulos, G. K. and DeFrances, M. C. Liver regeneration, *Science*, 276, pp. 60-66. 1997.
[11] How the Liver Works, http://www.cooperhealth.org/content/greystone_18102.asp, *Cooper University Hospital*. 2006.
[12] Arroyo, V.; Gines, P.; Rodes, S.; Schrier, R. W. Ascites and renal dysfunction in liver disease: pathogenesis, diagnosis, and treatment. Oxford: Blackwell Publishing. 2005.
[13] Arias, I. M.; Jakoby, W. B.; Popper, H.; Schachter, D.; Shafritz, D. A. The Liver: Biology and Pathobiology. New York: Raven Press. 1998.
[14] Chua, K.; Lim, W.; Zhang, P.; Lu, H.; Wen, J.; Ramakrishna, S.; Leong, K. W.; Mao, H. Stable immobilization of rat hepatocyte spheroids on galactosylated nanofiber scaffold, *Biomaterials*, 26, pp. 2537-2547. 2005.
[15] Catapano, G.; De Bartolo, L.; Vico, V.; Ambrosio, L. Morphology and metabolism of hepatocytes cultured in Petri dishes on films and in non-woven fabrics of hyaluronic acid esters, *Biomaterials*, 22, pp. 659-665. 2001.
[16] Ying, L.; Yin, C.; Zhuo, R. X.; Mao, H. Q.; Kang, E. T.; Neoh, K. G. Immobilization of Galactose Ligands on Acrylic Acid Graft-Copolymerized Poly(ethylene terephthalate) Film and Its Application to Hepatocyte Culture, *Biomacromolecules*, 4, pp. 157-165. 2003.
[17] Du, Y.; Chia, S.; Han, R.; Chang, S.; Tang, H.; Yu, H. 3D hepatocyte monolayer on hybrid RGD/galactose substratum, *Biomaterials*, Article in Press, pp. 1-12. 2006.
[18] Ding, Z.; Chen, J.; Gao, S.; Chang, J.; Zhang, J.; Kang, E. T. Immobilization of chitosan onto poly-$_L$-lactic acid film surface by plasma graft polymerization to control the morphology of fibroblast and liver cells, *Biomaterials*, 25, pp. 1059-1067. 2004.
[19] Yin, C.; Liao, K.; Mao, H.; Leong, K. W.; Zhou, R.; Chan, V. Adhesion Contact Dynamics of HepG2 Cells on Galactose-Immobilized Substrate, *Biomaterials*, 24, pp. 837-850. 2003.
[20] Wang, X. H.; Li, P. D.; Wang, W. J.; Feng, Q. L.; Cui, F. Z.; Xu, Y. X.; Song, X. H. Covalent immobilization of chitosan and heparin on PLGA surface, *International Journal of Biological Macromolecules Structure, Function and Interactions*, 33, pp. 95-100. 2003.
[21] Zhang, Y.; Wang, W.; Feng, Q.; Cui, F.; Xu, Y. A novel method to immobilize collagen on polypropylene film as substrate for hepatocyte culture, *Materials Science & Engineering C*, 26, pp. 657-663. 2006.
[22] Kurosawa, H.; Yuminamochi, E.; Yasuda, R.; Amano, Y. Morphology and Albumin Secretion of Adult Rat Hepatocytes Cultured on a Hydrophobic Porous Expanded Polytetrafluoroethylene Membrane, *Journal of Bioscience and Bioengineering*, 95, pp. 59-64. 2003.

[23] Lu, H.; Lim, W. S.; Want, J.; Tang, Z.; Zhang, P.; Leong, K. W.; Chia, S. M.; Yu, H.; Mao, H. Galactosylated PVDF Membrane Promotes Hepatocyte Attachment and Functional Maintenance, *Biomaterials*, 24, pp. 4893-4903. 2003.
[24] Dewez, J. L.; Lhoest, J. B.; Detrait, E.; Berger, V.; Dupont-Gillain, C. C.; Vincent, L. M.; Schneider, Y. J.; Bertrand, P.; Rouxhet, P. G. Adhesion of mammalian cells to polymer surfaces: from physical chemistry of surfaces to selective adhesion on defined patterns, *Biomaterials*, 19, pp. 1441-1445. 1998.
[25] Catapano, G.; Di Lorenzo, M. C.; Della Volpe, C.; De Bartolo, L; Milgiaresi, C. Polymeric membranes for hybrid liver support devices: the effect of membrane surface wettability on hepatocyte viability and functions. *Journal of Biomaterials Science: Polymer Edition*, 7, pp. 1017-1027. 1996.
[26] Tanaka, M.; Nishikawa, K.; Okubo, H.; Kamachi, H.; Kawai, T.; Matsushita, M.; Todo, S.; Shimomura, M. Control of hepatocyte adhesion and function on self-organized honeycomb-patterned polymer film, *Colloids and Surfaces A: Physicochemical and Engineering Aspects*, 284-285, pp. 464-469. 2006.
[27] Kim, S.; Hoshiba, T.; Akaike, T. Effect of carbohydrates attached to polystyrene on hepatocyte morphology on sugar-derivatized polystyrene matrices, *Journal of Biomedical Materials Research Part A*, 67A, pp. 1351-1359. 2003.
[28] Cho, C. S.; Seo, S. J.; Park, I. K.; Kim, S. H.; Kim, T. H.; Hoshiba, T.; Harada, I.; Akaike, T. Galactose-carrying polymers as extracellular matrices for liver tissue engineering, *Biomaterials*, 27, pp. 576-585. 2006.
[29] Kawase, M.; Shiomi, T.; Matsui, H.; Ouji, Y.; Higashiyama, S.; Tsutsui, T.; Yagi, K. Suppression of Apoptosis in Hepatocytes by Fructose-Modified Dendrimers, *Journal of Biomedical Materials Research*, pp. 519-524. 2001.
[30] Tirrell, M.; Kokkoli, E.; Biesalski, M. The Role of Surface Science in Bioengineered Materials, *Surface Science*, 500, pp. 61-83. 2002.
[31] Dubber, M.; Lindhorst, T. K. Synthesis of Chiral Carbohydrate-Centered Dendrimer, *Chemical Communications*, pp. 1265-1266. 1998.
[32] Wang, X. H.; Li, D. P.; Wang, W. J.; Feng, W. L.; Cui, F. Z., Xu, Y. X., Song, X. H. Covalent immobilization of chitosan and heparin on PLGA surface, *International Journal of Biological Macromolecules*, 33, pp. 95-100. 2003.
[33] Park, K-H. and Song, S. C. Morphology of spheroidal hepatocytes within injectable, biodegradable, and thermosensitive poly(organophosphazene) hydrogel as cell delivery vehicle, *Journal of Bioscience and Bioengineering*, 101, pp. 238-242. 2006.
[34] Park, I.; Yang, J.; Jeong, H.; Bom, H.; Harada, I.; Akaike, T.; Kum, S.; Cho, C. Galactosylated chitosan as a synthetic extracellular matrix for hepatocyte attachment, *Biomaterials*, 24, pp. 2331-2337. 2003.
[35] Li, J.; Pan, J.; Zhang, L.; Yu, Y. Culture of hepatocytes on fructose-modified chitosan scaffolds, *Biomaterials*, 24, pp. 2317-2322. 2003.
[36] Chung, T. W.; Yang, J.; Akaiki, T.; Cho, K. Y.; Nah, J. W.; Kim, S.; Cho, C. S. Preparation of Alginate/Galactosylated Chitosan Scaffold for Hepatocyte Attachment, *Biomaterials*, 23, pp. 2827-2834. 2002.
[37] Wang, X. H.; Li, D. P.; Wang, W. J.; Feng, Q. L.; Cui, F. Z., Xu, Y. X.; Song, X. H.; van der Werf, M. Crosslinked collagen/chitosan matrix for artificial livers, *Biomaterials*, 24, pp. 3213-3220. 2003.
[38] Balakrishnan, B. and Jayakrishnan, A. Self-cross-linking biopolymers as injectable in situ forming biodegradable scaffolds, *Biomaterials*, 26, pp. 3941-3951. 2005.
[39] Honiger, J.; Balladur, P.; Mariani, P.; Calmus, Y.; Vaubourdolle, M.; Delelo, R.; Capeau, J.; Nordlinger, B. Permeability and biocompatibility of a new hydrogel used for encapsulation of hepatocytes, *Biomaterials*, 16, pp. 753-759. 1995.
[40] Ringel, M.; von Mack, M. A.; Santos, R.; Feilen, P. J.; Brulport, M.; Hermes, M.; Bauer, A. W.; Schormann, W.; Tanner, B.; Schön, M. R.; Oesch, F.; Hengstler, J. G. Hepatocytes cultured in alginate microspheres: an optimized technique to study enzyme induction, *Toxicology*, 206, pp. 153-167. 2005.
[41] Zhu, J.; Wang, X.; Ng, S.; Quek, C.; Ho, H.; Lao, X.; Yu, H. Encapsulating live cells with water-soluble chitosan in physiological conditions, *Journal of Biotechnology*, 117, pp. 355-365. 2005.
[42] Allen, J. W.; Brunson, M.; Salomon, D. R. Advances in Bioartificial Liver Devices, *Hepatology*, 34, pp. 447-455. 2001.
[43] Tzanakakis, E.; Hess, D. J.; Sielaff, T. D.; Hu, W. Extracorporeal Tissue Engineered Liver-Assist Devices, *Annual Review in Biomedical Engineering*, 2, pp. 607-632. 2000.
[44] http://www.leber-dialyse.de/lebertherapien/leberdialyse/mars/main.htm, Hepanet.

[45] Hamilton, A. and Bower, A. Best of the rest: For you health, *Time*, 158, pp. 96-97. 2001.
[46] Seo, S.; Kim, I.; Choi, Y.; Akaike, T.; Cho, C. Enhanced liver function of hepatocytes cocultured with NIH 3T3 in the alginate/galactosylated chitosan, *Biomaterials*, 27, pp. 1487-1495. 2006.
[47] Higashiyama, S.; Noda, M.; Muraoka, S.; Uyama, N.; Kawada, N.; Ide, T.; Kawase, M.; Yagi, K. Maintenance of hepatocyte functions in coculture with hepatic stellate cells, *Biochemical Engineering Journal*, 20, pp. 113-118. 2004.
[48] Isoda, K.; Kojima, M.; Takeda, M.; Higashiyama, S.; Kawase, M.; Yagi, K. Maintenance of Hepatocyte Functions by Coculture with Bone Marrow Stromal Cells, *Journal of Bioscience and Bioengineering*, 97, pp. 343-346. 2004.
[49] Tsuda, Y.; Kikuchi, A.; Yamato, M.; Chen, G.; Okano, T. Heterotypic cell interactions on a dually patterned surface, *Biochemical and Biophysical Comm.*, 348, pp. 937-944. 2006.
[50] Elliot, J.; Knight, A.; Cowley, C. The Oxford compact dictionary & thesaurus, Oxford: Oxford University Press. 1997.
[51] Tomalia, D. A.; Baker, H.; Dewald, J.; Hall, M.; Kallos, G.; Martin, S.; Roeck, J.; Ryder, J.; Smith, P. Dendritic Macromolecules: Synthesis of Starburst Dendrimers, *Macromolecules*, 19, pg. 2466-2468. 1986
[52] Tomalia, D. A. and Frechet, J. M. Discovery of Dendrimers and Dendritic Polymers: A Brief Historical Perspective, *Journal of Polymer Science Part A: Polymer Chemistry*, 40, pp. 2719-2728. 2002.
[53] Newkome, G. R.; Yao, Z.; Baker, G. R.; Gupta, V. K. Cascade Molecules: A New Approach to Micelles. A [27]-Arborol, *Journal of Organic Chemistry*, 50, pp. 2003-2004. 1985.
[54] Wörner, C. and Mülhaupt, R. Polynitrile- and Polyamine-Functional Poly(trimethylene imine) Dendrimers, *Angew. Chem., Int. Ed. Engl*., 32, pp. 1306-1308. 1993.
[55] De Brabander-van den Berg, E. M. M. and Meijer, E. W. Poly(propylene imine) Dendrimers: Large-Scale Synthesis by Heterogeneously Catalyzed Hydrogenations, *Angew. Chem., Int. Ed. Engl*., 32, pp. 1308-13011. 1993.
[56] Hobson, L. J. and Feast, W. J. Poly(amidoamine) hyperbranced systems: synthesis, structure and characterization, *Polymer*, 40, pp. 1279-1297. 1999.
[57] Bosman, A. W.; Janssen, H. M.; Meijer, E. W. About Dendrimers: Structure, Physical Properties, and Applications, *Chem. Rev.*, 99, pp. 1655-1688. 1999.
[58] Hawker, C. J. and Fréchet, J. M. J. Preparation of Polymers with Controlled Molecular Architecture. A New Convergent Approach to Dendritic Macromolecules, *J. Am. Chem. Soc.*, 112, pp. 7638-7647. 1990.
[59] Moore, J. S. and Xu, Z. Synthesis of Rigid Dendritic Macromolecules: Enlarging the Repeat Unit Size as a Function of Generation Permits Growth to Continue, *Macromolecules*, 24, pp. 5893-5894. 1991.
[60] Turnbull, W. B. and Stoddart, J. F. Design and Synthesis of Glycodendrimers, *Reviews in Molecular Biotechnology*, 90, pp. 231-255. 2002.
[61] Cloninger, M. J. Biological Applications of Dendrimers, *Current Opinion in Chemical Biology*, 6, pp. 1-7. 2002.
[62] Klajnert, B. and Bryszewska, M. Dendrimers: Properties and Applications, *Acta Biochimica Polonica*, 48, pp. 199-208. 2001.
[63] Hawker, C. J.; Farrington, P. J.; Mackay, M. E.; Wooley, K. L.; Frechet, J. M. Molecular Ball Bearings: The Unusual Melt Viscosity Behavior of Dendritic Macromolecules, *J. Am. Chem. Soc.*, 117, pp. 4409-4410. 1996.
[64] Svenson, S. and Tomalia, D. A. Dendrimers in biomedical applications-reflections on the field, *Advanced Drug Delivery Reviews*, 57, pp. 2106-2129. 2005.
[65] Rockendorf, N. and Lindhorst, T. K. Glycodendrimers, *Topics in Current Chemistry*, 217, pp. 202-238. 2001.
[66] Tirrel, M.; Kokkoli, E.; Biesalski, M. The Role of Surface Science in Bioengineered Materials, *Surface Science*, 500, pp. 61-83. 2002.
[67] Baek, M. and Roy, R. Synthesis and Protein Binding Properties of T-Antigen Containing GlycoPAMAM Dendrimers, Bioorganic & Medicinal Chemistry, 10, pp. 11-17. 2002.
[68] Aoi, K.; Itoh, K.; Okada, M. Globular Carbohydrate Macromolecule "Sugar Balls". 1. Synthesis of Novel Sugar-Persubstituted Poly(amido amine) Dendrimers, *Macromolecules*, 28, pp. 5391-5393. 1995.
[69] Ashton, P. R.; Boyd, S. E.; Brown, C. L.; Nepogodiev, S. A.; Meijer, E. W.; Peerlings, H. W. I.; Stoddart, J. F. Synthesis of Glycodendrimers by Modification of Poly(propylene imine) Dendrimers, *Chem. Eur. J.*, 3, pp. 974-984. 1997.

[70] Ashton, P. R., Boyd, S. E.; Brown, C. L.; Jayaraman, N.; Stoddart, J. F. Synthetic carbohydrate dendrimers. 1. A convergent synthesis of carbohydrate-containing dendrimers, *Chemistry: A European Journal*, 2, pp. 1115. 1996.
[71] Colonna, B.; Harding, V. D.; Nerpgodiev, S. A.; Raymo, F. M.; Spencer, N.; Stoddart, J. F. Synthesis of Oligosaccharide Dendrimers, *Chemistry-A European Journal*, 4, pp. 1244-1254. 1998.
[72] Veprek, P. and Jezek, J. Peptide and Glycopeptide Dendrimers. Part II, *Journal of Peptide Science*, 5, pp. 203-220. 1999.
[73] Sadalapure, K. and Lindhorst, T. K. A General Entry into Glycopeptide "Dendrons", *Angew. Chem. Int. Ed.*, 39, pp. 2010-2013. 2000.
[74] Turnbull, W. B.; Pease, A. R.; Stoddart, J. F. Synthetic Carbohydrate Dendrimers, Part 8 – Toward the Synthesis of Large Oligosaccharide-Based Dendrimers, *ChemBioChem*, 1, pp. 70-74. 2000.
[75] Dubber, M. and Lindhorst, T. K. Synthesis of octopus glycosides: core molecules for the construction of glycoclusters and carbohydrate-centered dendrimers, *Carbohydrate Research*, 310, pp. 35-41. 1998.
[76] Kitov, P. I.; Sadowska, J. M.; Mulvey, G.; Armstrong, G. D.; Ling, H.; Pannu, N. S.; Read, R. J.; Bundle, D. R. Shiga-like toxins are neutralized by tailored multivalent carbohydrate ligands, *Nature*, 403, pp. 669-672. 2000.
[77] Dubber, M. and Lindhorst, T. K. Synthesis of Carbohydrate-Centered Oligosaccharide Mimetics Equipped with a Functionalized Tether, *J. Org. Chem.*, 65, pp. 5275-5281. 2000.
[78] Stevens, M. P. Polymer Chemistry an Introduction. New York: Oxford University Press, Inc. 1999.
[79] Fischer, D.; Li, Y.; Ahlemeyer, B.; Krieglstein, J.; Kissel, T. In Vitro Cytotoxicity Testing of Polycations: Influence of Polymer Structure on Cell Viability and Hemolysis, *Biomaterials*, 24, pp. 1121-1131. 2003.
[80] Jevprasesphant, R.; Penny, J.; Jalal, R.; Attwood, D.; Mckeown, N. B.; D'Emanuele, A. The Influence of Surface Modification on the Cytotoxicity of PAMAM Dendrimers, *International Journal of Pharmaceutics*, 252, pp. 263-266. 2003.
[81] Marcos, M.; Omenat, A.; Serrano, J. L. Structure-mesomorphism relationship in terminally functionalized liquid crystal dendrimers, *C. R. Chimie*, 6, pp. 947-957. 2003.
[82] Sali, S.; Grabchev, I.; Ghovelon, J.; Ivanova, G. Selective sensors for Zn^{2+} cations based on new green fluorescent poly(amidoamine) dendrimers peripherally modified with 1,8-naphthalimides, *Spectochimica Acta Part A*, 65, pp. 591-597. 2006.
[83] Ghosh, S. and Banthia, A. K. Towards fluorescence sensing polyamidoamine (PAMAM) dendritic architectures, *Tetrahedron Letters*, 43, pp. 6457-6459. 2002.
[84] Li, A.; Yang, F.; Ma, Y.; Yang, X. Electrochemical impedance detection of DNA hydridization based on dendrimer modified electrode, *Biosensors and Bioelectronics*, In Press, Corrected Proof. 2006.
[85] Li, M.; Wang, J.; Feng, L.; Wang, B.; Jia, X.; Jiang, L.; Song, Y.; Zhu, D. Fabrication of tunable colloid crystals from amine-terminated polyamidoamine dendrimers, *Colloids and Surfaces A*, 290, pp. 233-238. 2006.
[86] Grabchev, I.; Sali, S.; Chovelon, J. Functional properties of fluorescent poly(amidoamine) dendrimers in nematic liquid crystalline media, *Chemical Physics Letters*, 422, pp. 547-551. 2006.
[87] Méry, D. and Astruc, D. Dendritic catalysis: Major concepts and recent progress, *Coordination Chemistry Reviews*, 250, pp. 1965-1979. 2006.
[88] Reek, J. N. H.; Arévalo, S.; van Heerbeek, R.; Kamer, P. C. J.; van Leeuwn, P. W. N. M. Dendrimers in Catalysis, *Advances in Catalysis*, 49, pp. 71-151. 2006.
[89] Tauzani, R. and Alper, H. PAMAM dendrimer-palladium complex catalyzed synthesis of five-, six- or seven membered ring lactones and lactams by cyclocarbonylation methodology, *Journal of Molecular Catalysis A: Chemical*, 227, pp. 197-207. 2005.
[90] Gong, A.; Fan, Q.; Chen, Y.; Liu, H.; Chen, C.; Xi, F. Two-phase hydroformylation reaction catalysed by rhodium-complexed water-soluble dendrimers, *Journal of Molecular Catalysis A: Chemical*, 159, pp. 225-232. 2000.
[91] Haensler, J. and Szoka, F. C. J. Polyamidoamine Cascade Polymers Mediate Efficient Transfection of Cells in Culture, *Bioconjugate Chem.*, 4, pp. 372-379. 1993.
[92] Tang, M. X.; Redemann, C. T.; Szoka, F. C. In vitro gene delivery by degraded polyamidoamine dendrimers, *Bioconjugate Chem.*, 7, pp. 703-714. 1996.

[93] Luo, D.; Haverstick, K.; Belcheva, N.; Han, E.; Saltzman, W. M. Poly(ethylene glycol)-conjugated PAMAM dendrimer for biocompatible, high-efficiency DNA delivery, *Macromolecules*, 35, pp. 3456-3462. 2002.
[94] Arima, H.; Kihara, F.; Hirayama, F.; Uckama, K. Enhancement of gene expression by polyamidoamine dendrimer conjugates with alpha-, beta-, and gamma-cyclodextrins, *Bioconjugate Chem.*, 12, pp. 476-484. 2001.
[95] Bielinska, A.; KukowskaLatallo, J. F.; Johnson, J.; Tomalia, D. A.; Baker, J. R. Regulation of in vitro gene expression using antisense oligonucleotides or antisense expression plasmids transfected using starburst PAMAM dendrimers, *Nucleic Acids Res.*, 24, pp. 2176-2182. 1996.
[96] Beezer, A. E.; King, A. S. H.; Martin, I. K.; Mitchel, J. C.; Ywyman, L. J.; Wain, C. F. Dendrimers as potential drug carriers; encapsulation of acidic hydrophobes within water soluble PAMAM derivatives, *Tetrahedron*, 59, pp. 3873-3880. 2003.
[97] Chandrasekar, D.; Sistla, R.; Ahmad, F. J.; Khar, R. K.; Diwan, P. V. The development of folate-PAMAM dendrimer conjugates for targeted delivery of anti-arthritic drugs and their pharmacokinetics and biodistribution in arthritic rats, *Biomaterials*, 28, pp. 504-512. 2007.
[98] Wiwattanapatapee, R.; Lomlim, L.; Saramunee, K. Dendrimers conjugates for colonic delivery of 5-aminosalicylic acid, *Journal of Controlled Release*, 88, pp. 1-9. 2003.
[99] El-Sayed, M.; Ginski, M.; Rhodes, C.; Ghandehari, H. Transepithelial transport of poly(amidoamine) dendrimers across Caco-2 cell monolayers, *Journal of Controlled Release*, 81, pp. 355-365. 2002.
[100] Kawase, M.; Kurikawa, N.; Higashiyama, S.; Miura, N.; Shiomi, T.; Ozawa, C.; Mizoguchi, T.; Yagi, k. Effectiveness of Polyamidoamine Dendrimers Modified with Tripeptide Growth Factor, Glycyl-L-Histidyl-L-Lysine, for Enhancement of Function of Hepatoma Cells, *Journal of Bioscience and Bioengineering*, 4, pp. 433-437. 1999.
[101] Higashiyama, S.; Noda, M.; Yagi, K. Mixed-ligand modification of polyamidoamine dendrimers to develop an effective scaffold for maintenance of hepatocyte spheroids, *Journal of Biomedical Materials Research*, 64A, pp. 475-482. 2003.
[102] Söntjens, S. H. M.; Nettles, D. L.; Carnahan, M. A.; Setton, L. A.; Grinstaff, M. W. Biodendrimer-Based Hydrogel Scaffolds for Cartilage Tissue Repair, *Biomacromolecules*, 7, pp. 310-316. 2006.
[103] Duan, X. and Sheardown, H. Dendrimer crosslinked collagen as a corneal tissue engineering scaffold: Mechanical properties and corneal epithelial cell interactions, *Biomaterials*, 27, pp. 4608-4617. 2006.
[104] Lindhorst, T. K. Essentials of Carbohydrate Chemistry and Biochemistry. Wiley-VCH. 2000.
[105] Claus, R. E. and Schreiber, S. L. Ozonolytic Cleavage of Cyclohexene to Terminally Differentiated Products: Methyl 6-Oxohexanoate, 6,6-Dimethoxyhexanal, Methyl 6,6-Dimethoxyhexanoate, *Organic Synthesis*, 7, pp. 168. 1990.
[106] Peterson, J.; Ebber, A.; Allikmaa, V.; Lopp, M. Synthesis and CZE Analysis of PAMAM Dendrimers with an Ethylenediamine Core, *Proc. Estonian Acad. Sci. Chem.*, 50, pp. 156-166. 2001.
[107] Christova, D.; Velichkova, R.; Goethals, E. J.; Du Prez, F. E. Amphiphilic segmented polymer networks based on poly(2-alkyl-2-oxazoline) and poly(methyl methacrylate), *Polymer*, 43, pp. 4585-4590. 2002.
[108] Islam, M. T.; Shi, X.; Balogh, L.; Baker Jr., J. R. HPLC Separation of Different Generations of Poly(amidoamine) Dendrimers Modified with Various Terminal Groups, *Analytical Chemistry*, 77, pp. 2063-2070. 2005.
[109] Zhang, N.; Doucette, A. and Li, L. Two-Layer Sample Preparation Method for MALDI Mass Spectrometric Analysis of Protein and Peptide Samples Containing Sodium Dodecyl Sulfate, *Anal. Chem.*, 73, pp. 2968-2975. 2001.
[110] Jackson, C. L.; Chanzy, H. D.; Booy, F. P.; Drake, B. J.; Tomalia, D. A.; Bauer, B. J.; Amis, E. J. Visualization of Dendrimer Molecules by Transmission Electron Microscopy (TEM): Staining Methods and Cryo-TEM of Vitrified Solutions, *Macromolecules*, 31, pp. 6259-6265. 1998.
[111] Ying-Jie, W.; Meng-Dong, L.; Yu-Min, W.; Jian, D.; Qing-He, N. Simplified isolation and spheroidal aggregate culture of rat hepatocytes, *World Journal of Gastroenterology* , 4, pp. 74-76. 1998.
[112] Technical Support: Cell Culture Troubleshooting, *JRH Bioscience*
[113] MTT Cell Proliferation Assay Instructions, American Type Culture Collection, pp. 1-6. 2001.
[114] Biological evaluation of medical devices – Part 5: Tests for in vitro cytotoxicity, British Standards Institution, pp. 1-9. 2001.
[115] Reddy, G. V. S.; Rao, G. V.; Subramanyam, R. V. K.; Iyengar, D. S. A new novel and practical one pot methodology for conversion of alcohols to amines, *Synthetic Communications*, 30, pp. 2233-2237. 2000.

[116] Svobodova, L.; Snejdarkova, M.; Polohova, V.; Grman, I.; Rybar, P.; Hianik, T. QCM immunosensor based on Polyamidoamine dendrimers, *Electroanalysis*, 18, pp. 1943-1949. 2006.
[117] Chen, Q. Q.; Lin. L.; Chen, H. M.; Yang, S. P.; Yang, L. Z.; Yu, X. B. A Polyamidoamine dendrimer with peripheral 1,8-naphthalimide groups capable of acting as a PET fluorescent sensor for the rare earth cations, *Journal of Photochemistry and Photobiology A-Chemistry*, 180, pp. 69-74. 2006.
[118] Kiselev, A. V.; Il'ina, P. L.; Egorova, A. A.; Baranov, A. N.; Guryanov, I. A.; Bayanova, N. V.; Tarasenko, I. I.; Lesina, E. A.; Vlasov, G. P.; Baranov, V. S. Lysine dendrimers as vectors for delivery of genetic constructs to eukaryotic cells, *Russian Journal of Genetics*, 43, pp. 593-600. 2007.
[119] Guillot-Nieckowski, M.; Eisler, S.; Diederich, F. Dendritic vectors for gene transfection, *New Journal of Chemistry*, 31, pp. 1111-1127. 2007.
[120] Appel, R. Tertiary Phospane/Tetrachloromethane, a Versatile Reagent for Chlorination, Dehydration, and P-N Linkage, *Angewandte Chemie International Edition*, 14, pp. 801-811. 1975.
[121] Gibson, M. S. and Bradshaw, R. W. The Gabriel Synthesis of Primary Amines, *Angewandte Chemie International Edition*, *7*, pp. 919-930. 1968.
[122] Lee, I.; Athey, B. D.; Wetzel, A. W.; Meixner, W.; Baker, J. R. Jr. Structural Molecular Dynamics Studies on Polyamidoamine Dendrimers for a Therapeutic Application: Effects of pH and Generation, *Macromolecules*, 35, pp. 4510-4520. 2002.
[123] Fréchet, J. M. J.; Hawker, C. J.; Wooley, K. L. The Convergent Route to Globular Dendritic Macromolecules: A Versatile Approach to Precisely Functionalized Three Dimensional Polymers and Novel Block Copolymers, *Pure Appl. Chem.*, A31, pp. 1627-1645. 1994.
[124] Hay, G.; Mackay, M. E.; Hawker, C. J. Thermodynamic Properties of Dendrimers Compared with Linear Polymers: General Observations, J. Polymer Science: Part B: Polymer Physics, 39, 1766-1777. 2001.
[125] Maiti, P. K.; Cagin, T.; Lin, S. T.; Goddard, W. A. III. Effect of Solvent and pH on the Structure of PAMAM Dendrimers, *Macromolecules*, 38, pp. 979-991. 2005.
[126] Fernandez-Megia, E.; Correa, J.; Rodriquez-Meizoso, I.; Riguera, R. A Click Approach to Unprotected Glycodendrimers, *Macromolecules*, 39, pp. 2113-2120. 2006.
[127] Roos, E. J. and Schiller, M. E. Loading of biologically active solutes into polymer gels, United States Patent 5840338, 1998.
[128] Engelmayr, G.C.; Papworth, G.D.; Watkins, S.C.; Mayer, J.E. and Sacks, M.S. Guidance of engineered tissue collagen orientation by large-scale scaffold microstructures, *Journal of Biomechanics*, 39, pp. 1819-1831. 2006.
[129] Kim, H.; Murakami, H.; Chehroudi, B.; Textor, M. and Brunette, D.M. Effects of surface topography on the connective tissue attachment to subcutaneous implants, *International Journal of Oral & Maxillofacial Implants*, 21, pp. 354-365. 2006.
[130] Dogan, A.K.; Gumusderelioglu, M. and Aksoz, E. Controlled release of EGF and bFGF from dextran hydrogels in vitro and in vivo, *Journal of Biomedical Materials Research Part B-Applied Biomaterials*, 74B, pp. 504-510. 2005.
[131] Katime, I.; Diaz de Apodaca, E. and Rodriguez, E. Effect of Crosslinking Concentration on Mechanical and Thermodynamic Properties in Acrylic Acid-*co*-Methyl Methacrylate Hydrogels, *Journal of Applied Polymer Science*, 42, pp. 4016-4022. 2006.
[132] Caykara, T. and Turan, E. Effect of the amount and type of the crosslinker on the swelling behavior of temperature-sensitive poly(N-*tert*-butylacrylamide-*co*-acrylamide) hydrogels, *Colloid and Polymer Science*, 284, pp. 1038-1048. 2006.
[133] Unal, B. and Hedden, R. Gelation and swelling behavior of end-linked hydrogels prepared from linear poly(ethylene glycol) and poly(amidoamine) dendrimers, *Polymer*, 47, pp. 8173-8182. 2006.
[134] Epperson, J. D.; Ming, L.; Baker, G. R.; Newkome, G. R. Paramagnetic Cobalt(II) as an NMR Probe of Dendrimer Structure: Mobility and Cooperativity of Dendritic Arms, *J. Am. Chem. Soc.*, 123, pp. 8583-8592. 2001.
[135] Tomalia, D. A. Dendrons/Dendrimers. The convergence of quantized dendritic building blocks/architectures for applications in nanotechnology, *Chemistry Today*, 23, pp. 41-45. 2005.
[136] Stechemesser, S. and Eimer, W. Solvent-Dependent Swelling of Poly(amido amine) Starburst Dendrimers, *Macromolecules*, 30, pp. 2204-2206. 1997.

[137] De Bartolo, L.; Morelli, S.; Piscioneri, A.; Lopez, L. C.; Favia, P.; d'Agostino, R.; Drioli, E. Novel membranes and surface modification able to activate specific cellular responses, *Biomolecular Engineering*, 24, pp. 23-26. 2007.
[138] Bhadriraju, K. and Hansen, L. H. Hepatocyte adhesion, growth and differentiated function on RGD-containing proteins, *Biomaterials*, 21, pp. 267-272. 2000.
[139] Fürst, W. M. S and Banerjee, A. Release of Glutaraldehyde From an Albumin-Glutaraldehyde Tissue Adhesive Causes Significant In Vitro and In Vivo Toxicity, *The Annals of Thoracic Surgery*, 79, pp. 1522-1528. 2005.
[140] Lin, F. H.; Yao, C. H.; Sun, J. S.; Liu, H. C.; Huang, C. W. Biological effects and cytotocity of the composite composed by tricalcium phosphate and glutaraldehyde cross-lined gelatin, *Biomaterials*, 19, pp. 905-917. 1998.
[141] Jones, K. D. Membrane immobilization of nucleic acids: Part 3: Covalent linkage and system manufacturability, *IVD Technology*, 2001.
[142] Jones, K. D. Membrane immobilization of nucleic acids: Part 3: Covalent linkage and system manufacturability, *IVD Technology*, p. 39. Nov. 2001.
[143] Kiernan, J. A. Formaldehyde, formalin, paraformaldehyde and glutaraldehyde: What they are and what they do, *Microscopy Today*, 1, pp. 8-12. 2000.
[144] Caudane, J.; Laurent, E.; Vert, M. Poly(ε-caprolactone)-Based Organogels and Hydrogels with Poly(ethylene glycol) Cross-Linkings, *Macromolecular Rapid Communications*, 25, pp. 1865-1869. 2004.
[145] Gombotz, W. R.; Guanghui, W.; Horbett, T. A.; Hoffman, A. S. Protein adsorption to poly(ethylene oxide) surfaces, *Journal of Biomedical Materials Research*, 25, pp. 1547-1562. 1991.
[146] Kumar, R. and Katare, O. P. Lecithin Organogels as a Potential Phospholipid-Structured System for Topical Drug Delivery: A Review, *AAPS PharmSciTech*, 6, pp. E298-E310. 2005.
[147] John, G.; Zhu, G.; Li, J.; Dordick, J. S. Enzymatically Derived Sugar-Containing Self-Assembled Organogels with Nanostructured Morphologies, *Angew. Chem. Int. Ed*., 45, pp. 4772-4775. 2006.
[148] Sugimoto, P. M.; Watrin, A.; Chiquet, M.; Hunziker, E. B. BMP-2 induces the expression of chondrocyte-specific genes in bovine synovium-derived progenitor cells cultures in three-dimensional alginate hydrogel, *Osteoarthritis Cartilage*, 13, pp. 527-536. 2005.
[149] Yu, X.; Dillon, G. P.; Bellamkonda, R. B. A laminin and nerve growth factor-laden three-dimensional scaffold for enhanced neurite extension, *Tissue Eng.*, 5, pp. 291-304. 1999.
[150] Fisher, J. P.; Jo, S.; Mikos, A. G.; Reddi, A. H. Thermoreversible hydrogel scaffolds for articular cartilage engineering, *J. Bio. Mat. Res. A*, 71A, pp. 268-274. 2004.
[151] Agrawal, P.; Gupta, U.; Jain, N. K. Glycoconjugated peptide dendrimers-based nanoparticulate system for the delivery of chloroquine phosphate, *Biomaterials*, 28, pp. 3349-3359. 2007.
[152] Chihara, Y.; Arima, H.; Arizono, M.; Wada, K.; Hirayama, F.; Uekama, K. Serum-resistant gene transfer activity of mannosylated dendrimer/alpha-cyclodextrin conjugate (G3), *J. Incl. Phenom. Macro.*, 56, pp. 89-93. 2006.
[153] Lee, N.; Jang, W.; Yu, S; Im, J.; Chung, S. Synthesis of glycodendrimers having *scyllo*-inositol as the scaffold, *Tetrahedron Letters*, 46, pp. 6063-6066. 2005.
[154] Farahani, T. D.; Entezami, A. A.; Mobedi, H.; Abtahi, M. Degradation of Poly(D,L-lactide-*co*-glycolide) 50:50 Implant in Aqueous Medium, *Iranian Polymer Journal*, 14, pp. 753-763. 2005.
[155] Park, I. K.; Yang, J.; Jeong, H. J.; Bom, H. S.; Harada, I.; Akaike, T.; Kim, S.; Cho, C. S. Galactosylated chitosan as a synthetic extracellular matrix for hepatocytes attachment, *Biomaterials*, 24, pp. 2331-2337. 2003.
[156] Takei, R.; Suzuki, D.; Hoshiba, T.; Nagaoka, M.; Seo, S. J.; Cho, C. S.; Akaike, T. Role of E-cadherin Molecules in Spheroid Formation of Hepatocytes Adhered on Galactose-Carrying Polymer as an Artificial Asialoglycoprotein Model, *Biotechnology Letters*, 27, pp. 1149-1156. 2005.
[157] Hansen, L. K.; Hsiao, C. C.; Friend, J. R.; Wu, F. J.; Bridge, G. A.; Remmel, R. P.; Cerra, F. B.; Hu, W. S. Enhanced morphology and function in hepatocytes spheroids: A model of tissue self-assembly, *Tissue Engineering*, 4, pp. 65-74. 1998.
[158] Atherton, E.; Sheppard, R. C. Solid Phase peptide synthesis: a practical approach. IRL Press, Oxford, England. 1989.

APPENDIX A:

SUPPORTING DATA FOR DENDRIMER SYNTHESIS

A.1 Scheme 1

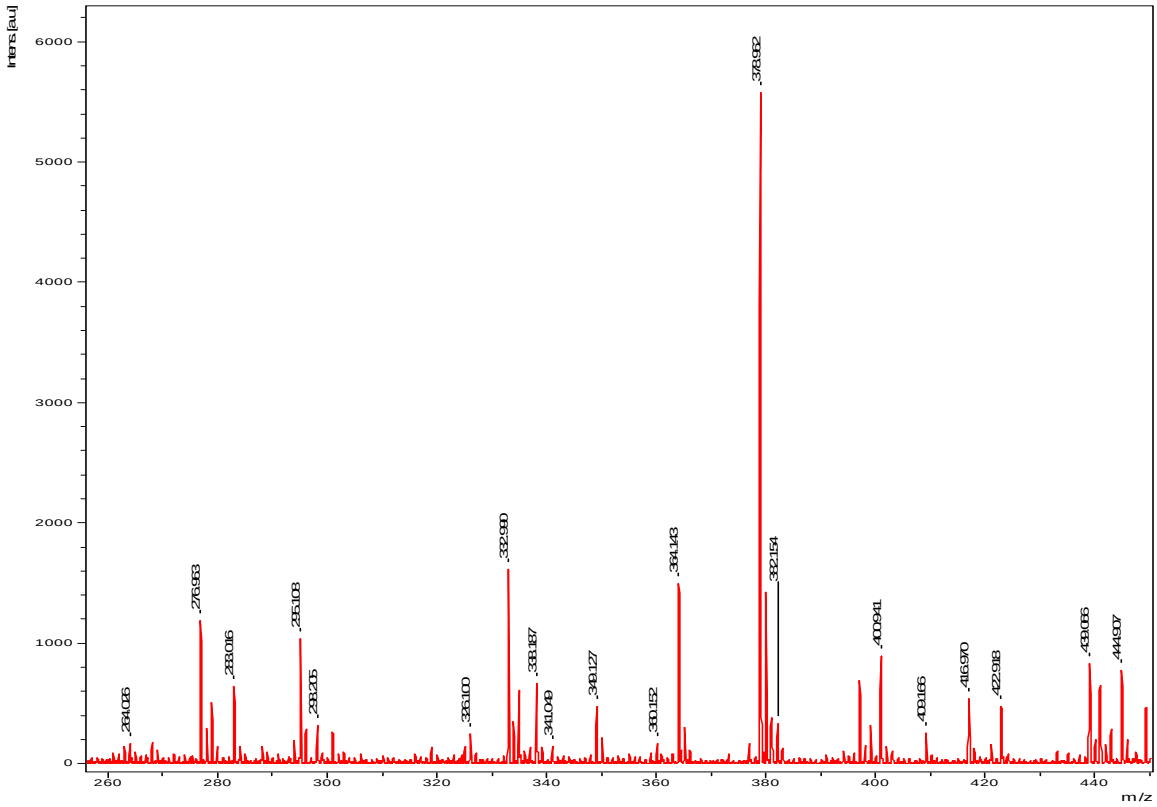

Figure A-1: MALDI-TOF-MS for product 2

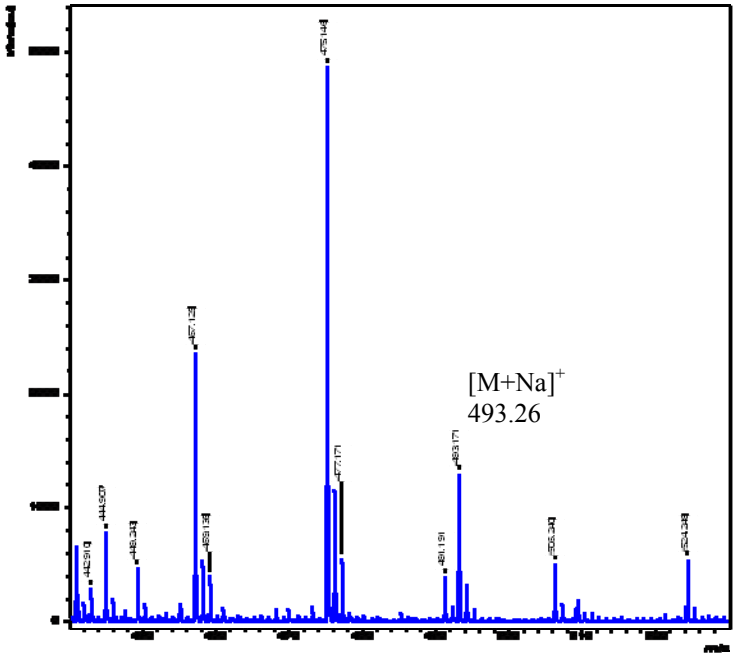

Figure A-2: MALDI-TOF-MS for product 3

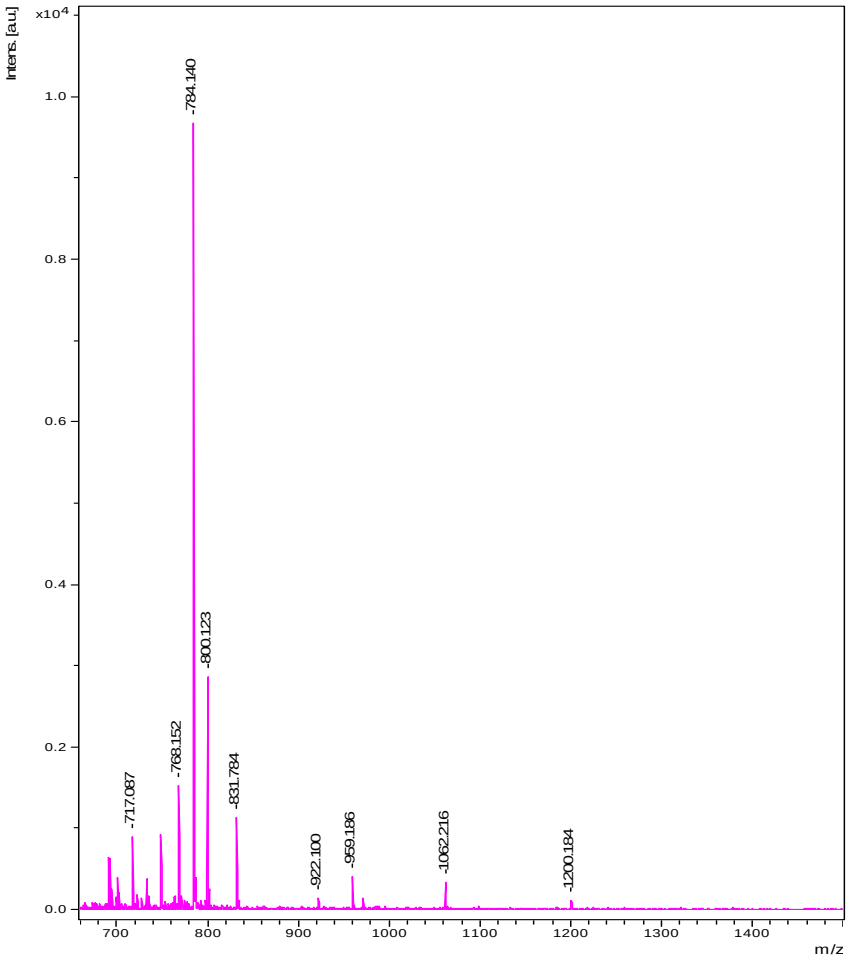

Figure A-3: MALDI-TOF-MS for product 4

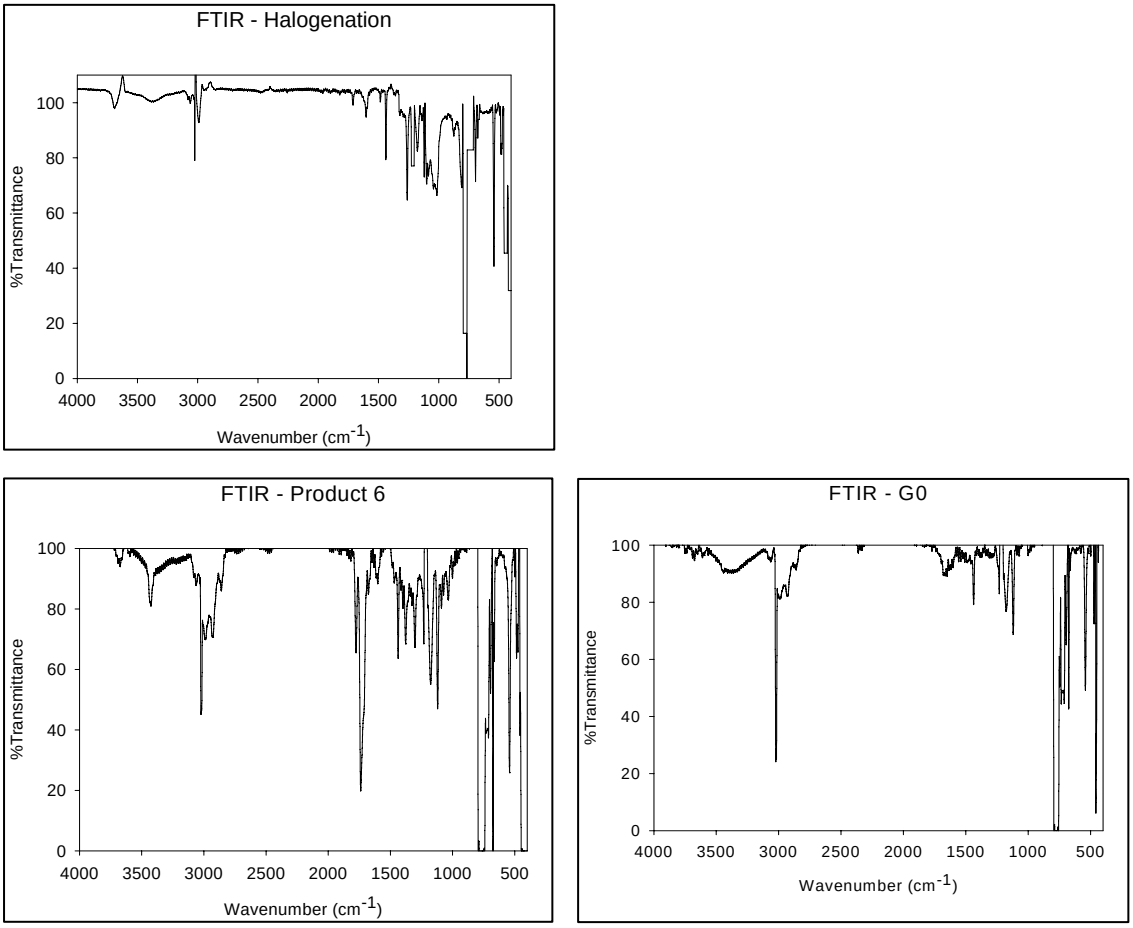

Figure A-4: FTIR spectra of product 5 (upper left), product 6 (lower left) and 7 (lower right)

A.2 Scheme 2

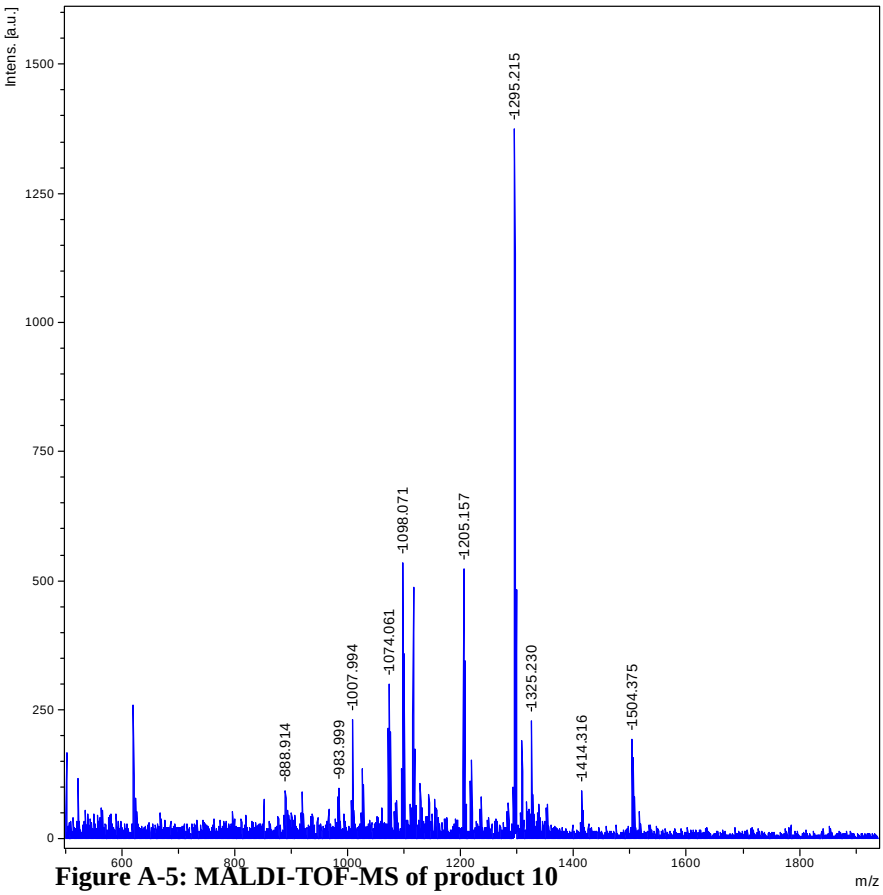

Figure A-5: MALDI-TOF-MS of product 10

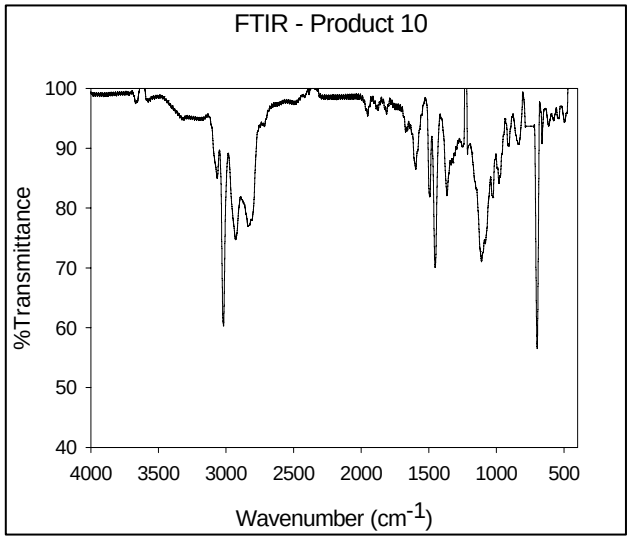

Figure A-6: FTIR spectrum of *scheme-2* product 10

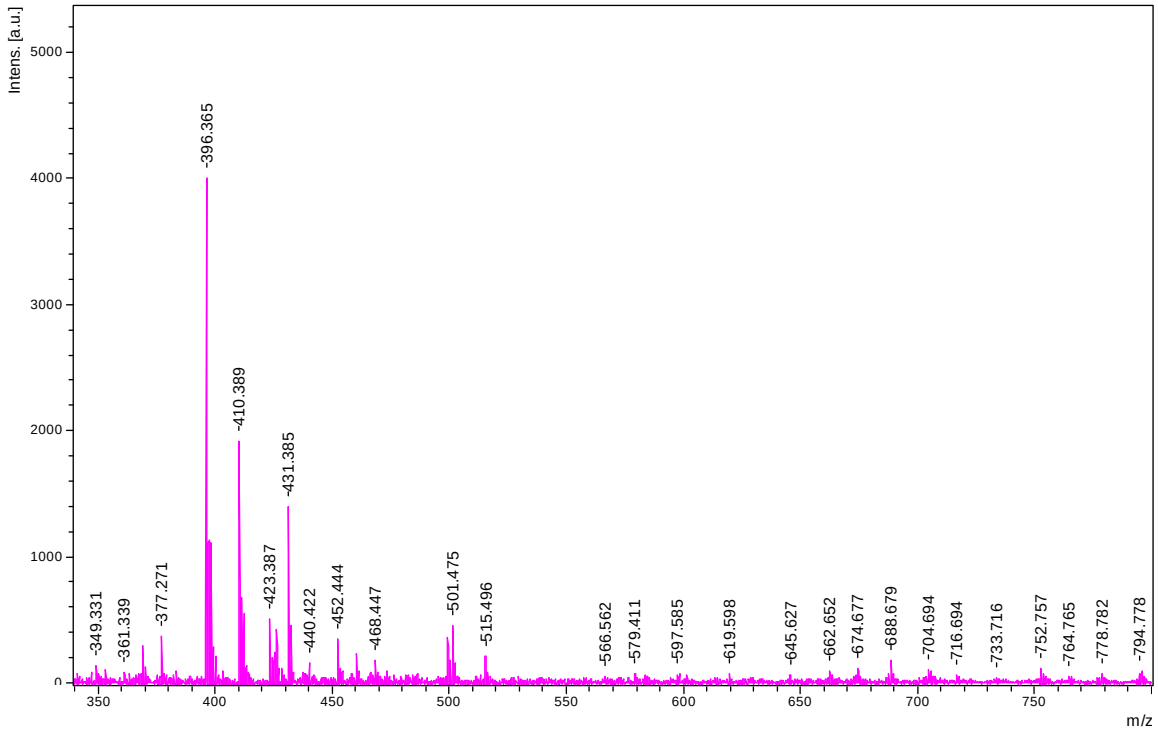

Figure A-7: MALDI-TOF-MS of *scheme-2* GO galactose-centered PAMAM dendrimer

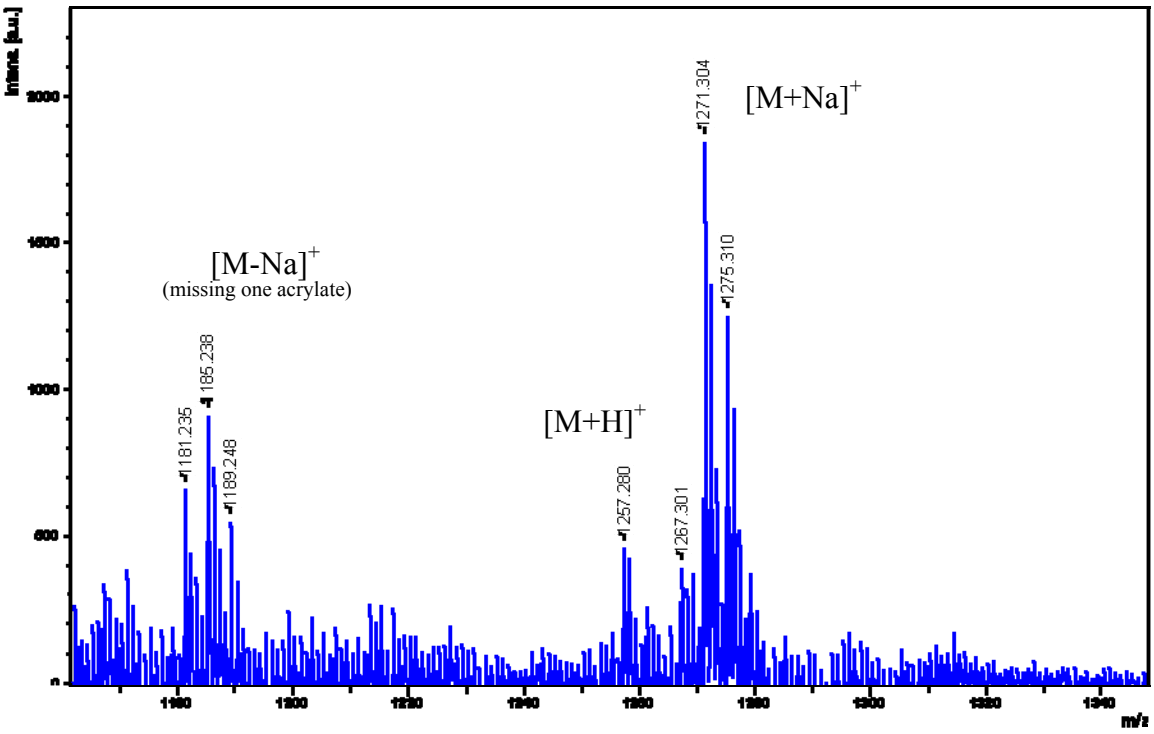

Figure A-8: MALDI-TOF spectrum of G0.5 dendrimer.

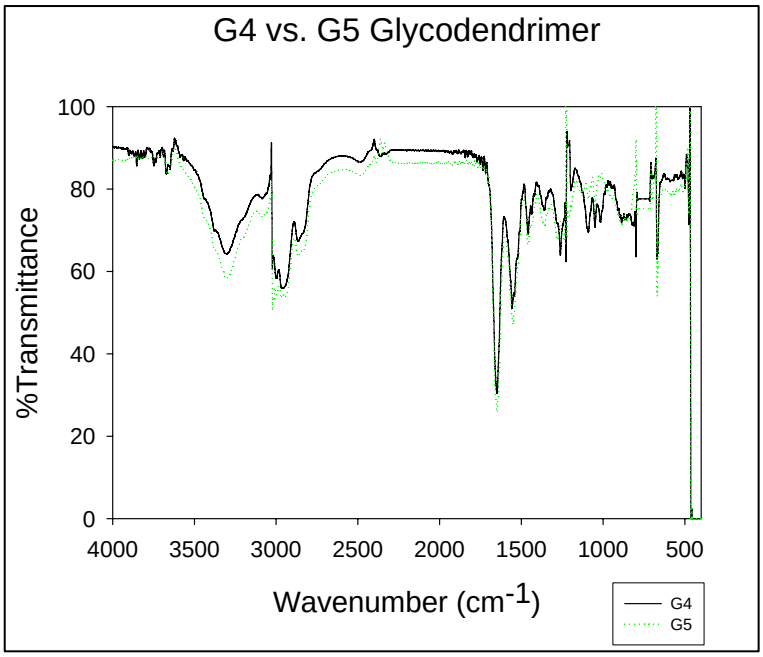

Figure A-9: FTIR spectra of G4 and G5 dendrimers.

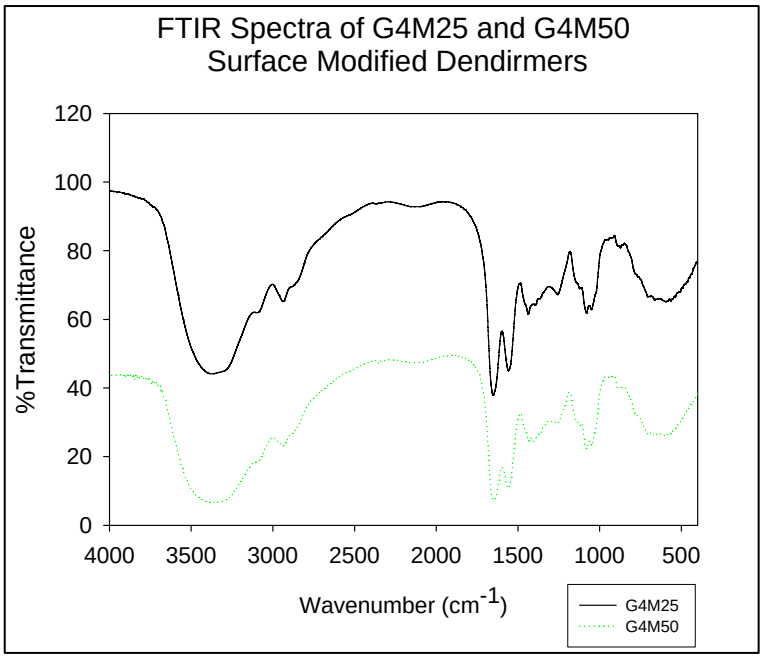

Figure A-10: FTIR spectra of G4 surface modified dendrimers.

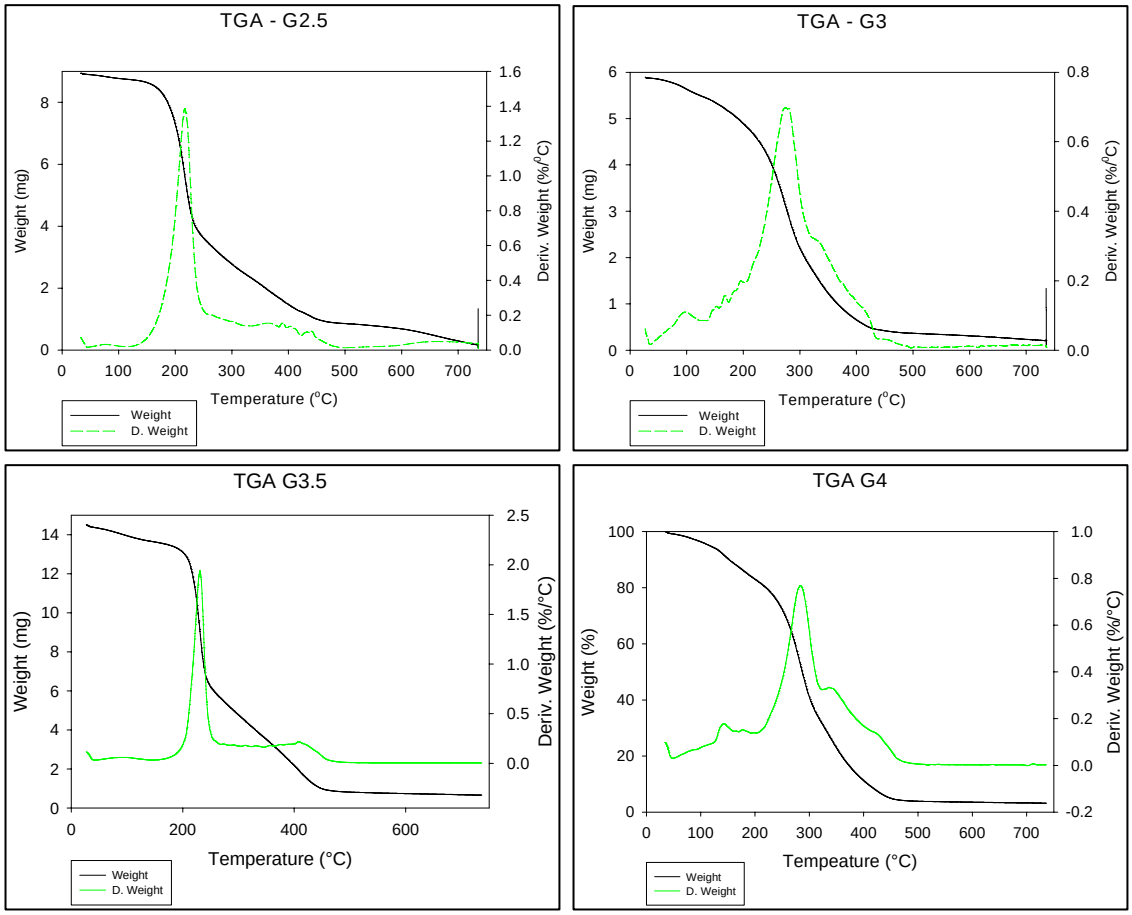

Figure A-11: TGA analysis of G2.5 (upper left), G3.5 (lower left), G3 (upper right) and G4 (lower right) glycodendrimers

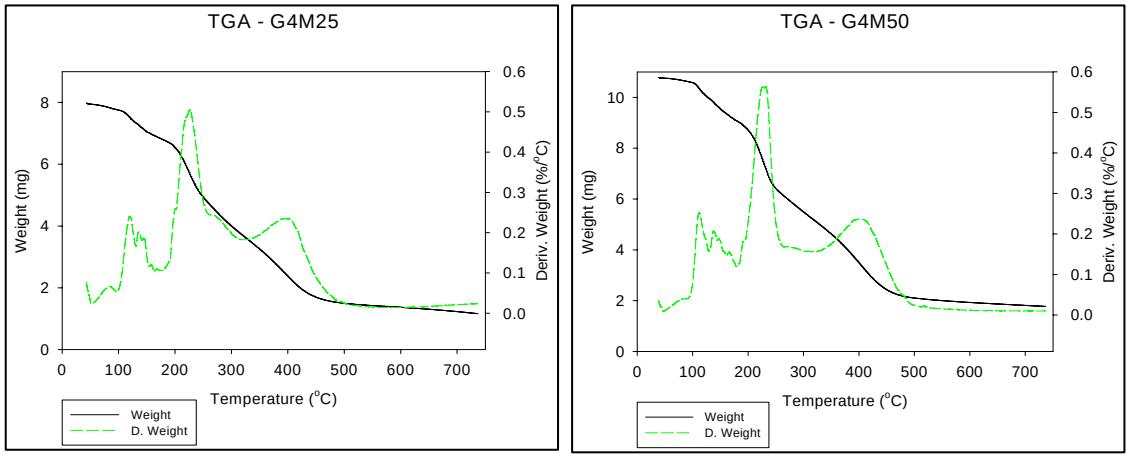

Figure A-12: TGA analysis of G4M25 and G4M50 surface modified glycodendrimers

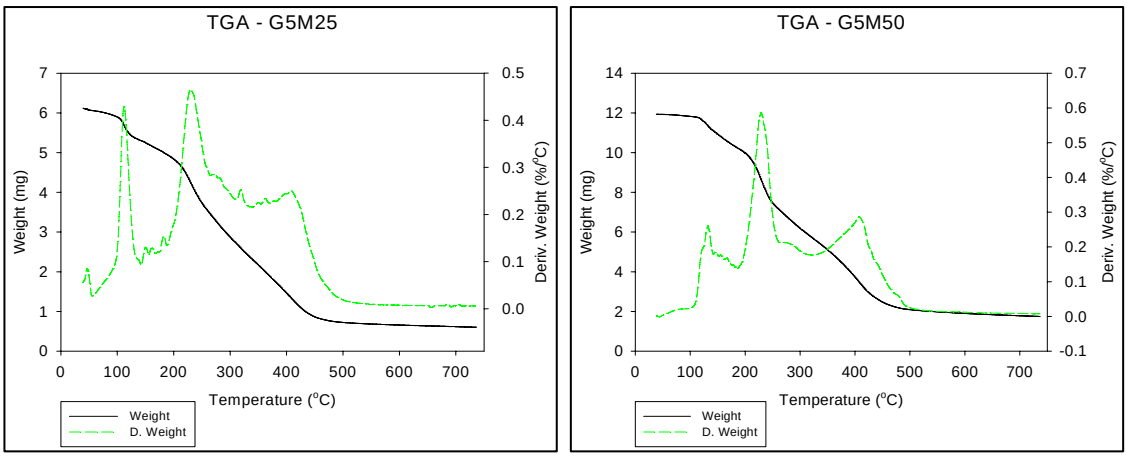

Figure A-13: TGA analysis of G5M25 and G5M50 surface modified glycodendrimers

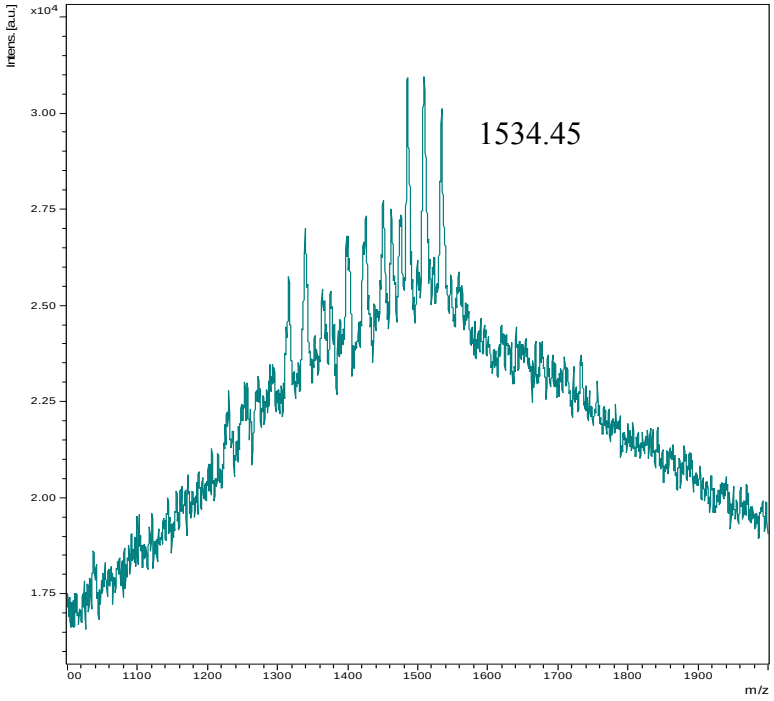

Figure A-14: MALDI-TOF spectrum of G1 dendrimer

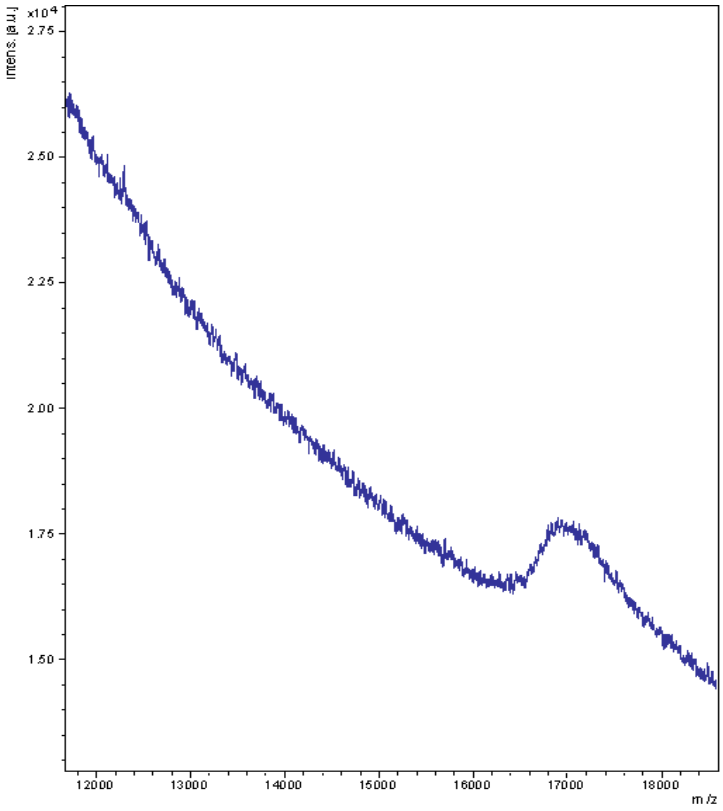

Figure A-15: MALDI-TOF spectrum of G4 dendrimer

APPENDIX B:

SUPPORTING DATA FOR DENDRIMER GELATION

B.1 PEG-DGE

This section contains additional FTIR, SEM, TGA and XPS data for PEG-DGE crosslinked glycodendrimer gels.

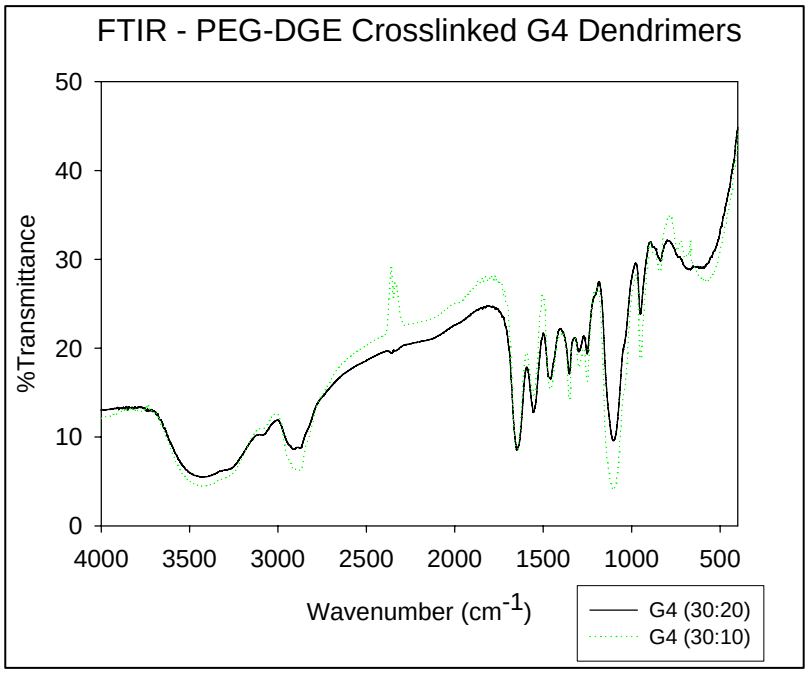

Figure B-1: FTIR spectra comparison between varying gel compositions of crosslinker and dendrimer.

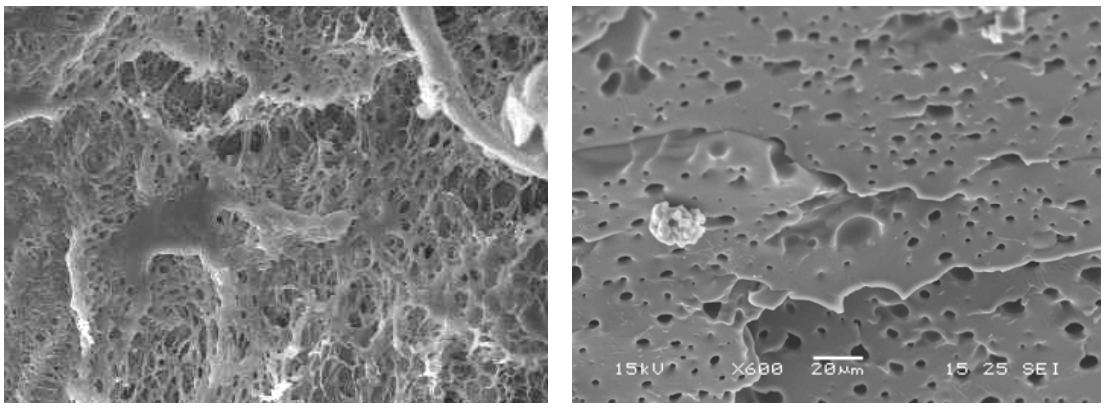

Figure B-2: SEM images of (left) G5 (30:40) and (right) G4 (30:20)

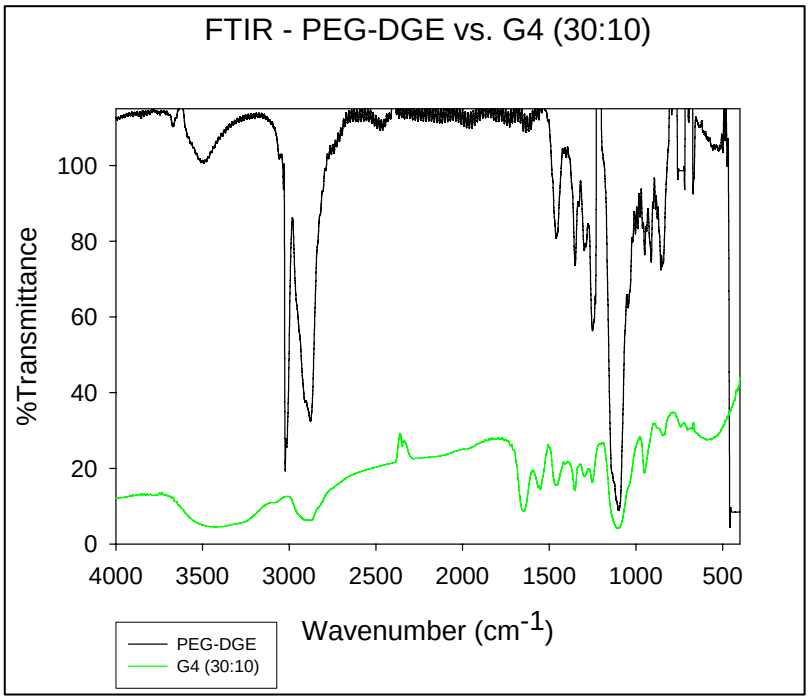

Figure B-3: FTIR spectra comparison between PEG-DGE crosslinker and G4 (30:10) crosslinked gel

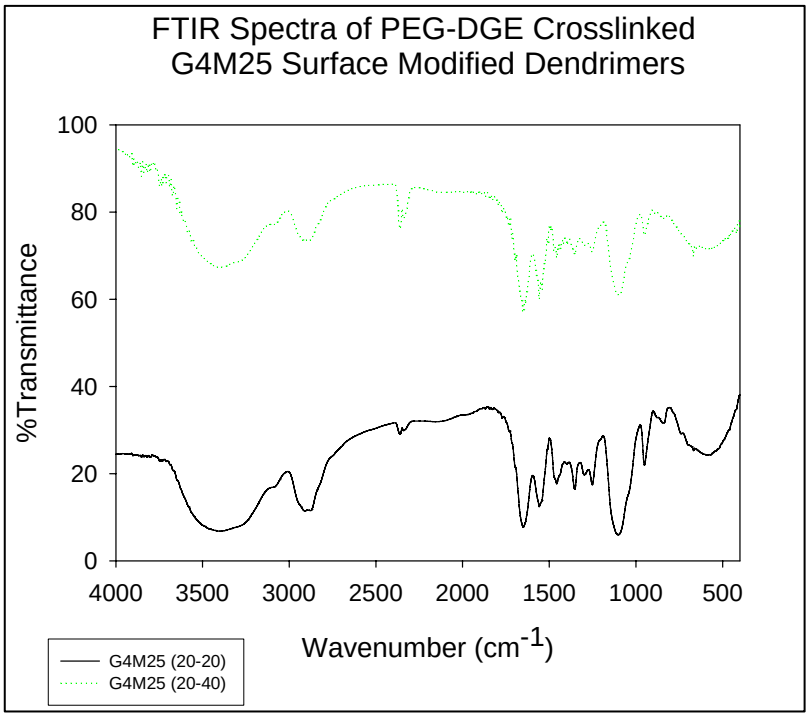

Figure B-4: Comparison between FTIR spectra of varying gel compositions (PEG-DGE:G4M25).

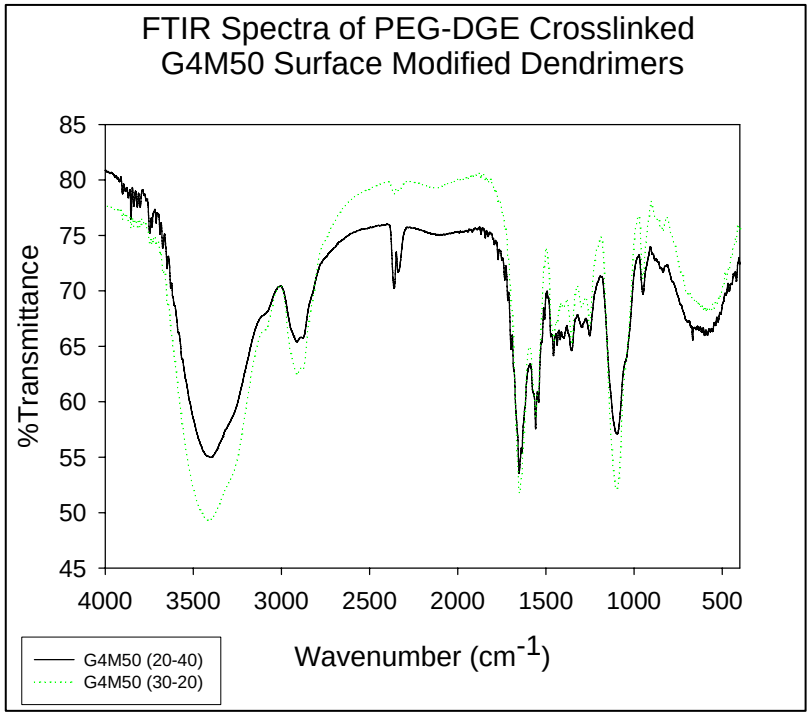

Figure B-5: Comparison between FTIR spectra of varying gel compositions (PEG-DGE:G4M50).

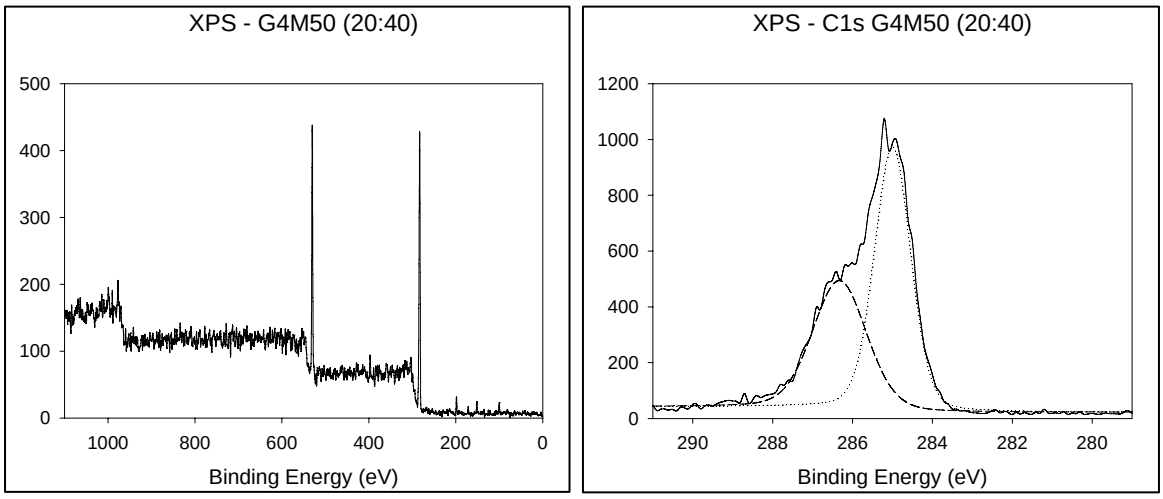

Figure B-6: XPS wide scan (left) and C 1s Peak (right) for G4M50 (20:40) gel

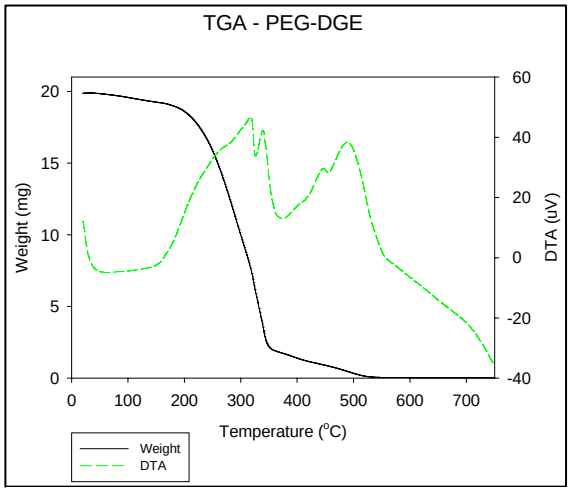

Figure B-7: TGA analysis of PEG-DGE crosslinking agent

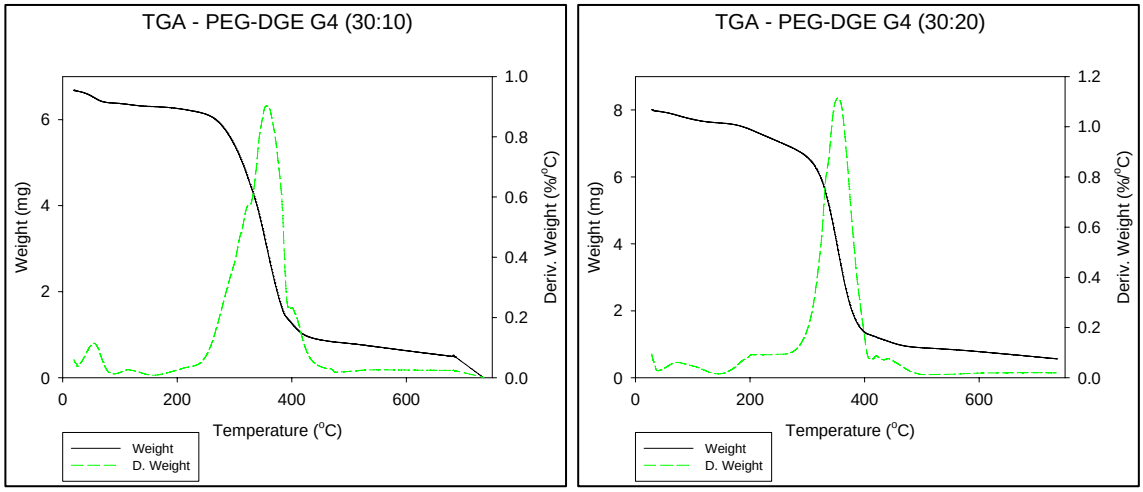

Figure B-8: TGA analysis of (left) PEG-DGE G4 (30-10) and (right) G4 (30-20) gels

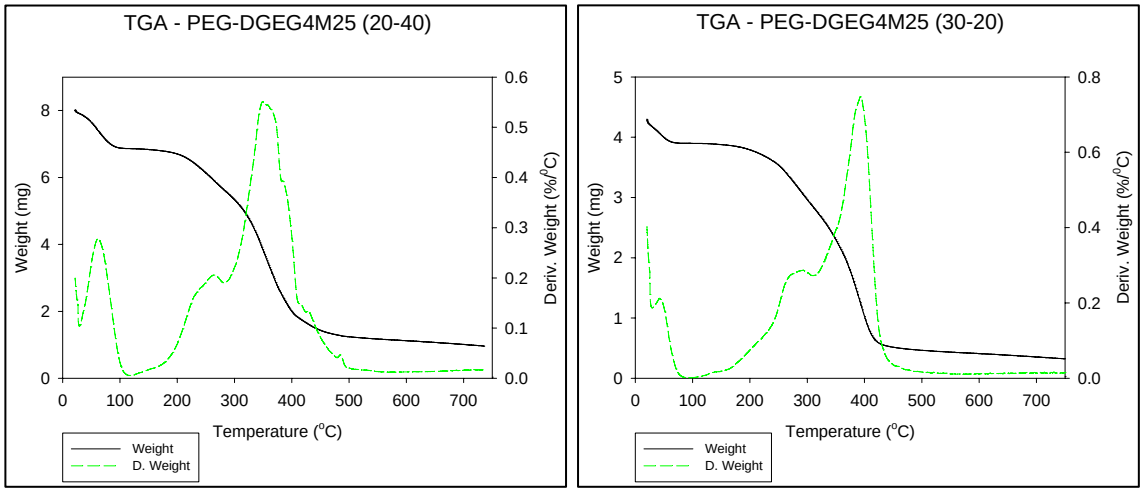

Figure B-9: TGA analysis of (left) PEG-DGE G4M25 (20:40) and (right) G4M25 (30:20) gels

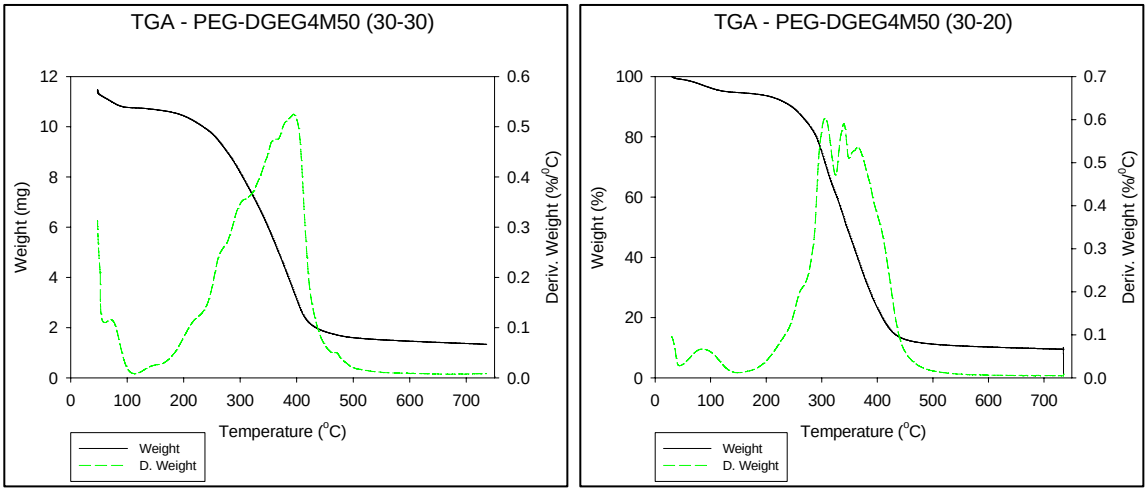

Figure B-10: TGA analysis of (left) PEG-DGE G4M50 (30:30) and (right) G4M50 (30:20) gels

B.2

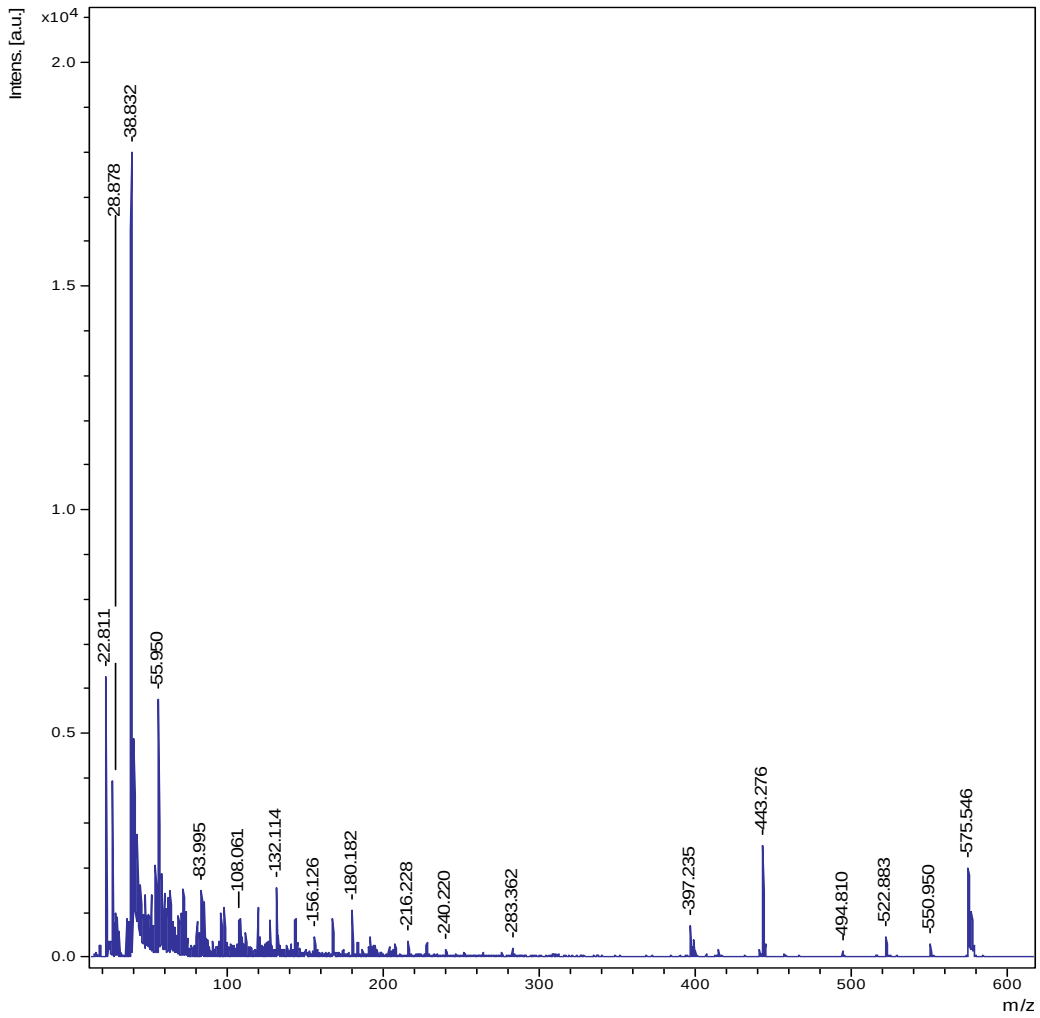

Figure B-11: Solid phase MALDI-TOF-MS on G4M25 (30:20) gel sample

Glutaraldehyde

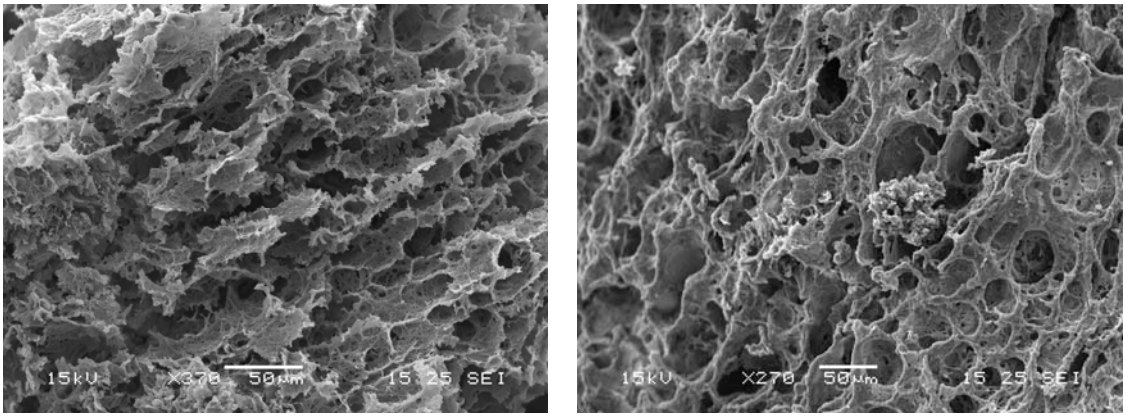

Figure B-12: SEM images of glutaraldehyde crosslinked G4 glycodendrimers, spongier samples

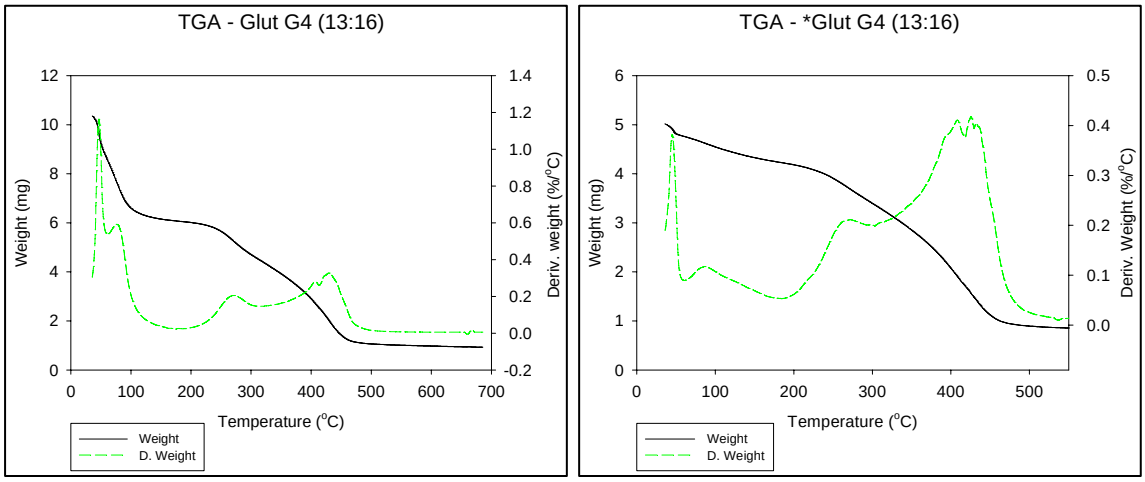

Figure B-13: TGA analysis of glutaraldehyde crosslinked G4 dendrimers in aqueous (left) and organic (right) solution. *Crosslinking performed in methanol.

B.3 PEG-DA

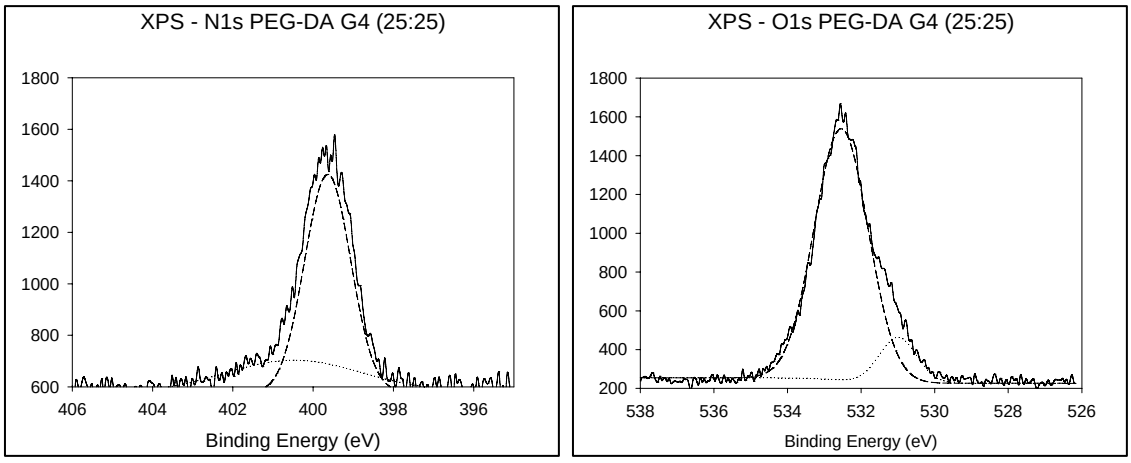

Figure B-14: N1s Peak (left) and O1s Peak (right) for PEG-DA G4 (25:25) gel

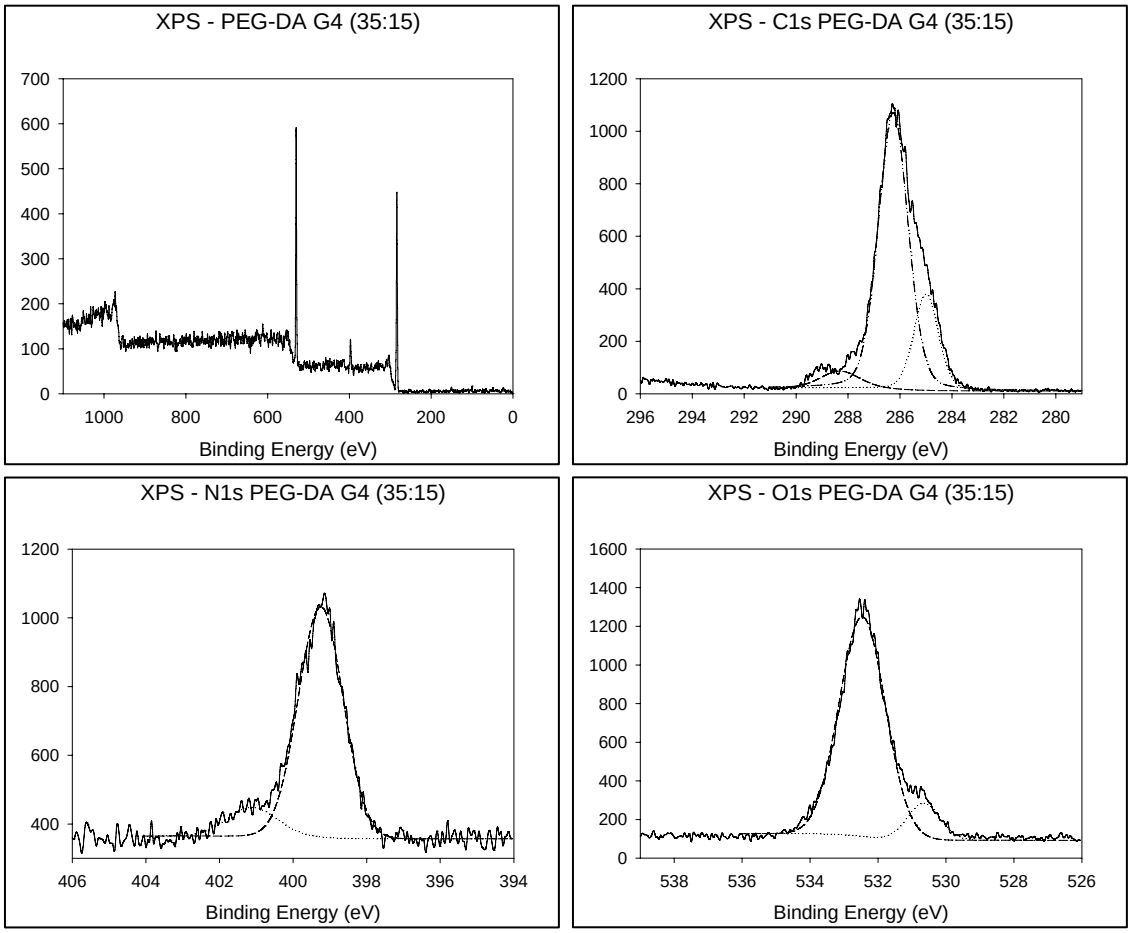

Figure B-15: XPS wide scan (upper left), N1s Peak (lower left), C1s Peak (upper right) and O1s Peak (lower right) for PEG-DA G4 (35:15) gel

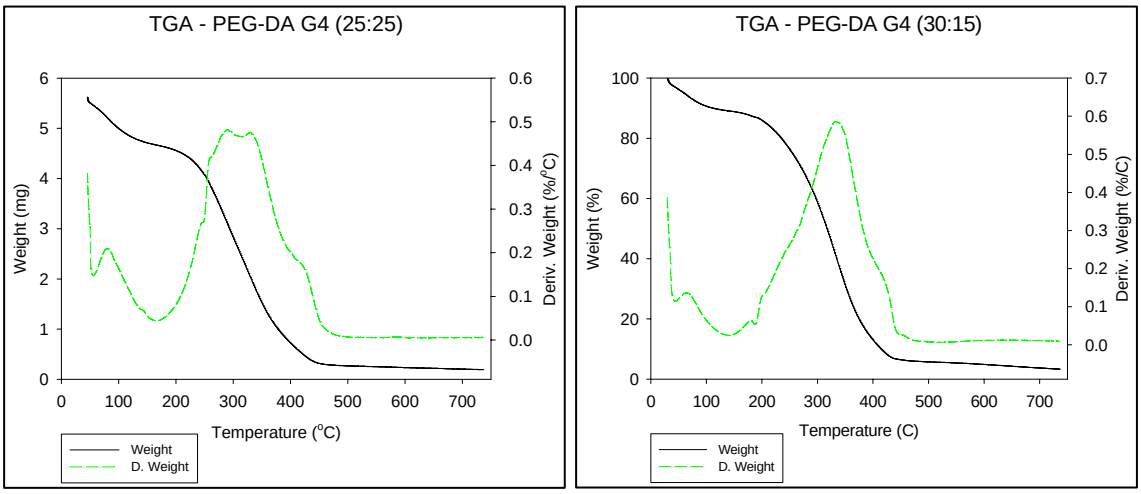

Figure B-16: TGA analysis of a PEG-DA G4 (25:25) (left) and PEG-DA G4 (30:15) gel samples

APPENDIX C:

SUPPORTING DATA FOR CELL CULTURE STUDIES

C.1 Cytotoxicity Studies

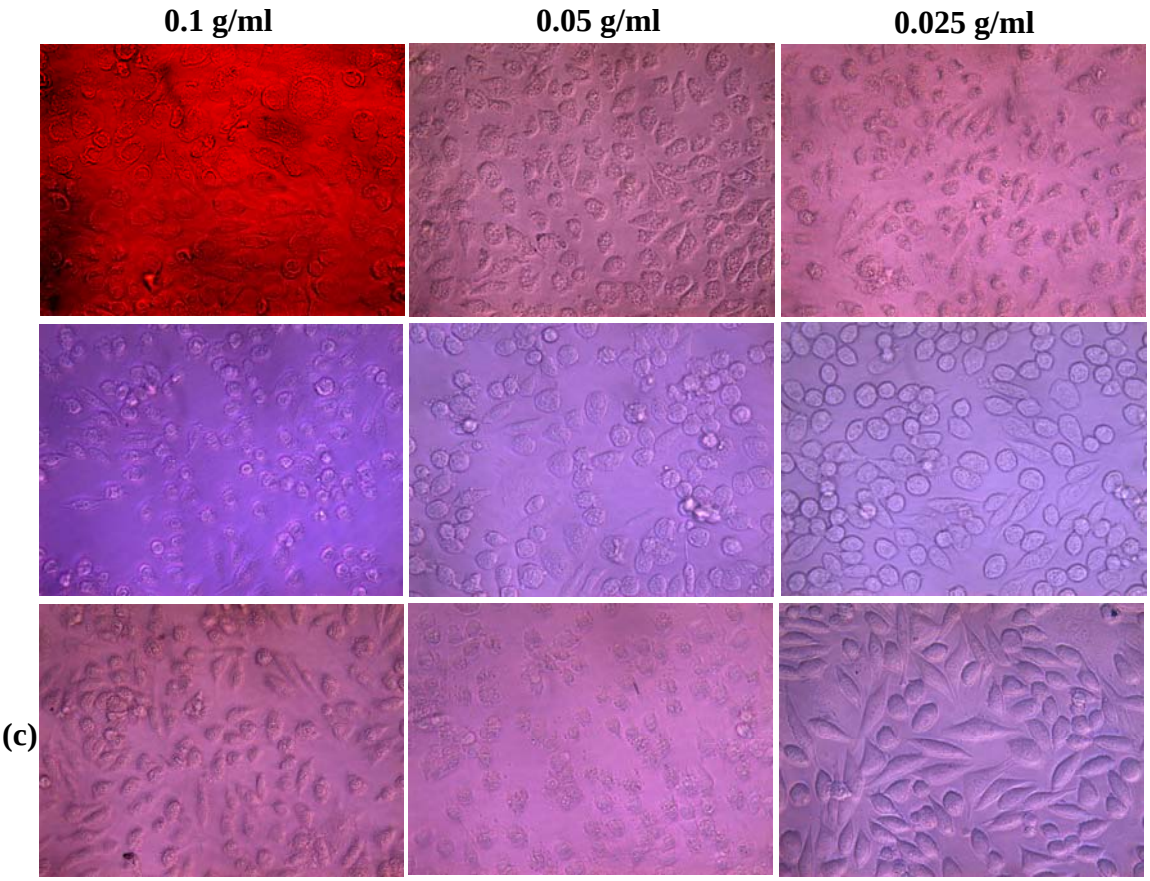

Figure C-1: Solution phase cytotoxicity tests of (a) G5, (b) G5-M25 and (c) G5-M50 dendrimers. Photos were taken after 3 hours (x20 magnification).

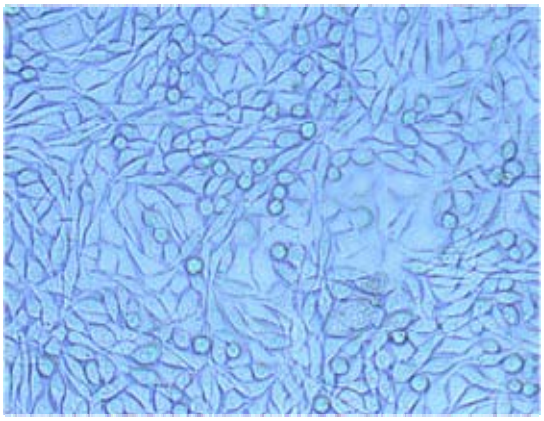

Figure C-2: L929 cell culture at confluence

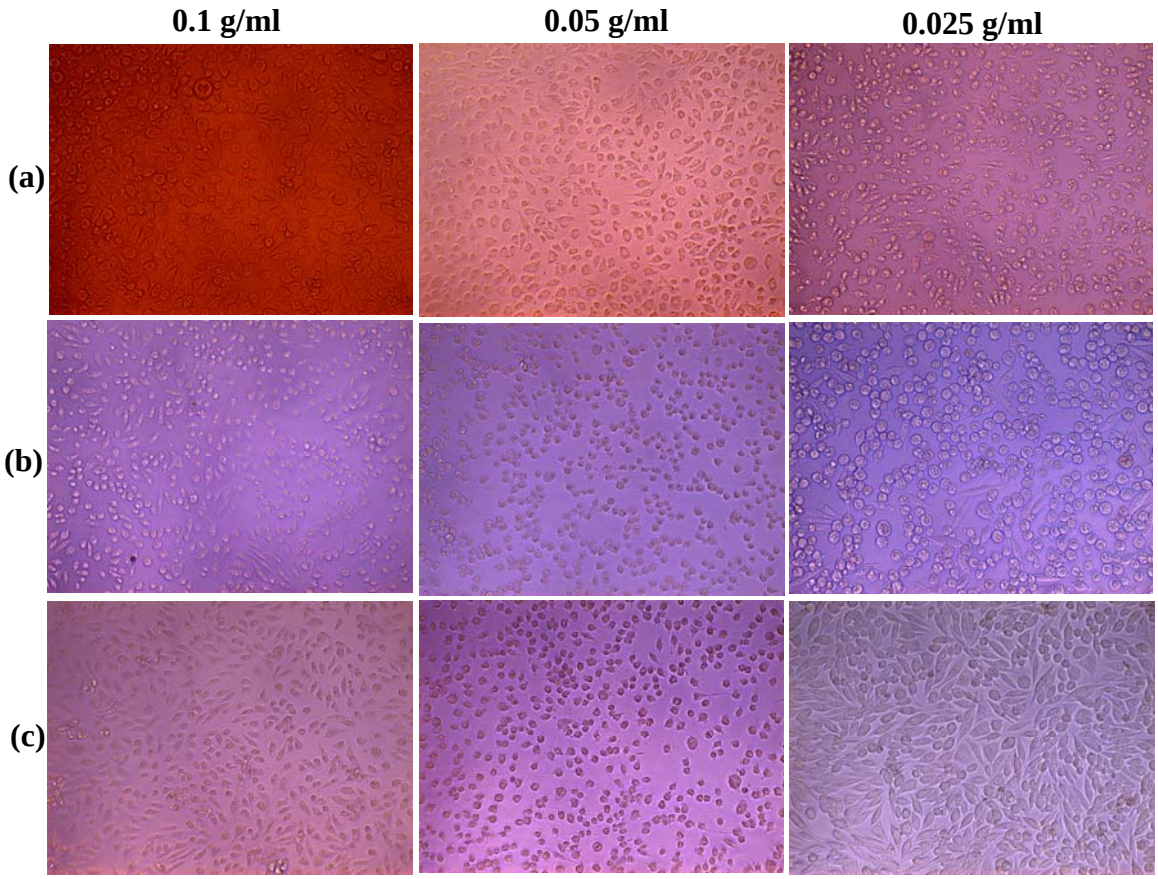

Figure C-3: Solution phase cytotoxicity tests of (a) G5, (b) G5-M25 and (c) G5-M50 dendrimers. Photos were taken after 28 hours (x10 magnification).

C.2 Functional Assays

Table C-1: Additional EROD cell culture analysis

Sample	Day 3	Day 6	Day 9	Day 13	Day 16
G4 (30:20)	122±40	487±310	640±232	521±266	329±81
G4M50 (20:40)	33±51	473±371	995±71	504±141	489±162
G5M50 (40:20)	112±26	1004±444	730±320	253±359	89±73
G5M50 (20:40)	242±26	775±432	696±308	100±91	118±104
Blank	115±13	88±64	-o-	421±58	368±140

APPENDIX D:

SUPPORTING INFORMATION FOR SIDE STUDIES

D.1 Glycine Coupling to Trehalose

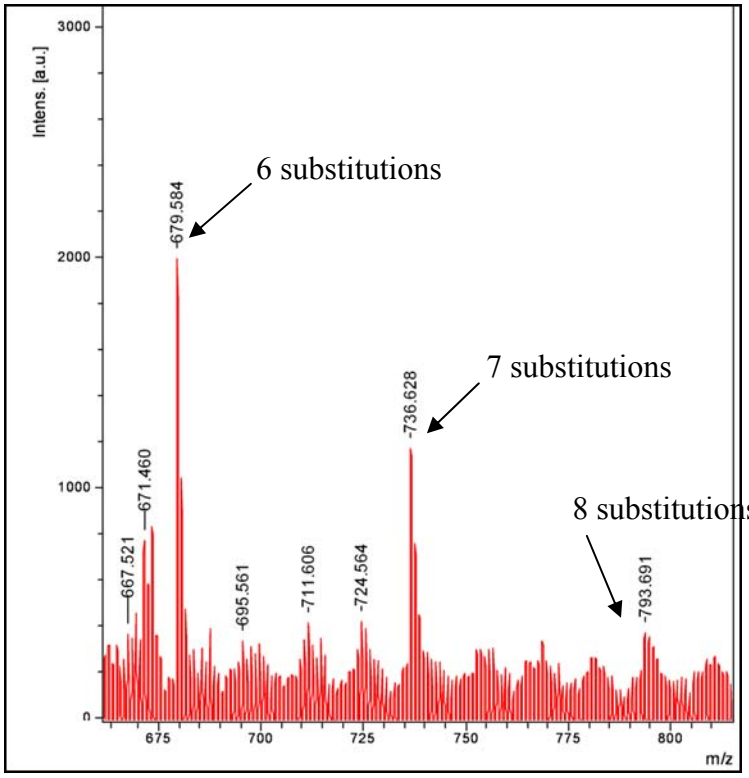

Figure D-1: MALDI-TOF-MS of Trehalose-glycine coupled carbohydrate

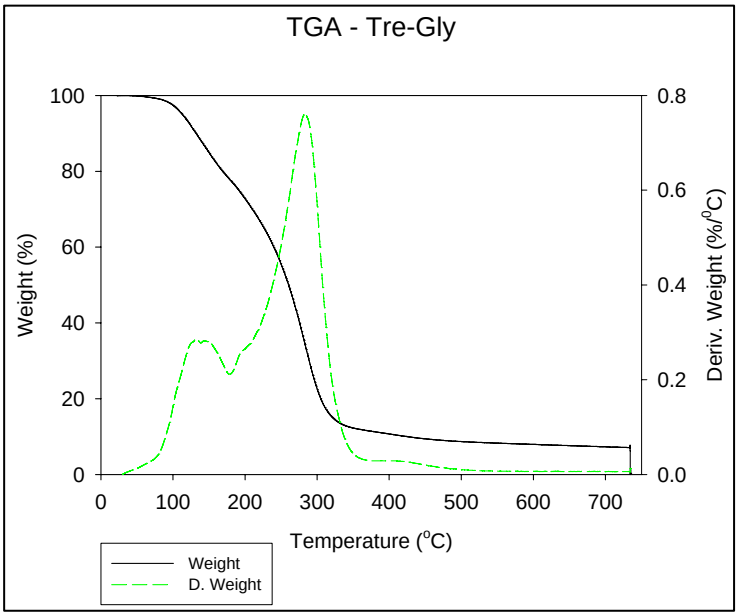

Figure D-2: TGA analysis of crude glycine-trehalose coupled product